

THESIS FOR THE DEGREE OF DOCTOR OF PHILOSOPHY (PHD)

**Phagocytic efficiency of human monocyte-derived dendritic cells is affected
by the peptidoglycan modifications in *Lactobacillus casei* BL23 and tumor-
derived soluble factors**

by

Márta Tóth

Supervisor

Prof. Dr. Attila Bácsi



UNIVERSITY OF DEBRECEN

DOCTORAL SCHOOL OF MOLECULAR CELL AND IMMUNE BIOLOGY

DEBRECEN, 2023

TABLE OF CONTENTS

1. ABBREVIATIONS	4
2. INTRODUCTION	4
3. THEORETICAL BACKGROUND	6
3.1. General aspects of the microbiota	6
3.2. Participants of the mucosal immune system	8
3.2.1. Mucus layer and the epithelium	8
3.2.2. Immunological compartmentalization of the GI tract	10
3.3. Microbiota and its contribution to the homeostasis	12
3.4. Antigen sampling by CD11c ^{high} intestinal DC subpopulations	14
3.5. Ingestion processes after antigen sampling by the DCs	17
3.6. Structure and composition of the PG.....	18
3.7. The role of PG hydrolases in the bacterium's life	20
3.8. The <i>Lactobacillus casei</i> group (LCG).....	22
3.9. Tumor-mediated actions affect the phagocytic efficiency and functions of myeloid cells	24
4. AIMS OF THE STUDY	26
4.1. Part I. Analyzing the effects of human symbiont <i>L. casei</i> BL23 and its PG modifications on human moDC-mediated inflammatory and effector T-cell responses	26
4.2. Part II. Studying the effects of different tumor cell line-derived soluble factors on the differentiation program and phagocytic potential of moDCs.....	26
5. MATERIALS AND METHODS	27
5.1. Bacterial strains and growth conditions	27
5.2. Extraction of peptidoglycan	28
5.3. Human monocyte separation and differentiation to dendritic cells	29
5.4. Maintenance of the tumor cell lines and generation of tumor cell line-derived conditioned media	30
5.5. Activation of moDCs with bacteria or their derived PG fragments	30
5.6. Analysis of the cell surface marker expression and cell viability of dendritic cells by flow cytometry	31
5.7. Cytokine and chemokine measurements by enzyme-linked immunosorbent assays (ELISA)	31
5.8. Enzyme-linked immunospot (ELISpot) assays	31
5.9. Phagocytosis assay by flow cytometry.....	32
5.10. Confocal microscopy.....	33
5.11. Bioinformatical analyses for generation of heatmaps and correlograms.....	33
5.12. Statistical analyses.....	33
6. RESULTS	35
6.1. Part 1. Analyzing the effects of human symbiont <i>L. casei</i> BL23 and its PG modifications on human moDC-mediated inflammatory and effector T-cell responses	35

6.1.1. <i>L. casei</i> ΔLc-p75 mutant bacteria can not alter the moDC activation program but influence the inflammatory cytokine production by moDCs	35
6.1.2. Absence of Lc-p75 in <i>L. casei</i> does not influence the antigen presentation and co-stimulation but promotes an attenuated T-cell response by bacteria-exposed moDCs	38
6.1.3. Purified peptidoglycan extracted from WT or Lc-p75 mutant <i>L. casei</i> demonstrates similar moDC-activating potential	42
6.1.4. Modified bacterial morphology leads to defective phagocytosis by moDCs	45
6.1.5. Blocked uptake of WT <i>L. casei</i> induces diminished inflammatory and T-cell polarizing moDC responses	48
6.2. Part II. Studying the effects of different tumor cell line-derived soluble factors on the differentiation program and phagocytic potential of moDCs.....	54
6.2.1. TU-CMs alter the phenotypic properties of moDCs	54
6.2.2. Mediators derived from different tumor cell lines modify the phagocytic capacity of moDCs ..	59
6.2.3. Correlation analyses reveal associations between the expression of different cell surface markers and phagocytosis by adenocarcinoma- or melanoma-derived CM-educated moDCs.....	61
7. DISCUSSION.....	64
7.1. Peptidoglycan modifications of <i>L. casei</i> BL23 influence the inflammation-inducing capacity of monocyte-derived dendritic cells	64
7.2. Phagocytosis of <i>L. casei</i> BL23 is an elemental step in the induction of moDC activation	67
7.3. Soluble mediators derived from melanoma and adenocarcinoma cell lines differentially affect the differentiation and phagocytic activity of moDCs	69
8. SUMMARY.....	71
9. ÖSSZEFOGLALÁS.....	72
10. REFERENCES	73
11. PUBLICATION LIST PREPARED BY THE KENÉZY LIFE SCIENCES LIBRARY.....	81
12. KEYWORDS	84
12.1 Keywords.....	84
12.2 Kulcsszavak.....	84
13. ACKNOWLEDGEMENT	85
14. APPENDIX	87

1. ABBREVIATIONS

AMP	– antimicrobial peptide
APC	– antigen presenting cell
BMDC	– bone marrow derived dendritic cell
cDC	– conventional dendritic cell
CyD	– cytochalasin D
DC	– dendritic cell
dexDC	– dexamethasone-treated dendritic cell
EGF	– epidermal growth factor
FAE	– follicle- associated epithelium
GALT	– gut- associated lymphoid tissues
GI	– gastrointestinal
IDC	– immature dendritic cell
IEC	– intestinal epithelial cell
IFN	– interferon
IFR	– interfollicular region
Ig	– immunoglobulin
IL	– interleukin
ILF	– isolated lymphoid follicle
ISC	– intestinal stem cell
LAB	– lactic acid bacteria
<i>L. casei</i>	– <i>Lactobacillus casei</i>
LCG	– <i>Lactobacillus casei</i> group
LP	– lamina propria
MDP	– muramyl- dipeptide
Mf	– macrophage
MHC	– major histocompatibility complex
moDC	– monocyte-derived dendritic cell
MLN	– mesenteric lymph node
MUC	– mucin
NAG	– N-acetylglucosamine
NAM	– N-acetylmuramic acid
NK	– natural killer
NOD2	– nucleotide binding oligomerization domain 2
PBL	– peripheral blood lymphocyte
PBMC	– peripheral blood mononuclear cell
PG	– peptidoglycan
PGH	– peptidoglycan-hydrolase
PP	– Peyer’s patch
PRR	– pattern recognition receptor
SED	– subepithelial dome
sIgA	– secretory IgA
SIRP α	– signal regulatory protein α
TAM	– tumor-associated macrophage
Th	– helper T cell
Treg	– regulatory T cell
TNF	– tumor necrosis factor
TLR	– Toll-like receptor
TU-CM	– tumor cell line-derived conditioned media
WT	– wild-type

2. INTRODUCTION

Loads of external and internal factors challenge daily the host throughout life. According to the nature of the exposing factors which can be harmless such as microbiota and harmful like pathogens and transformed self-cells, the immune system needs to react with a proper response against them. The microbiota has co-evolved with the human host, colonizes the mucosal surfaces and the skin after birth, and exerts many kinds of beneficial effects. Therefore, tolerogenic immune responses are demanded to be induced against the microbiota members and it is necessary to avoid promoting inflammation. In contrast to this, generating an inflammatory response against pathogens and transformed self-cells is crucial for the efficient elimination of threats.

Inducing the proper immune response needs precise regulation and cooperation between the innate and adaptive immune cells. Since dendritic cells (DCs) have a unique ability to migrate to the secondary lymphoid organs and activate T cells, they form a bridge between innate and adaptive immunity and can shape the developing T cell responses according to the nature of the antigens. Therefore, DCs in the periphery have to make direct contact with the antigens in which different endocytic processes play a central role.

Symbiotic bacteria such as *Lactobacillus* and their metabolites interact with the host cells in different ways. DCs and other immune and non-immune cells are equipped with a plethora of receptors that sense the bacterial components. The direct interaction between the bacterium and the host cells often relies on the bacterial cell wall and its constituents like polysaccharides, glycolipids, and the peptidoglycan (PG) layer. The immunomodulatory actions of the PG have been known for a long time. Alterations in the PG structure by enzymes such as acetyltransferases or peptidoglycan hydrolases (PGH) largely affect their modulatory potentials.

Similarly, transformed cancer cells manipulate the immune responses against themselves. Since DCs have a complex immunological activity, modifying their differentiation and functions by the cancer cells via secreted factors seems to be crucial for the evasion of DC-mediated immune responses.

Considering the complicated relationship between the microbiota or cancer cells and the DCs, the potential mechanisms are under intense research. However, the bacterial species-specific actions and the unique immunomodulatory properties of the different cancer cells present a great challenge in these studies. This work is dedicated to deepening the knowledge about the symbiotic bacteria- and cancer cell-exerted immunomodulatory properties.

3. THEORETICAL BACKGROUND

3.1. General aspects of the microbiota

The emerging importance of microbiota can be well-characterized by the fact, that over the past decade \$1.7 billion was spent on human microbiota research regarding its medical aspects¹. Even though researchers use the terms microbiota and microbiome interchangeably; they do not mean the same. Microbiota is defined as “the assemblage of living microorganisms presents in a defined environment”, while the microbiome includes “not only the community of the microorganisms, but also their theatre of activity”, which involves the molecules, structural elements, metabolites produced by the microorganisms and all mobile genetic elements, phages, viruses, and extracellular DNA derived from dead cells (**Figure 1**)^{2,3}. However, a consensus is still lacking regarding the integration of viruses, phages, plasmids, and mobile genetic elements into the microbiome.

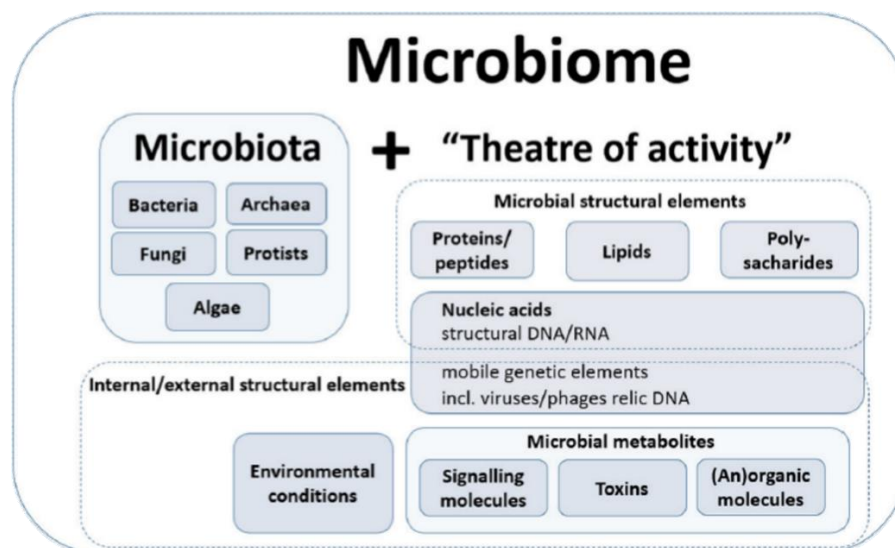


Figure 1. Determination of microbiome and microbiota. The term microbiome refers to the community of microorganisms together with internal and external factors and elements. The term microbiota defines only the living microorganisms in a defined place, i.e., Bacteria, Archaea, Fungi, Algae and Protists³.

Based on these, the human microbiota contains microorganisms from the domains bacteria and archaea, and kingdoms fungi, algae, and protists². These microorganisms reside on the human skin and inside the body on the mucosal surfaces, including in the oral cavity, gastrointestinal (GI) tract, the airways, and reproductive tract^{4,5}. Among these tissues, the GI tract harbors the most abundant microbiota. Microbial communities can be further classified within GI tract according to the different anatomical sites and their physiological

characteristics. In the small intestine, the short transit time, and the high levels of oxygen, bile acids and antimicrobial molecules limit the success of bacterial growth and survival, thus the rapidly proliferating, facultative anaerobic species (such as Lactobacillaceae) adhering to the mucus/epithelial layer can survive in such conditions^{6,7}. In contrast, in the colon the anaerobic conditions and the presence of complex carbohydrates favor the growth of anaerobic species (including Prevotellaceae, Rikenellaceae, Lachnospiraceae) forming a diverse and dense community^{6,7}. Differences can be established also between the transverse sections of the intestines, namely, in the luminal content and in the mucus layers according to the distance from the epithelium, diverse microbiota composition can be detected.

Microorganisms established different types of relationships with the host. Symbiotic species live in mutualism or commensalism with the host, whilst pathobionts are potentially pathogenic species and can cause diseases in immunocompromised people or in dysbiosis when healthy microbiota composition is disrupted⁸, for example upon excessive antibiotic treatments. It has long been demonstrated that symbiotic microorganisms exert many beneficial effects on the host. The best-studied mutualistic microbiota members are bacteria, so-called probiotic bacteria. However, the interactions between the host and other microbiome members such as fungi and viruses are also gaining increasing attention⁴.

A plethora of valuable effects are attributed to probiotic bacteria, including maintaining and reinforcing the intestinal epithelium integrity^{9,10}, restraining the adhesion of pathogens^{11,12}, and assisting in the digestion resulting in energy accumulation, vitamin and metabolite production¹³⁻¹⁵. Additionally, probiotics support immune system development and manipulate immune responses^{16,17}. In the absence of microbiota, the primary and secondary lymphoid organs, such as the mucosae-associated lymphoid tissue, spleen, and thymus contain a low number of immune cells for example CD4⁺ and CD8⁺ T cells, intraepithelial lymphocytes, regulatory T cells (Treg) and invariant natural killer T cells and reduced secretory immunoglobulin A (sIgA) level. These observations are derived from germ-free mice, an excellent model to study the effect of monocolonization with one bacterial strain or colonization with standard microbiota. Interestingly, it has been demonstrated that restoration of the microbiota in germ-free mice can reverse the defects of the immune system but only within a certain time window, in the first week after birth¹⁸. In humans, the first year of life seems to be pivotal, because excessive antibiotic and disinfectant usage in this period could have serious consequences in later life including the development of allergies, asthma¹⁹, inflammatory bowel diseases²⁰, obesity²¹, and type I and II diabetes mellitus²². These observations indicate that

microbial exposures in early life may have lifelong consequences and that the disruption of the individual microbiota can contribute to the development of chronic inflammatory disorders.

3.2. Participants of the mucosal immune system

3.2.1. Mucus layer and the epithelium

Distinguishing the innocent substances derived from the food and microbiota from pathogen-derived molecules is indispensable for avoiding excessive inflammatory processes. Therefore, tolerance induction is crucial against food- and microbiota-derived antigens and immunogenic immune responses must be generated against pathogen-derived antigens. The induction of the appropriate immune response relies on the operation of the mucosal immune system, which involves many types of defense layers protecting the body's most vulnerable surfaces, the mucosae, and the skin, including physical, chemical, microbiological and immunological defenses. The mucosae-associated lymphoid tissues can be subdivided according to the tissue sites, namely NALT, BALT, GALT, GOALT and SALT, which refer to nasal-, bronchus-, gut, genital organ- and skin-associated lymphoid tissues^{23,24}. Hereafter, the GALT will be detailed.

The first line of defense is provided by the mucus layer. The mucus consists of hydrophilic branched glycoproteins secreted by goblet cells in both the small and large intestines. However, the structure of the mucus layer is largely different between the small and large intestines. The mucus in the small intestine is one-layered and attached loosely to the epithelium, thus the nutrients and the digestive enzymes can be easily passed through it. This may also apply to the bacterial content of the lumen, but the abundant number of antimicrobial molecules can limit its access²⁵. The mucus layer consists of mainly the gel-forming mucin-2 (MUC2) and MUC6 in the duodenum²⁶. Similarly, MUC2 is the main component in the large intestinal mucus layer. However, in the large intestine it forms 2 layers; an inner, directly attached to the epithelial layer which is barely penetrable for the microorganisms and an outer, loosely attached one²⁵. Beside the barrier function, mucus has an anchoring role and serves as an energy and carbon source for certain bacterial species. Members of the microbiota can be fixed to the outer mucus layer via sIgA²⁷ or adhesins, including pili, flagella, and mucus-binding proteins expressed by the bacteria such as *Lactobacillus* or *Bacteroides* species²⁸. Furthermore, the O-glycan residues of the mucin can be degraded to monosaccharides by bacterial species like *Akkermansia muciniphila* (*A. muciniphila*), *Bacteroides thetaiotaomicron* (*B. thetaiotaomicron*) and *Bifidobacterium bifidum* (*B. bifidum*), which express mucus-degrading

enzymes like glycosidases, sialidases and sulphatases²⁹. The monosaccharides can be further exploited by other mucus-anchoring bacteria such as Lachnospiraceae³⁰ (**Figure 2**).

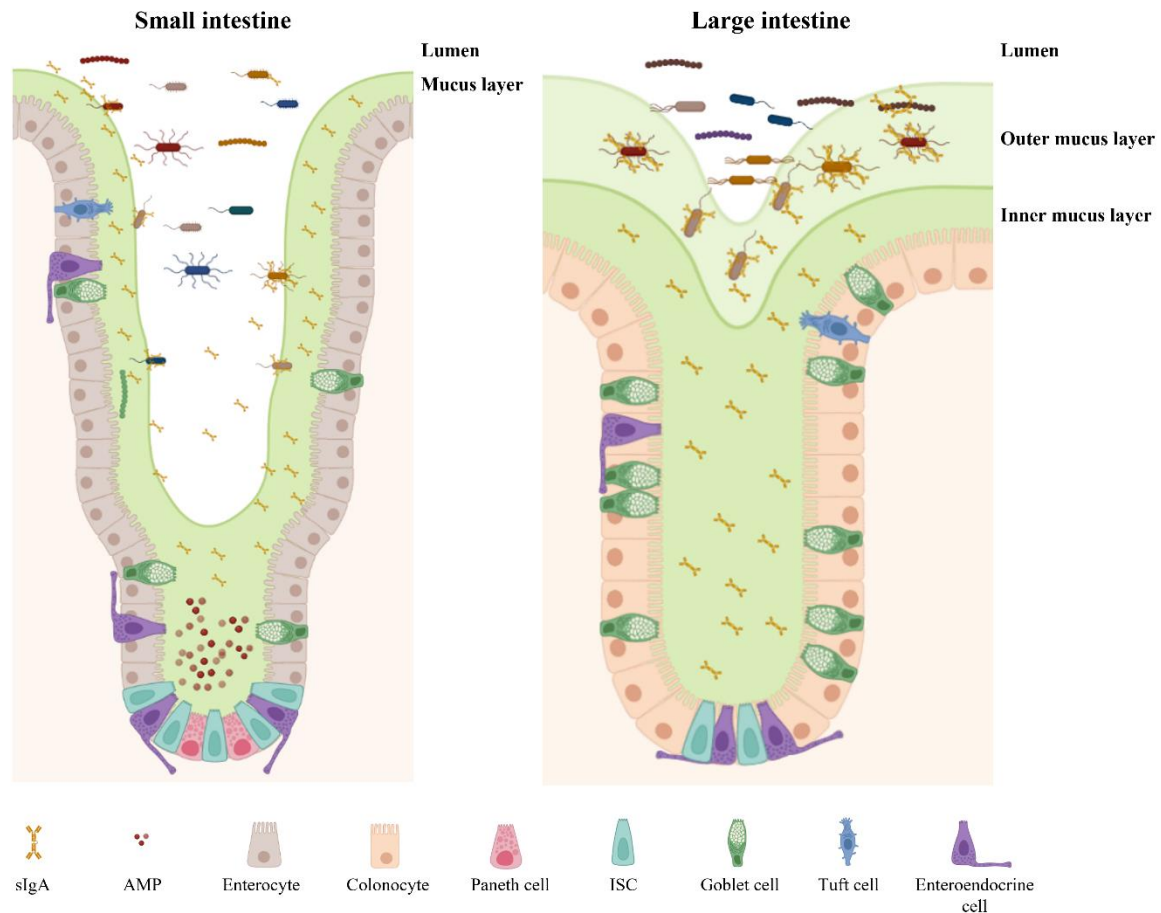


Figure 2. Structure and composition of the mucus and epithelial layers in the small and large intestines. Thin, one-layered mucus covers the small intestine. Bacteria from the microbiota can adhere to the mucus layer via sIgA or with bacterial molecules such as adhesins or pili. Specialized epithelial cells between the enterocytes can be found in the epithelium; Paneth cells release antimicrobial peptides, enteroendocrine cells produce gut hormones, goblet cells secrete mucin, and tuft cells help in the induction of immune responses by cytokine secretion. Epithelial cells are replaced by intestinal stem cells, which reside in the crypts along with Paneth cells and enteroendocrine cells (left panel). In the large intestine, the mucus is two-layered; the inner one is barely penetrable for the bacteria, while the outer layer is rich in them. Paneth cells are missing in the large intestine (right panel). The figure was created in BioRender. Abbreviations: sIgA: secretory IgA; AMP: antimicrobial peptide; ISC: intestinal stem cell.

Beneath the mucus layer(s) the epithelium of the GI tract performs various tasks. Food is digested in the small intestine and the absorption of the ions, water, macro- and micronutrients require transport mechanisms between (paracellular) and through (transcellular) the enterocytes³¹. Besides, the epithelium has to create a physical barrier against the invasion of dangerous molecules and microbes, like toxins and pathogens³². A selectively permeable seal is formed between adjacent intestinal epithelial cells (IECs) by tight junction proteins including

occluding, claudin and junctional adhesion molecules. Besides, IECs can recognize the invading microorganisms via their various pattern recognition receptors (PRRs) and respond with the production of many kinds of cytokines and chemokines^{33,34}. Moreover, specialized epithelial cells have unique functions. The formerly described goblet cells secrete mucin, whilst Paneth cells, which reside at the bottom of the crypts, produce antimicrobial peptides (AMPs) and enzymes, including lysozyme C, α -defensins and the lectin type regenerating islet-derived protein 3 α ³⁵. These antimicrobials are efficient in the disruption of the Gram+ and Gram-bacterial cell wall. Paneth cells highly express nucleotide binding oligomerization domain 2 (NOD2) which regulates their α -defensin production³⁶. Furthermore, NOD2-deficient mice have altered microbiota indicating that Paneth cells play a role in the regulation of microbiota composition³⁷. They also support the differentiation of leucine-rich repeat-containing G-protein coupled receptor 5 positive intestinal stem cells (ISCs) to any epithelial cells by secreted factors, like epidermal growth factor (EGF) and Wnt3a, a key molecule in the induction of ISC proliferation and differentiation³⁸. The other two secretory cell types are the enteroendocrine cells and the tuft cells. Enteroendocrine cells secrete gut hormones, including glucagon-like peptide 1, glucose-dependent insulintropic polypeptide and cholecystokinin controlling food digestion and absorption, appetite, and insulin release³⁹. Tuft cells produce various soluble mediators such as interleukin (IL)-25, thymic stromal lymphopoietin, acetylcholine and prostaglandins upon stimulation and can sense the presence of pathogens, mainly helminths and protozoa⁴⁰. Lastly, the microfold (M) cells will be described in the 3.2.2 subsection.

3.2.2. Immunological compartmentalization of the GI tract

Cellular and humoral factors of the immune system are localized in every defense layer of the intestinal wall; sIgA molecules are attached to the mucus layer, intraepithelial immune cells are present between the IECs, and a huge number of immune cells are in the *lamina propria* (LP). These elements act in concert to maintain the tolerance against the microbiota members and induce the elimination of pathogens or toxic molecules. The immunological compartments can be categorized into inductive sites: the GALT including the Peyer's patches (PPs), appendix, the numerous isolated lymphoid follicles (ILFs), and the draining mesenteric lymph nodes (MLNs). In these places, the naïve adaptive immune cells are subjected to priming and differentiation. LP and the epithelium are the effector sites in which primed cells are localized and fulfill their functions⁴¹.

PPs are found along the small intestine with increasing frequency towards the terminal ileum, where they compose a lymphoid ring⁴². PPs are covered with follicle-associated

epithelium (FAE) rich in M cells, which are embedded between the enterocytes to sample the luminal content of the gut and equipped with molecules like glycoprotein 2, uromodulin or peptidoglycan recognition protein 1 facilitating the endo- and transcytosis by the M cells and selection between bacteria^{43,44}. SIgA-opsonized or intact particulate and soluble antigens are transported to the underlying subepithelial dome (SED) full of highly phagocytosing myeloid antigen presenting cells (APCs) such as macrophages (Mfs) and DCs⁴⁵. Besides, adaptive B cell subsets expressing IgA, IgM, or IgG are in the follicles, while naïve, regulatory and memory T cell subpopulations are found in the interfollicular regions (IFRs)^{41,46,47} (**Figure 3**).

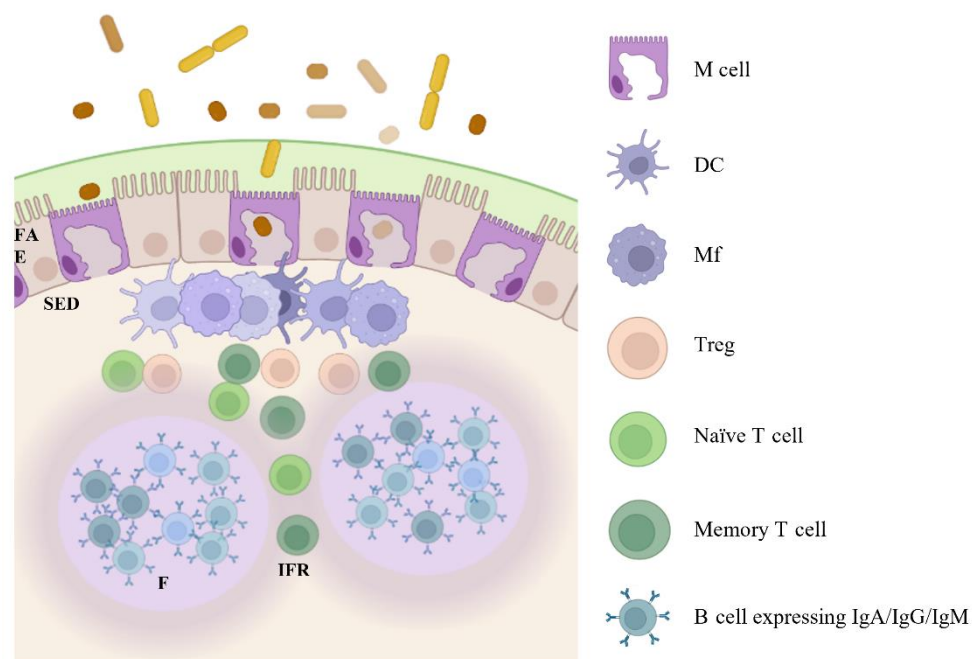


Figure 3. Schematic representation of the Peyer's patch. FAE of the PP is barely covered by mucus and is permeable to the particles and soluble antigens. M cells are located between enterocytes and allow the entry of the antigens to the SED. Beneath the FAE, myeloid-derived APCs, i.e., Mfs and DCs encounter the antigens. Besides, naïve, memory and regulatory T cells and IgA, IgM and IgG-expressing B cells are localized in the dome. Figure was created in BioRender. Abbreviations: PP: Peyer's patch, FAE: follicle associated epithelium, SED: subepithelial dome, IFR: interfollicular region, F: follicle, DC: dendritic cell, Mf: macrophage, Treg: regulatory T cells, APC: antigen presenting cell.

Interestingly, Junker et al. demonstrated, that T cells isolated from human ileal, and colon lymphoid follicles differentiated to interferon (IFN) γ -, tumor necrosis factor (TNF) α -, and IL-2-secreting T cells upon anti-CD3/CD28 stimulation in contrast to rodents in which regulatory cytokines including IL-4 or IL-10 were produced by such T cells⁴⁸ indicating that results from mice are not always applicable to humans.

The structure of the vermiform appendix is highly resembles the PP. The FAE contains M cells⁴⁹ and the dome region is rich in monocytes and CD86⁺ DCs⁵⁰. Furthermore, naïve and

central memory T cells⁵¹, Tregs, and B cells at different developmental and activation stage⁵² are in the T and B cell zones indicating that adaptive immune responses can be induced in the appendix.

ILFs are the smallest lymphoid organelle among the gut's lymphoid structures; however, there are approx. 30,000 ILFs in the human small and large intestines making them a remarkable immunological compartment in the human body⁵³. The surface of the ILFs is covered by FAE with M cells. SED is enriched in CD11c⁺ APCs and B cell follicles enclosed by T cells⁵⁴. Like PPs and appendix, ILFs also contain various T and B cell subtypes, including naïve and memory B and T cells and Tregs as well. It has also been shown that T-cell independent IgA class switching can take place in murine ILFs. DCs and Mfs express APRIL (a proliferation-inducing ligand), which elicits the activation-induced deaminase expression in the B cells required for isotype switching⁴⁵. Additionally, T-cell dependent IgA1, IgA2 and IgG antibody responses can be also generated in the ILFs⁵⁵.

Activation and differentiation of naïve T cells can also be executed in the draining mesenteric lymph nodes by DCs from the inductive or effector sites of the immunological compartments. It has previously been reported that MLNs are crucial for the induction of oral tolerance; presentation of the food antigens occurs primarily in the MLNs not in any other lymphoid tissue in the intestine⁵⁶. Moreover, DCs continuously migrate from the LP and PP to the MLN to induce tolerance⁵⁷. However, tolerance induction against microbiota members rather occurs in the LP or PP more than in the MLNs.

As an immunological effector site, LP contains many kinds of myeloid- and lymphoid-derived effector cells including Mfs, DCs, natural killer (NK) cells, mast cells, effector and memory Th1, Th17 cells, and regulatory T and B cells to orchestrate the gut immune responses and maintain the homeostasis^{58,59}. Intraepithelial lymphocytes located between the IECs also contribute to pathogen clearance and tolerance induction against the microbiota members⁶⁰.

3.3. Microbiota and its contribution to the homeostasis

The host's encounter with the microbiota-derived metabolites begins already in the womb, this process is called immune imprinting⁴. It has previously been demonstrated that the short chain fatty acid acetate can cross the placenta and acts on epigenetic mechanisms influencing Treg differentiation. Moreover, the maternal microbial factors shape the fetus' immune system and affect the development of potential pathological conditions later in life, such as asthma⁶¹. Therefore, the mother's diet and usage of antibiotics are important during pregnancy. The pioneer species first colonizing the newborn's skin and mucosal surfaces

depend on the type of delivery; newborns get members from the vaginal and fecal microbiota by vaginal birth; in the case of Cesarean section microbiota members from the mother's skin become the first colonizing species. The diversity of microbiota in childhood rapidly increases because of breast milk or formula feeding and the new environmental factors. Adult microbiota composition is relatively stable as compared to children's microbiota. However, with changing the diet, increasing pollution and antibiotic use adult's microbiota can also be drastically altered⁴.

Radical disruption of the diversity and composition of the individual microbiota i.e., dysbiosis can lead to serious consequences implying the importance of the symbiotic microbes in the host's life. Direct and indirect mechanisms exerted by the microorganisms help in the protection against pathogenic colonization, maintenance of the epithelial barrier integrity and the development and education of the immune system. It has been demonstrated that *Bacteroides* spp can prevent the *Klebsiella pneumoniae* (*K. pneumoniae*) infection via directly enhancing the macrophage killing ability mediated by intestinal IL-36 γ ⁶² or indirectly via production of acetate causing intracellular acidification of *K. pneumoniae* and blocking its growth⁶³. In another study, Kim et al. observed that a lantibiotic derived from *Blautia producta*, a member of a 4-strain cooperative bacterial consortium can directly inhibit the growth of vancomycin-resistant enterococcus⁶⁴. Furthermore, forming long chains by inhibiting cell septation is a survival strategy for pathogens, such as uropathogenic *Escherichia coli* (*E. coli*) to avoid phagocytosis by the immune cells or increase antibiotic resistance⁶⁵. The auto- and coaggregation properties of probiotic bacteria can actively restrain pathogenic colonization and biofilm formation. It has recently been shown that three *Lactobacillus* strains could inhibit the growth, adhesion, and biofilm formation of *Gardnerella vaginalis*, a bacterial vaginosis-causing pathogen⁶⁶. In addition to this, bacteria and their secreted molecules such as indole are involved in the protection of the epithelial barrier via enhancement and maintenance of tight-junction proteins' expression⁶⁷.

Microbiota-derived molecules serve as ligands for numerous PRRs and locally act on IECs and immune cells or influence the functions of extraintestinal organs. Polysaccharide A produced by *Bacteroides fragilis* (*B. fragilis*) is recognized by Toll-like receptor (TLR)1/TLR2 heterodimer together with Dectin-1 by DCs and induces anti-inflammatory gene expression via cAMP response element-binding protein contributing to the differentiation of peripheral Tregs⁶⁸. In contrast, segmented filamentous bacteria assist in the differentiation of Th17 cells in mice⁶⁹. It is well-known that muramyl-dipeptide (MDP) the smallest active fragment of the Gram+ bacterial PG is a ligand for the cytosolic NOD2 receptor highly expressed by Paneth

cells and CD11c⁺ myeloid cells controlling the microbiota composition and inflammatory cytokine secretion^{70,71}.

3.4. Antigen sampling by CD11c^{high} intestinal DC subpopulations

Symbiotic bacteria have to make direct or indirect interactions with host cells to exert their modulatory effects. Direct interactions can be implemented via different ways. FAE on PPs is exposed to various stimuli to a great extent due to its fewer goblet and Paneth cell content as compared to the villous epithelium. The reduced protection allows pathogens to exploit the route through the M cells reaching the underlying tissues. For example, the invasion protein of *Yersinia pseudotuberculosis* species binds to integrin $\beta 1$ on M cells in mice⁷². Furthermore, *Listeria monocytogenes* uses internalin B binding to a yet undescribed M cell receptor⁷³. The antigen uptake can be facilitated by opsonization via sIgA, despite M cells don't express the classical Fc α receptor I⁷⁴. However, it has been uncovered that the apical Dectin-1 plays an essential role in the transcytosis of sIgA-antigen complexes through the M cells and these complexes are internalized by CX₃CR1⁺ DCs⁷⁵. The CX₃CR1⁺ DC subpopulation in the SED, which expresses CD11b, CD11c and lysozyme M, is called LysoDC. LysoDC has a powerful phagocytic capacity, and it is capable to penetrate FAE and able to sample the luminal antigens by extending their dendrites via M cell-specific transcellular pores without disrupting the epithelial integrity^{76,77}. Moreover, they can acquire antigens from M cell-derived microvesicles⁷⁸ and from apoptotic M cells⁷⁷. It is worth noting that recently a DC-independent antigen uptake was described by an activated B cell subpopulation which makes close contact with the PP M cells internalizing the specific antigen⁷⁹. These overall demonstrate that M cells are the main antigen source in the PP.

In an elegant mouse study from 2015, it has been demonstrated that the LysoDCs originate from circulating CCR2⁺ monocytes but do not express inflammatory monocyte-derived genes such as Cd209a, Nos2 or Tnf. Furthermore, LysoDCs were able to upregulate the co-stimulatory CD40 and CD86 and major histocompatibility complex II (MHCII) expression upon TLR7 stimulation by R848 ligand and secrete IL-6 and TNF α . They were also capable to induce the priming of naïve Th cells toward IFN γ -secreting Th1 cells⁸⁰. Nevertheless, four different subsets of the LysoDCs have been observed recently with both shared and distinct functions⁸¹.

Additional three CD11c⁺ DC subsets can be distinguished in the PP's different locations in the mouse small intestine: CD8 α ⁺ cDC1 DC subset and CD11b⁺ cDC2 DCs are localized in the IFR, whereas double negative (DN) DCs shuttle between SED and IFR. DN DCs are

considered to be the immature counterpart of the CD11b⁺ cDC2 DCs. Since the available literature about the PP DC subsets is derived from mice experiments, **Table 1** summarizes the origin, localization, phenotype, and function of the mouse PP DC subsets. The blood CD8 α ⁺ DC subset shares a common gene signature with the human blood CD141⁺ cDC1 subset but there are no available data about the human equivalent of the PP CD8 α ⁺ DC subset. Note that some of the human counterparts of the murine PP DC subsets, for example LysoDCs are already discovered⁷⁷. Besides, plasmacytoid DCs and distinct Mf populations are also found in the PP⁸².

CD11c ^{high} MHCII ^{high} DC subsets	Origin	Localization	Phenotype	Antigen acquisition	Function	T cell activation
CD8 α ⁺ cDC1	CDP	IFR	SIRP α ⁻ /CD11b ⁷ /CD8 α ⁺	Antigens from other Mf or DC subsets	IL-12 secretion after bacterial stimulation	IFN γ -producing T cells
CD11b ⁺ cDC2	CDP	IFR	SIRP α ⁺ /CD11b ^{int/+} /CD8 α ⁻	Antigens from other Mf or DC subsets	IL-6, IL-10 secretion IgA switching induction	IL-4-, IL-6- and IL-10-secreting T cells
DN cDC2 (immature)	CDP	SED/IFR	SIRP α ⁺ /CD11b ⁷ /CD8 α ⁻	Penetration across the epithelium Interaction with M cells	IL-12 secretion Cross-presentation of viral antigens	IFN γ -producing T cells
LysoDC	Monocyte	SED/F/IFR	SIRP α ⁺ /CD11b ⁺ /CX ₃ CR1 ⁺	Protrusions in M cell transcellular pores Penetration across the epithelium IgA-coated antigen uptake	High phagocytic activity IL-6, TNF α secretion IgA switching induction	IL-6 or IFN γ -producing T cells

Table 1: Main characteristics of the mouse PP DC subsets^{80,82–84}. Abbreviations: CDP: common DC progenitor, SED: subepithelial dome, F: follicle, IFR: interfollicular region.

Similarly to the PP, LP also contains various CD11c^{high} DC subtypes whose differentiation programs and functional properties are conserved between mice and humans⁸⁵. In mice, CD103 and CD11b markers are frequently used to distinguish the LP DC subsets: cDC1 DCs positive for CD103 and negative for CD11b and two cDC2 subsets: both positive for CD11b and positive/negative for CD103⁴⁷. In humans, instead of CD11b signal regulatory protein α (SIRP α) is used for the identification of the subsets: mouse cDC1 is equivalent to CD103⁺SIRP α ⁻; however, only one cDC2 population has been previously described in humans, which involves CD103⁺SIRP α ⁺ cells. A third DC subpopulation was discovered in the human LP, which is CD103⁻SIRP α ⁺ and has similarities to monocyte-derived DCs⁸⁶. However, more recent studies classify it as cDC2⁸⁷. Moreover, a distinct subset has been previously demonstrated, which expresses CX₃CR1⁸⁸. The characteristic markers and transcription factors

and T-cell activation properties of the human cDC1 and cDC2 subsets are summarized in **Table 2**.

cDC subsets	cDC1	cDC2	cDC2
Defining markers	CD103 ⁺ SIRP α ^{lo/-}	CD103 ⁺ SIRP α ⁺	CD103 ⁻ SIRP α ⁺
Transcription factors	IRF8, BCL6	IRF4, BLIMP1	?
Additional markers	CLEC9A, CXRI, CD141, CD13, CD26	CD1c, CD101, CD207, CD209	CD101
Function	Promote cytotoxic CD8 ⁺ T cell response	Promote T cells into Treg and Th17	Promote T cells into Th1 cells

Table 2. Main characteristics of the human intestinal LP cDC subsets. Abbreviations: BCL6, B cell lymphoma 6; BDCA, blood DC Ag; BLIMP1, B lymphocyte-induced maturation protein-1; CLEC9A, C-type lectin domain containing 9A; IRF, IFN regulatory factor; SIRP α , signal regulatory protein α ; XCR1, X-C motif chemokine receptor 1⁸⁷ (modified).

Acquisition of the antigen by the DC subpopulations can take place by multiple mechanisms in the LP. CX₃CR1⁺ DCs are able to extend their dendrites between the IECs and directly sample the luminal content of the gut^{88,89}. Similarly, it has been demonstrated that CD103⁺ DCs translocate to the epithelium and sample antigen from the lumen via their dendrites in the ileum and activate T cells⁹⁰. SIRP α ⁻ cDC1 can cross-present viral antigens derived from apoptotic epithelial cells and migrate to the T-cell zone in the MLN⁵⁷. Additionally, indirect mechanisms assist in the antigen sampling. McDole et al. reported that goblet cells deliver low molecular weight soluble antigens to the underlying CD103⁺ DCs⁹¹. Furthermore, IgG-coated antigens can also pass through the epithelial cells via the neonatal Fc receptor⁹². Non-migratory CX₃CR1⁺ Mfs can also hand over acquired antigen to CD103⁺ DCs via gap junction transfer and induce oral tolerance⁹³ (**Figure 4**).

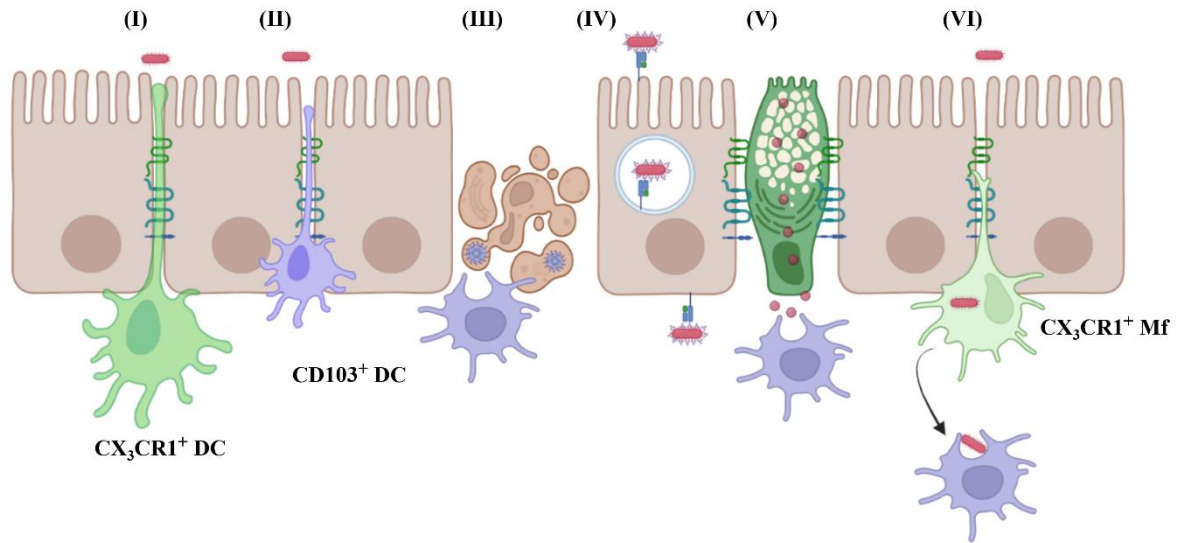


Figure 4. Potential antigen sampling mechanisms across the LP epithelium. DC subsets acquire antigens in different ways: **I.** CX_3CR1^+ DCs protrude their dendrites paracellularly between the enterocytes into the gut lumen. A tight junction is formed between the DC's dendrite and the epithelial cells thus, the barrier integrity is not harmed. **II.** Ileal $CD103^+$ DCs can translocate to the epithelium and extend their dendrites sampling soluble and particulate antigens. **III.** Apoptotic, virally infected epithelial cells can be engulfed by $CD103^+$ DCs. **IV.** IgG-coated antigens bind to the FcRn on the surface of the enterocytes and are transported by the vesicular system to the basolateral area in which phagocytes can uptake them. **V.** Low molecular weight soluble antigens can be transported by the goblet cell to the $CD103^+$ DCs. **VI.** Non-migratory, poor T-cell polarizing CX_3CR1^+ Mfs extend their dendrites to the lumen sampling the antigen and pass to the $CD103^+$ DCs. Created in BioRender. Abbreviations: DC: dendritic cell, FcRn: neonatal Fc receptor, Mf: macrophage.

3.5. Ingestion processes after antigen sampling by the DCs

Tissue-resident, immature DCs (IDCs) are equipped with the machinery required for all known endocytic processes: phagocytosis, macropinocytosis for the large particles and dynamin-dependent and independent endocytosis for small antigens^{94,95}. During the DC maturation, endocytic activity rapidly decreases and the antigen processing and presentation are becoming more prominent⁹⁶.

Phagocytosis and macropinocytosis play a role in the engulfment of particles larger than 500 nm size such as bacteria and apoptotic cells. Moreover, both processes are actin-dependent, but their regulation and the involved receptors and molecules are greatly different. The phagocytic process is highly regulated and initiated by the recognition of the opsonized material via cell surface receptors, generally Fc, complement receptors and PRRs like Dectin-1, and proceeds with the engagement of other receptors inducing the membrane distortion and phagosome generation⁹⁵. However, it is hard to determine which receptor actually promotes the internalization⁹⁷.

Macropinocytosis or “cell drinking” is constitutively active in professional APCs thus, in the absence of threats, macropinocytosis assists in maintaining the DC-dictated peripheral tolerance via self-peptide presentation⁹⁸. It involves the engulfment of extracellular fluid together with particles like bacteria. Initially, macropinocytosis was thought to be a barely regulated process with non-selective membrane uptake. However, the view has changed and revealed that the process is growth factor receptor signaling- and Na⁺/H⁺ exchanger-dependent^{95,99}. Under inflammation or in the presence of infection, DCs mostly rely on macropinocytosis in the antigen uptake. Moreover, it has been reported that macropinocytosis is necessary for MHCII-mediated antigen presentation by the DCs. Treatment with macropinocytosis inhibitors caused a marked reduction in the naïve T-cell priming ability of the DCs¹⁰⁰.

Particles smaller than 500 nm like bacterial cell wall components can be engulfed by macro- or micropinocytosis and other endocytic processes, like clathrin- or caveolin-dependent endocytic processes which can be dynamin-dependent or independent. It has been reported that MDP entry in the Mfs uses a clathrin- and dynamin-dependent endocytic pathway, which is necessary for NOD2 signaling¹⁰¹. In a study carried out this year, Popescu et al. have demonstrated that the internalization of the *Bacillus anthracis* PG polymer and larger fragments of various sizes takes place mostly via actin-dependent pathways¹⁰². However, dynamin-dependent endocytosis also contributes to the engulfment by 20-30 %. In another investigation, it has been shown that epithelial cells are able to use two independent pathways for the uptake of cell wall purified from *Streptococcus pneumoniae*¹⁰³. The dynamin- and clathrin-dependent pathway uses platelet-activating factor receptor in complex with the bacterial cell wall and a non-canonical pathway resembled macropinocytosis. Interestingly, TLR2 engagement with bacterial cell wall did not necessarily induce the internalization of the bacterium but promoted an inflammatory response. These studies demonstrate that the internalization pathways can vary between human cells.

3.6. Structure and composition of the PG

PG is the largest constituent of the Gram+ bacterial cell wall, consisting of long-glycan strands with repeating units of N-acetylglucosamine (NAG) and N-acetylmuramic acid (NAM) linked with β -1,4 bonds¹⁰⁴⁻¹⁰⁶. The NAM and NAG residues can be O-acetylated or N-deacetylated¹⁰⁵. The long strands are cross-linked by short peptide chains. The most common peptide sequence is composed of L- and D-amino acids in the following order: L-alanine, D-glutamine, L-lysine, D-alanine, D-alanine. The third amino acid in the rod-shaped Gram+ and

all Gram- bacteria can be alternatively meso-diaminopimelic acid or L-ornithine¹⁰⁵. The first L-alanine forms a lactyl bond with the carboxyl group of NAM (**Figure 5**). However, the structure and the composition of the mature PG are strikingly species-specific^{106,107}.

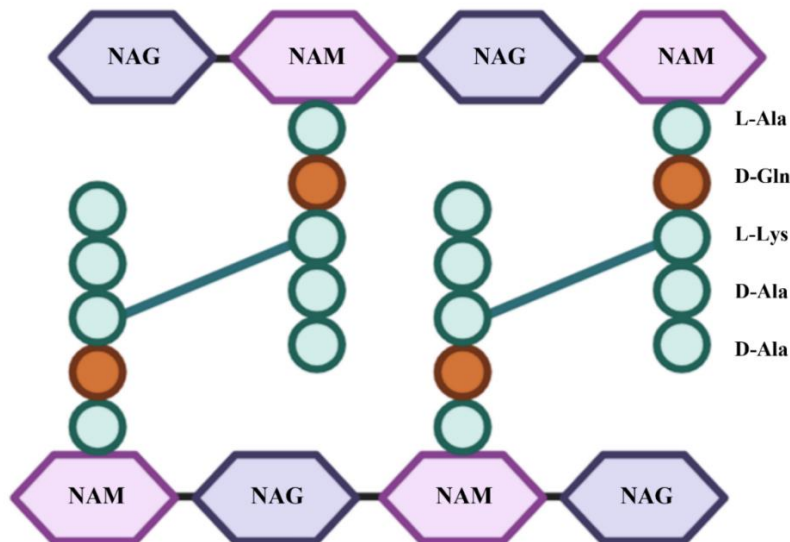


Figure 5. Common composition and structure of the Gram+ PG stem. The main glycan strands are composed of NAM and NAG. The strands are interconnected with short peptide sequences. The common peptide chain consists of L-Ala, D-Gln, L-Lys and two D-Ala residues and is linked with intrapeptide bridges. Structural and compositional variations are frequently found in the peptide chains. Created in BioRender. Abbreviations: NAM: N-acetylmuramic acid, NAG: N-acetylglucosamine, L-Ala: L-alanine, D-Gln: D-glutamine, L-Lys: L-lysine, D-Ala: D-alanine

Post-synthetic modifications and alterations in the peptidoglycan backbone can fundamentally change the bacterium's fate. O-acetylation of the NAM in *Staphylococcus aureus* (*S. aureus*) makes the bacterium resistant to the lysozyme¹⁰⁸. N-glycolylated PG of *Mycobacterium tuberculosis* increases the immunogenicity, mutation in the enzyme responsible for the N-glycolylation induced decreased TNF α production by Mfs¹⁰⁹.

The cell wall diversity is further amplified by the anchoring residues of the cell wall carbohydrate chains such as exopolysaccharides and teichoic acids. The observation showing that removal of the polysaccharides from *Lactobacillus* (*L.*) *casei* (renamed to *Lacticaseibacillus casei*) cell wall completely abrogated the IL-12 production by Mfs implies strong immunomodulatory actions of the cell wall constituents¹¹⁰. Similarly, the purified lipoteichoic acid derived from *L. plantarum* caused elevated pro-inflammatory cytokine and chemokine secretion by human peripheral blood mononuclear cells (PBMCs)¹¹¹. However, it has been demonstrated that the cell wall elements of microbiota members may have beneficial effects on the host, e.g., exopolysaccharides and capsular polysaccharides derived from lactic

acid bacteria (LAB) exert antimicrobial, antiviral, antifungal, and antibiofilm activities¹¹². Similarly, microbiota-derived PG or PG muropeptides present various favorable effects on the host. Previously, it has been reported that microbiota PG fragments were released systemically from the gut lumen into the circulation in the absence of infection and were detected even in the bone marrow¹¹³. The transferred PG components were bioactive because they could induce NOD1-dependent NF- κ B activation in HEK293 cells. Moreover, NOD1 mediated PG recognition efficiently primed and restored the neutrophil functions and killing ability in microbiota-deficient mice¹¹³. Additionally, a recent study has demonstrated that PG-sensing molecules and receptors are expressed in a developing brain suggesting the critical role of maternal microbiota during pregnancy^{114,115}.

Release of the PG fragments involves different mechanisms. Both pathogenic and symbiotic Gram+ bacteria constantly secrete membrane vesicles¹¹⁶ which contain PG components¹¹⁷. Furthermore, in *Helicobacter pylori*, type IV secretion systems can transport radiolabeled PG from the bacterium to the cytoplasm of the host cells¹¹⁸. After phagocytosis, the whole bacterium is degraded in the phagolysosomes and peptide transporters like the members of the SLC15 family in epithelial cells and DCs play a role in the delivery of NOD1 and NOD2 ligands to the cytosol¹¹⁹. In a study with *L. acidophilus*, apart from NOD2, PG is recognized by many types of PRRs including NOD1, NOD-leucine rich repeat and pyrin domain-containing (NLRP) 3, NLRP1, and PG-binding proteins. These receptors sense PG fragments with various structures, sizes, and compositions, including disaccharide-di-, tri-, tetra- or pentapeptides so called muropeptides¹²⁰.

3.7. The role of peptidoglycan hydrolases in the bacterium's life

The precise cleavage of the muropeptides is dependent on bacterium species-specific enzymes so called PGHs which contribute to the PG synthesis, turnover, recycling, and degradation¹²¹. Due to the action of the PGHs, muropeptides are generated which can be utilized in the PG turnover and recycling or released to the environment. The PGHs can be grouped according to the cleaved bond (**Figure 6**).

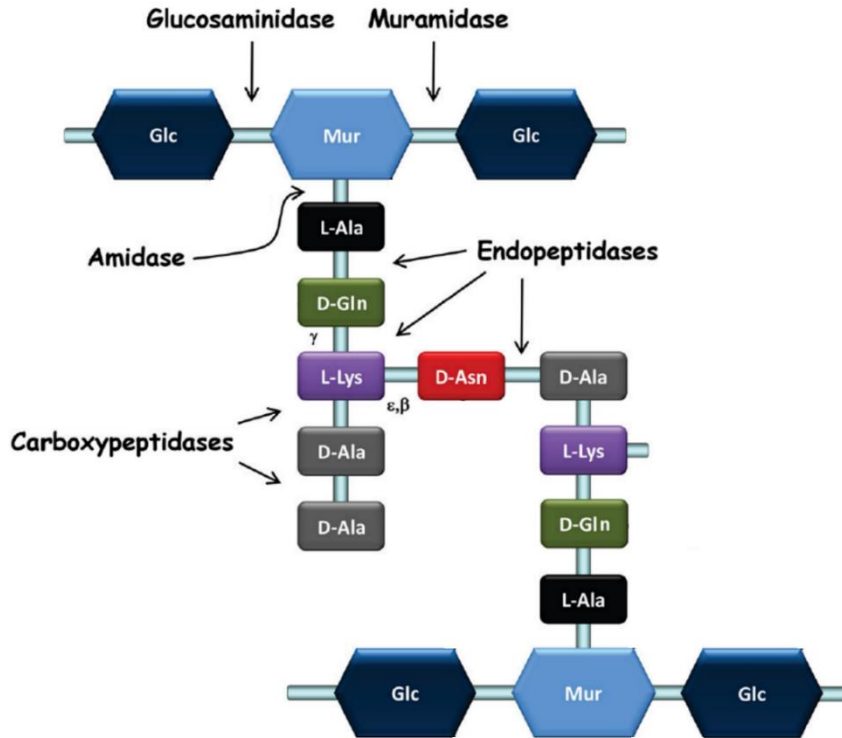


Figure 6. PG structure of *Lactococcus lactis* (*L. lactis*) with the PGHs. This type of PG structure is characteristic for *L. lactis* and many lactobacilli. The cleavage sites of different PGHs are illustrated with arrows. Abbreviations: Glc: N-acetylglucosamine, Mur: N-acetylmuramic acid, L-Ala: L-alanine, D-Gln: D-glutamine, L-Lys: L-lysine, D-Ala: D-alanine, D-Asn: D-asparagine¹⁰⁵ (modified).

These enzymes perform a variety of functions: they control the separation of the daughter cells by cleaving the septum during proliferation. The absence of AmiA, AmiB, AmiC enzymes causes filamentation of *E. coli*¹²². Furthermore, they determine the shape and size of the bacterium; during growth PGHs ensure that the PG polymer can stretch around the bacterium and provide space for the integration of new PG¹²³. In *Bacillus subtilis*, single inactivation of the cwI or lytE endopeptidases causes shorter bacterial size, whereas the double mutant is non-viable¹²⁴. They also control the length of the glycan strands and the degree of the peptide cross-linking. These physical features influence the rigidity of the cell wall which can mean the survival of the bacterium in unfavorable conditions¹²¹. In addition, it has been demonstrated that *Pseudomonas aeruginosa* can deliver Tse1 and Tse3 PGHs by type VI secretion system to the enemy cell competing for the niche¹²⁵.

Beside their role in the degradation of PG, PGHs can be released into the environment by symbiotic bacteria. It has previously been reported that Msp1 (p40) and Msp2 (p75) enzymes from *L. rhamnosus* (renamed to *Lacticaseibacillus rhamnosus*) can prevent cytokine-induced apoptosis through stimulation of Akt protein in mouse and human IECs¹²⁶. Moreover, it has

been observed that p40 can limit epithelial cell injury and ameliorate inflammation in colitis via activation of EGF receptor¹²⁷. Besides, EGF receptor-dependent APRIL expression in IECs is also mediated by the *L. rhamnosus*-derived p40 and leads to IgA production¹²⁸. The homologues of these proteins were later found in the other two bacteria of the *L. casei* group, *L. casei* and *L. paracasei*^{129,130}. The p75 enzyme of the *L. casei* BL23 (Lc-p75) has a remarkable effect on the PG structure and bacterial morphology¹³¹. Lc-p75 is one of the main PGHs with γ -D-glutamyl-L-lysyl-endopeptidase activity. In the absence of Lc-p75, the proportion of disaccharide-dipeptide and acetylated disaccharide-dipeptide PG subunits are significantly reduced in Lc-p75 mutant *L. casei*¹³¹. Additionally, bacteria form long-chains because the septum between the daughter cells is not cleaved (**Figure 7**).

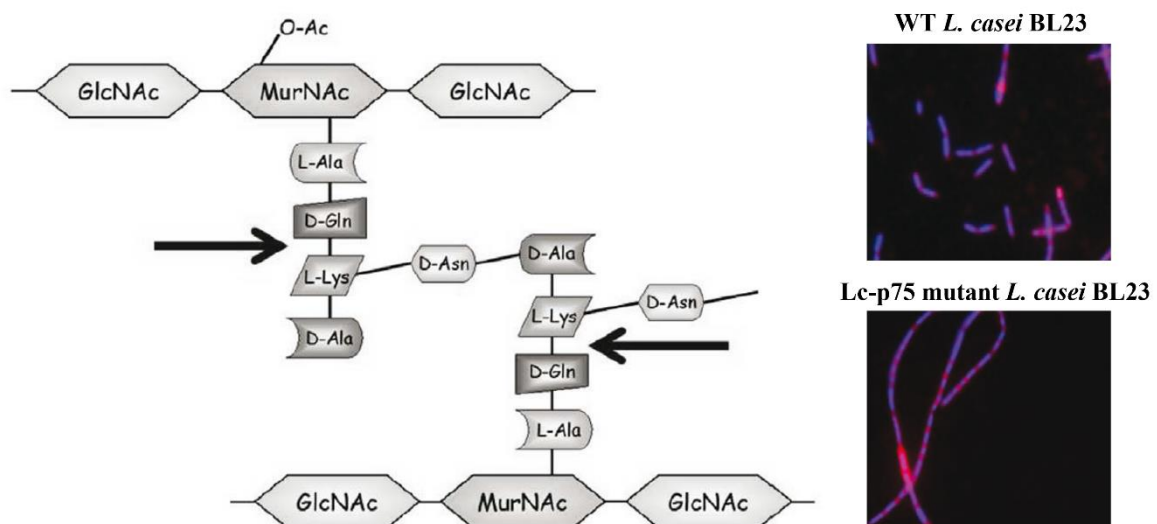


Figure 7. Structure of the *L. casei* BL23 PG with the cleavage site of the Lc-p75 enzyme and the morphology of the wild-type (WT) and Lc-p75 mutant *L. casei* BL23. Lc-p75 cleaves the peptide chain between the second (D-Gln) and third (L-Lys) amino acid (indicated by arrows), thereby playing a significant role in the septum cleavage upon proliferation. The absence of Lc-p75 PGH causes long-chain, filamentous phenotype in the mutant strains (below right) as compared to the WT (top right). Bacteria were stained with FM4-64 membrane dye and DAPI. Abbreviations: GlcNac: N-acetylglucosamine, MurNac: N-acetylmuramic acid, O-Ac: O-Acetylation, L-Ala: L-alanine, D-Gln: D-glutamic acid, L-Lys: L-lysine, D-Ala: D-alanine, D-Asn: D-asparagine¹³¹(modified).

3.8. The *Lactobacillus casei* group (LCG)

Lactobacilli are Gram+, rod-shaped, facultative anaerobic bacteria belonging to the LAB and efficiently colonizing the vertebrate intestinal system. The members of the LCG are widely used in daily life in dairy products or in fermented food productions¹³². Nevertheless, they are one of the most studied probiotic bacteria due to their health-related applications. It

has been demonstrated that the risk of allergy was decreased via early life colonization with LCG in 5-year-old children regardless of the allergic heredity¹³³. Furthermore, they exert favorable effects on gut-related diseases such as obesity and diarrhea¹³⁴. Besides, *L. rhamnosus* JB1 positively affects brain function via the vagus nerve. JB1 diminished the elevation of corticosterone induced by stress and influenced the expression of GABA receptors. Overall, these result in reduced depressive behavior and anxiety in mice¹³⁵. In the last decades, it has been reported by several studies that members of the LCG may have anti-cancer activities. It has recently been demonstrated that *L. casei* ATCC393 reduced the size of colon carcinoma by 80 %, adhered to the cancer cells and induced their apoptosis¹³⁶. LCG members are able to indirectly suppress tumor growth either by secreting mediators or via their immunomodulatory actions. In a study from 2020, the authors reported that *L. casei* HZ1 secreted LHH1, an AMP with strong antibacterial and antifungal activities, that exhibited anticancer properties against various immortalized cell lines¹³⁷. Additionally, in 2016 Lenoir et al. showed that *L. casei* BL23 protected the mice against experimentally-induced colorectal cancer via fine-tuning the regulatory and immunogenic Th responses¹³⁸. Furthermore, bacteria from LCG group have stimulatory effects on innate immune cells such as NK cells causing elevated cytotoxicity of these cells against the tumors. A proposed mechanism for how the LCG bacteria can indirectly instruct the NK cell-mediated cytotoxicity is the induced production of IL-12, a known NK cell-activating cytokine, by DCs and Mfs^{139,140}. Along with other microbiota members, LCG also contributes to colonization resistance and increased epithelial barrier integrity (**Figure 8**).

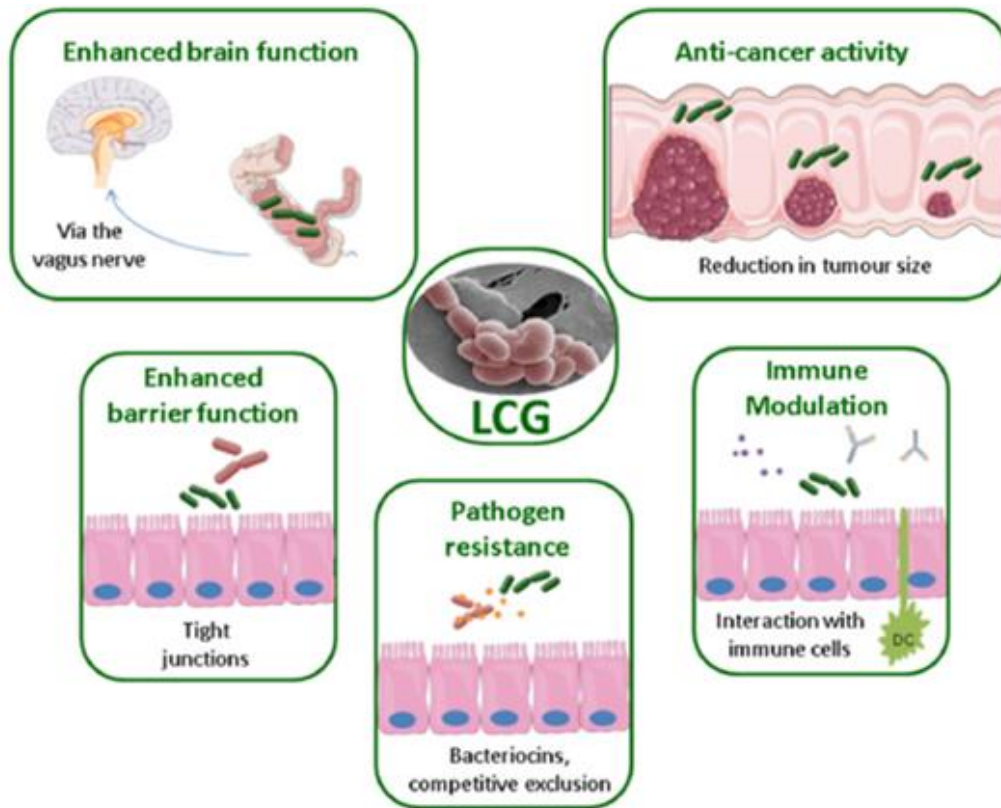


Figure 8. Modulatory activities exerted by the LCG members on the human host. As symbiotic bacteria, members of the LCG reside mainly in the human small intestines in which they contribute to the colonization resistance and make direct and indirect contacts with the host cells. These interactions result in benefits to the human host including enhanced brain functions and reduced depressive behavior, stronger barrier integrity, anti-cancer activities and immunomodulation¹³⁴.

3.9. Tumor-mediated actions affect the phagocytic efficiency and functions of myeloid cells

Myeloid-derived DCs and Mfs are professional phagocytic cells that are able to engulf tumor cells and present tumor-derived antigens. The CD141⁺ cDC1 subset is extremely effective in cross-presentation activating CD8⁺ cytotoxic T cells against the tumors¹⁴¹. One of the possible mechanisms hijacking immune recognition by tumor cells is the inhibition of their uptake by phagocytic cells. Among many phagocytosis inhibitory proteins or “don’t eat me” signals, including CD200, CD47 and the newly discovered CD24 are expressed by the tumor cells, whereas their interaction partners i.e., CD200R, SIRP α and Siglec10 are expressed by the phagocytic Mfs and DCs^{142,143}. The engagement can mediate the block of the inflammatory response and the uptake of the tumor cells. The pattern of the expressed don’t eat me signals is probably tumor specific¹⁴⁴.

Another escape mechanism of the tumor cells is modulating the differentiation of immune cells bearing suppressive features. To do so, monocytes are excellent candidates due

to their extremely high plasticity. In the tumor microenvironment monocytes are differentiated into tumor-associated macrophages (TAM) or DCs (**Figure 9**).

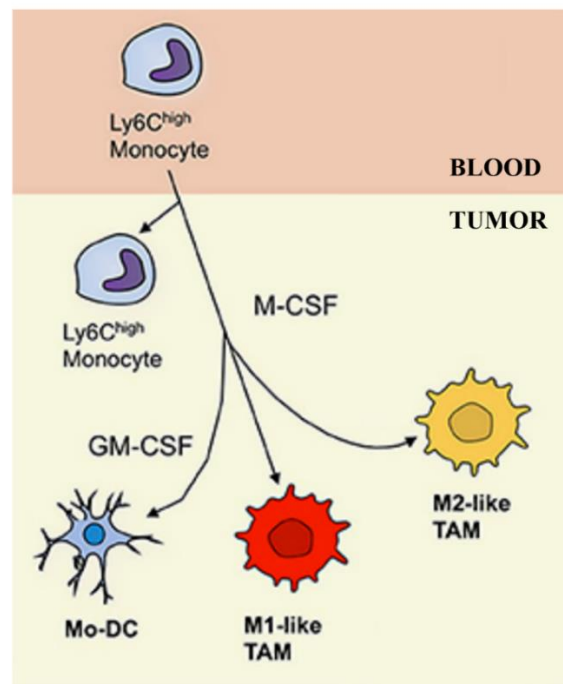


Figure 9. Ontogeny of tumor-associated monocyte-derived cells in mice. *Ly6C^{high} monocytes from the blood are recruited to the tumor site and differentiated to M1- or M2-like tumor-associated macrophages (TAMs) or monocyte-derived DCs (moDCs). For the differentiation of TAMs, M-CSF is needed, whereas moDC differentiation requires GM-CSF¹⁴⁵(modified).*

The differentiation of monocytes toward DCs can be modified by tumor-derived soluble factors. In a recent study with prostate cancer stroma-derived factors, monocyte-derived DCs (moDCs) expressed CD209/DC-SIGN, CD14 and the co-inhibitory molecule PD-L1 due to the actions of stroma-derived factors. These tumor-infiltrating DCs produced the immunoregulatory IL-10 cytokine but their IL-12 secretion was less prominent¹⁴⁶. Not only the differentiation, but the functions of the DCs are also modulated by the tumor-derived factors. For example, mucin-1 (MUC1) preferentially overexpressed by many tumors attracts IDC to the tumor site and induces the differentiation of a semimature DC subtype. In vitro, MUC1 promoted the expression of CD83, co-stimulatory CD80, CD86, CD40, and antigen-presenting MHCII by the moDCs. However, MUC1-exposed moDCs produced IL-6, TNF α and IL-10, but failed to secrete IL-12¹⁴⁷. Furthermore, many types of cancers release neuropeptides promoting tumor progression¹⁴⁸. Among them, substance P diminishes the phagocytic capacity of moDCs¹⁴⁹. However, the secreted soluble mediators exhibit extreme tumor-specificity.

4. AIMS OF THE STUDY

4.1. Part I. Analyzing the effects of human symbiont *L. casei* BL23 and its PG modifications on human moDC-mediated inflammatory and effector T-cell responses

The first interface between the symbiotic bacterium and host cells is the bacterial PG. Therefore, alterations in the PG structure may induce modified responses by the host's immune cells. In our work, we aspired to explore the modulatory mechanisms of PG-manipulated *L. casei* BL23 on human moDCs. We aimed to investigate:

- the inflammation-inducing potential of wild-type and Lc-p75 mutant *L. casei* BL23,
- the effect of wild-type and Lc-p75 mutant *L. casei* BL23 on the moDC's Th cell-stimulatory capacity,
- the impact of the PG's structural differences on its moDC-activating capacity,
- the importance of the morphological appearance in the induction of the moDC activation and the role of phagocytosis in the *L. casei*'s immunomodulation.

4.2. Part II. Studying the effects of different tumor cell line-derived soluble factors on the differentiation program and phagocytic potential of moDCs

Tumor-derived soluble factors influence the differentiation and functions of the DCs. However, the *in vitro* experimental systems to investigate and compare their modulatory effects are still incomplete. Our goal was to compare the effects of different adenocarcinoma- and melanoma cell line-derived soluble factors on the differentiation and function of moDCs as the followings:

- characterizing the phenotypic appearance of different tumor-promoted moDCs,
- investigating the phagocytic potential of moDCs differentiated in the presence of adenocarcinoma- and melanoma-derived conditioned media,
- finding potential correlations between the expression of different DC markers and phagocytic properties of the moDC.

5. MATERIALS AND METHODS

5.1. Bacterial strains and growth conditions

L. casei BL23 and its Δ Lc-p75 mutant derivative obtained by deletion of *lcabl_02770* gene encoding the Lc-p75 PGH were used in this study provided by Dr. Marie-Pierre Chapot-Chartier. They were inoculated from frozen glycerol stocks on MRS agar plates and cultured at 37°C for 48 h to obtain isolated colonies. Single colonies were diluted in MRS broth (BD Difco, Fisher Scientific, Co.L.L.C, PA, US) and propagated for 16 h at 37°C until the beginning of the stationary phase. Fluorescent mCherry strains were obtained by transformation with a plasmid encoding red fluorescent mCherry protein (pTS-mCherry; kind gift of Jerry M. Wells, Wageningen University, the Netherlands). The fluorescent strains were cultured with 5 μ g/ml erythromycin (Merck KGaA, Darmstadt, Germany) added to MRS medium to select the plasmid. Optical density (OD) of 1 at 600 nm corresponds to 2.5×10^8 cells per ml for the wild-type *L. casei* BL23 strain, as calculated from the dilution series of liquid bacterial culture and colony counting.

To verify that the same OD values for cell suspensions of the long-chain forming mutant or WT strain correspond to similar numbers of bacterial cells (**Figure 10A**), after a 16-h cultivation period, bacteria in suspension at various OD_{600nm} were stained with 4',6-diamidino-2-phenylindole (DAPI), a fluorescent DNA dye, and the bacteria-associated fluorescence was measured. We observed that for both strains, the OD_{600nm} values were perfectly correlated with the fluorescence intensity level and thus with the cell number (**Figure 10B**).

The cultivation of the bacteria was performed by the author of the thesis, and the determination of the correspondence between OD values and bacteria number was carried out by Dr. Krzysztof Regulski at INRA Institute, France.

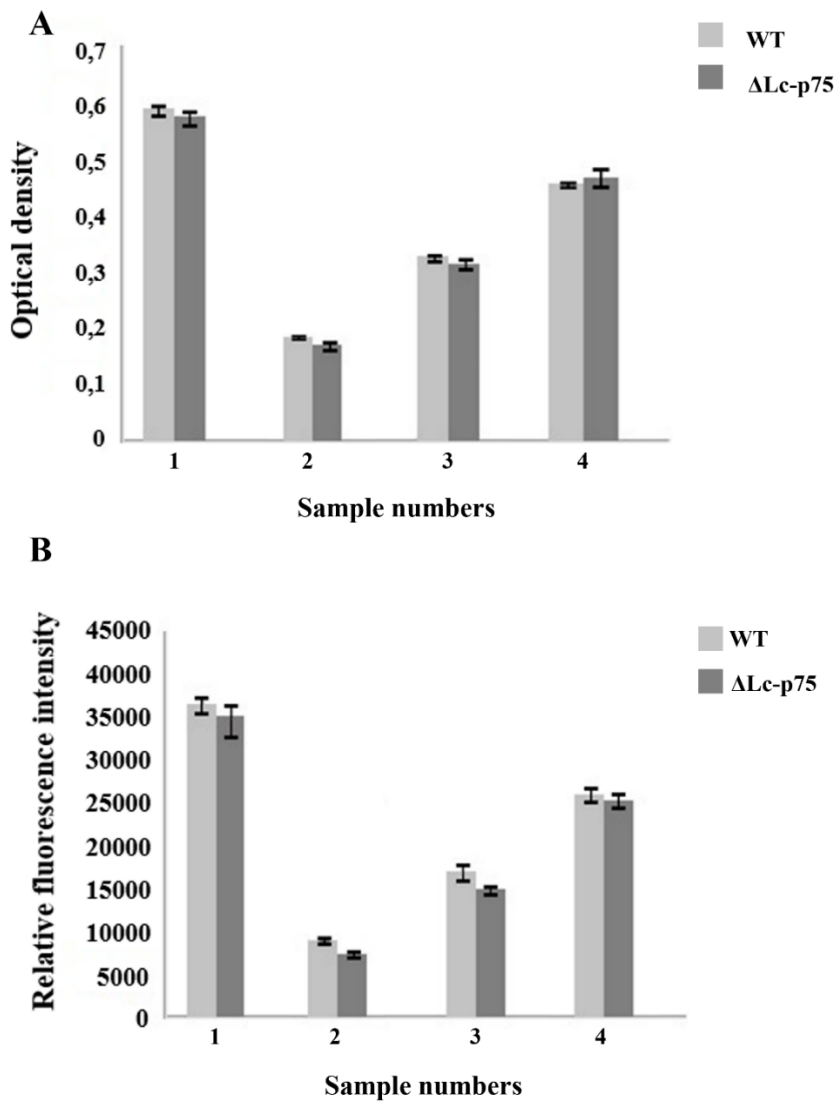


Figure 10. Correspondence between OD_{600nm} of bacterial suspension and bacteria number as detected by DAPI staining for WT *L. casei* BL23 and its *Lc-p75* mutant counterpart. OD_{600} values (A) and relative fluorescence intensity (B) after DAPI staining were detected at the same time, after 16 h of culturing for each sample (numbered 1 to 4) and strain using a Tecan Infinite M200 multimode microplate reader.

5.2. Extraction of peptidoglycan

PG was extracted from *L. casei* strains as previously described with some modifications¹³¹. Cells from a 500 ml exponentially growing culture (OD_{600} , 0.3) were chilled on ice and collected by centrifugation. Cells were suspended in deionized H_2O and boiled for 10 min. They were then resuspended in 5% (w/v) SDS in 50 mM Tris-HCl pH 7.0 and boiled for 25 min. The pellet obtained by centrifugation at $20,000 \times g$ for 10 min, was resuspended in 4% (w/v) SDS in Tris-HCl buffer and boiled again for 15 min. Cell walls were recovered by centrifugation at $20,000 \times g$ for 10 min and washed six times with deionized H_2O to remove

SDS. The cell wall pellet was then treated with Pronase (2 mg/ml) for 90 min at 60°C, by α -amylase (50 μ g/ml) for 2 h at 37°C, by DNase (50 μ g/ml) and RNase (50 μ g/ml) for 4 h at 37°C, and lipase (50 μ g/ml) and finally by trypsin (200 μ g/ml) for 16 h at 37°C. The final pellet was then treated with 2% SDS in Tris-HCl (50 mM pH 7.0.) and washed with deionized H₂O. The insoluble pellet was treated with 48% hydrofluoric acid overnight at 4°C to remove wall polysaccharides. After centrifugation, the pellet (containing PG) was washed several times with 0.25 M Tris-HCl (pH 7.0) and deionized H₂O. The final pellet was lyophilized and stored at -20°C.

PG was extracted by Dr. Krzysztof Regulski at INRA Institute, France.

5.3. Human monocyte separation and differentiation to dendritic cells

Leukocyte-enriched buffy coats were obtained from healthy blood donors and drawn at the Regional Blood Center of the Hungarian National Blood Transfusion Service (Debrecen, Hungary) in accordance with the written endorsement of the Director of the National Blood Transfusion Service (OVSzK 3572-2/2015/5200) and the Regional and Institutional Research Ethical Committee of the University of Debrecen, Faculty of Medicine (Debrecen, Hungary). Written informed consent was collected from the blood donors prior to blood donation; their data were processed and stored in accordance with the directives of the European Union.

PBMCs were isolated from buffy coats using a Ficoll-Paque Plus (Amersham Biosciences, Uppsala, Sweden) density gradient centrifugation. Monocytes were purified from PBMCs by magnetic cell separation by applying CD14-specific antibody-coated microbeads and a VarioMACS magnet following the manufacturer's instruction (MiltenyiBiotec, Bergisch Gladbach, Germany). The homogeneity of the isolated CD14⁺ monocytes was greater than 90-95% in all experiments. The autologous monocyte depleted peripheral blood lymphocytes (PBL) fraction was used as a T cell source in the ELISpot assays.

For the experiments with wild-type (WT) and Lc-p75 mutant *L. casei*, isolated monocytes were seeded at 1×10^6 /ml concentration in serum-free AIM-V medium (Thermo Fisher Scientific, Waltham, MA, USA) complemented with 100 ng/ml IL-4 (PeproTech EC, London, UK) and 80 ng/ml GM-CSF (Gentaur Molecular Products, Brussels, Belgium) and were differentiated to moDCs for 5 days. Half of the medium was changed on day 2, supplemented with 100 ng/ml IL-4 and 80 ng/ml GM-CSF. When indicated, moDCs were pretreated with 15 μ M Cytochalasin D (CyD, Merck KGaA) dissolved in dimethyl-sulfoxide (DMSO, Serva Electrophoresis GMBH, Germany) for 30 min to block the phagocytosis. DMSO was used as vehicle control.

Purified monocytes were seeded for four days at a density of 1.5×10^6 /ml concentration in RPMI1640 medium (Merck KGaA) supplemented with 10% fetal calf serum (FCS, Thermo Fisher Scientific) and 1% antibiotic/antimycotic solution (Hyclone, Shrewsbury, MA, USA) or in the presence of tumor cell line-derived conditioned media (TU-CM) at a ratio of 1:1. The medium also contained 100 ng/ml IL-4 (PeproTech) and 80 ng/ml GM-CSF (Gentaur Molecular Products). When indicated, 0.25 μ M dexamethasone (Merck KGaA) was added to the monocyte cultures generating monocyte-derived dexamethasone DCs (dexDCs) which are considered to be regulatory DCs^{150,151}.

Isolation and differentiation of the monocytes to DCs and the blocking of the phagocytosis were performed by the author of the thesis. Monocyte separation and differentiation to DCs in the presence of tumor cell line-derived conditioned media (TU-CM), as well as generation of dexDCs were carried out by Dr. Anett Türk-Mázló.

5.4. Maintenance of the tumor cell lines and generation of tumor cell line-derived conditioned media

MDA-MB231 (human breast adenocarcinoma), HeLa (human cervical adenocarcinoma), HT29 (human colorectal adenocarcinoma), WM278 (primary melanoma), WM1617 (metastatic counterpart of WM278 melanoma), WM983A (primary melanoma) and WM983B (metastatic counterpart of WM983A melanoma) were maintained in RPMI 1640 medium complemented with 10% FCS and 1% antibiotic/antimycotic solution.

Supernatants were discarded from the cell lines; cells were washed, and media were replaced by fresh ones. Cultures were rested for 48 h. TU-CM were harvested and spun at 3000 rpm for 5 min. The collected TU-CM was used in the differentiation process of monocytes to dendritic cells.

Maintenance of the tumor cell lines, and generation of TU-CM were carried out by Dr. Anett Türk-Mázló.

5.5. Activation of moDCs with bacteria or their derived PG fragments

On day 5 of *in vitro* moDC differentiation, bacteria were washed twice with cold PBS and were added to the moDCs at a ratio of 1 (moDC): 4 (bacteria) for the indicated incubation periods. Untreated moDCs (IDC-immature DC) were used as a control.

Purified bacterial PG samples were resuspended in deionized water and sonicated with Branson Sonifier 450 until they became clear. 10 μ g/ml PG fragments were used to activate the moDCs for 24 h. Each experiment was repeated with at least three independent donors.

Activation of the moDCs either with bacteria or PG fragments was performed by the author of the thesis.

5.6. Analysis of the cell surface marker expression and viability of dendritic cells by flow cytometry

After a 24-h stimulation of moDCs by bacteria, cells were stained with fluorescence-conjugated monoclonal antibodies: CD83-fluorescein isothiocyanate (FITC), CD80-FITC, CD86-phycoerythrin (PE) and human leukocyte antigen- (HLA) DQ-FITC (BioLegend, San Diego, CA, US) or left unlabeled as a control.

For the TU-CM experiments moDCs were stained with anti-human CD14-FITC, CD209/DC-SIGN-PE, CD1a-FITC, CD1d-Peridinin-Chlorophyll-Protein (PerCP), CD86-PE, PD-L1-PE, HLA-ABC-FITC, and HLA-DR-FITC.

Non-specific antibody binding was blocked using heat-inactivated mouse serum. The moDC population was gated according to the forward/side scatter parameters. Fluorescence intensities were measured by an ACEA NovoCyte 2000R cytometer (Agilent, Santa Clara, CA, US); data analyzes were performed using the FlowJo vX.0.7 software (Tree Star Inc., Ashland, OR, US). Viable and nonviable cells were dissected by flow cytometry after labeling the freshly collected, non-fixed cells with 0.5 µg/ml 7-Amino-actinomycin D (7-AAD) (Merck KGaA).

Flow cytometric measurements were performed by the author of the thesis regarding the experiments with bacteria, whereas phenotypic changes of TU-CM educated moDCs were measured by Dr. Anett Türk-Mázló.

5.7. Cytokine and chemokine measurements by enzyme-linked immunosorbent assays (ELISA)

Supernatants of stimulated moDCs were harvested after 24 h and the concentrations of IL-1β, IL-6, TNF-α, IL-12p70, IL-10, IL-23, and IL-8 were measured using BD OptEIA ELISA kits following the manufacturer's instructions (Becton Dickinson, BD Biosciences, US). OD was detected at 450 nm on a SynergyTM HT Multi-Detection Microplate reader (Bio-Tek Instruments, VT, USA) and KC4 v3.4 software. Data were evaluated using Microsoft Excel.

ELISA analyses were carried out by the author of the thesis.

5.8. Enzyme-linked immunospot (ELISpot) assays

Bacteria-stimulated moDCs were counted, washed and co-cultured with autologous PBL at a ratio of 1:20 for 3 days at 37°C in a 5% CO₂ atmosphere in AIM-V medium. On day

4, cells were harvested, counted, and subjected to IFN γ , IL-17A and IL-4 Ready Set Go ELISpot assays according to the instructions of the manufacturer (eBioscience, San Diego, CA, USA). Unstimulated moDCs and PBL cultures alone served as negative controls. Briefly, 3×10^5 cells/well were seeded in CTL-Test medium (Cellular Technology Limited, Cleveland, OH, USA) for 40-48 h at 37°C to the MultiScreen-HTS PVDF plates (Millipore S.A., Molsheim, France) pre-coated with IFN γ -, IL-4-, or IL-17A-specific capture antibodies. 0.5 μ g/ml purified anti-human CD3 antibody (BD Biosciences) was added to the coating buffer containing the IL-4- and IL-17A-specific capture antibodies for the mitogenic stimulation of CD3⁺ T cells. Identification of the cytokine release was performed by biotinylated IFN γ , IL-4, or IL-17A-specific antibodies in the presence of horseradish peroxidase enzyme (HRP) conjugated to streptavidin. Then the colorigenic substrate, 3-amino-9-ethylcarbazole (AEC Substrate Set, BD Biosciences) was added to the plates. Color development was stopped by tap water, and air-dried plates were evaluated by a computer-assisted ELISpot image analyzer (Series 1 ImmunoSpot Analyzer, ImmunoSpot Version 4.0 Software Academic, Cellular Technology Limited, Shaker Heights, OH, USA).

ELISpot assays were performed by the author of the thesis.

5.9. Phagocytosis assay by flow cytometry

To assess the differences between the uptake of WT and Lc-p75 *L. casei* by moDCs, the cells and mCherry-expressing bacteria were co-incubated at a ratio of 1:4 for 3 or 24 h at 37°C in a 5% CO₂ atmosphere or on ice as a control. After the incubation periods, moDCs were labeled with allophycocyanin (APC)-conjugated anti-CD1a monoclonal antibody (BioLegend, San Diego, CA, US).

To test the phagocytic capacity of the different TU-CM-educated moDCs, the cells and mCherry-expressing WT *L. casei* were co-incubated at a ratio of 1:4 for 4 h at 37°C and 4°C. Unstimulated moDCs and dexDCs were used as controls.

Fluorescent intensities were measured using ACEA NovoCyte 3000 RYB flow cytometer (Agilent). Data were analyzed by the FlowJo vX.0.7 software. The moDC population was gated according to the forward/side scatter parameters by excluding the non-internalized bacteria. The frequency of phagocytic cells was determined as a percentage of mCherry-positive cells or according to the median values of mCherry fluorescence intensity (MFI). Similarly, the ratio of the bacteria internalization was determined in the CD1a⁺ and the CD1a⁻ moDC subpopulations as a percentage of mCherry positive cells.

Phagocytosis assays were carried out by the author of the thesis regarding the experiments with bacteria, whereas TU-CM educated moDCs were investigated by Dr. Anett Türk-Mázló.

5.10. Confocal microscopy

To identify the localization of the internalized bacteria inside the moDCs, confocal microscopic analysis was performed. Zeiss LSM 880 confocal laser scanning microscope (Carl Zeiss, Oberkochen, Germany) equipped with 40x water immersion objective (NA 1.2) was applied to illustrate the uptake of WT *L. casei* by TU-CM-conditioned moDCs after 4 h and the phagocytosis of WT and Lc-p75 mutant *L. casei* cells by moDCs after 24 h. For the excitation of DAPI a 405 nm diode laser; for FITC the 488 nm line of an Argon ion laser; for mCherry a 543 nm He-Ne laser and for APC a 633 nm He-Ne laser was used. Fluorescence emissions of DAPI and FITC were detected in the wavelength range of 410-485 and 490-610 nm, respectively, while the detection of mCherry was executed with 575-695 nm band-pass filter. For the detection of APC, 640-745 nm band-pass filter was used. Z-stack images were collected at 1 μm intervals from the bottom to the top of the cells. Images, montage, and orthogonal views were visualized using ImageJ 1.53c (Wayne Rasband, National Institute of Health, USA) based on Java 1.8.1_172.

Confocal microscopic measurements were carried out by Dr. Tímea Szendi-Szatmári, whereas the visualization of the images was performed by the author of the thesis.

5.11. Bioinformatical analyses for generation of heatmaps and correlograms

Bioinformatical analyses were performed using R (version 4.1.3) and RStudio (version 1.4.1717). The expression data of cell surface markers and phagocytosis data were included in the dataset. Heatmaps were visualized with *pheatmap* function of *pheatmap* package (version 1.0.12). Values were normalized using z-score and scaled by the columns. Correlation matrices were calculated using *cor* function of the *base* RStudio package (version 4.1.3). Correlograms from correlation matrices were plotted by *ggcorrplot* library (version 0.1.3) with *ggcorrplot* function.

Bioinformatical analyses were performed by the author of the thesis.

5.12. Statistical analyses

Plotting the data and statistical analyses were performed using GraphPad Prism v8.0 (GraphPad Software Inc., San Diego, CA, USA). Two groups were compared with paired, two-tailed Student's t test. Comparison of more than two groups was performed by One-way

ANOVA followed by Tukey's post hoc test. Comparison of two independent variables was executed by Two-way ANOVA followed by Tukey's post hoc test. Results are displayed as mean \pm standard deviation (SD). Differences were statistically significant at $p < 0.05$. Significance was determined as * $p < 0.05$; ** $p < 0.01$, *** $p < 0.001$; **** $p < 0.0001$ or as # $p < 0.05$; ## $p < 0.01$, ### $p < 0.001$; #### $p < 0.0001$.

Statistical analyses were carried out by the author of the thesis regarding the bacterial experiments, whereas data from experiments with TU-CM were analyzed by Dr. Anett Türk-Mázló.

6. RESULTS

6.1. Part 1. Analyzing the effects of human symbiont *L. casei* BL23 and its PG modifications on human moDC-mediated inflammatory and effector T-cell responses

6.1.1. *L. casei* Δ Lc-p75 mutant bacteria can not alter the moDC activation program but influence the inflammatory cytokine production by moDCs

Since Lc-p75 is one of the major PGHs in *L. casei* BL23, its absence leads to aberrant peptidoglycan structure and morphology¹³¹ as compared to rod-shaped wild-type bacteria (**Figure 11**).

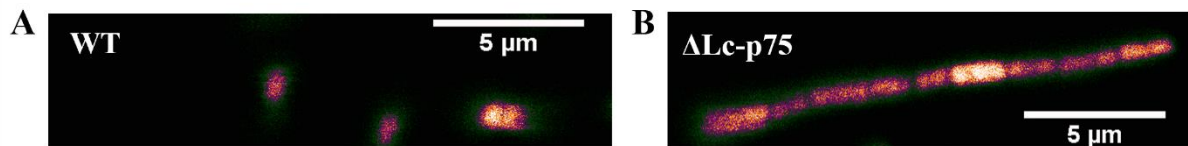


Figure 11. The absence of Lc-p75 PGH modifies the morphology of *L. casei* BL23. Confocal microscopic pictures about mCherry-expressing wild-type (WT) (A) and Lc-p75 mutant (B) *L. casei* were taken by Zeiss LSM 880 confocal laser scanning microscope with 40x objective.

Bacterial PG, a major structural cell wall component originating from pathogens or probiotic bacteria triggers DC activation. Therefore, we investigated firstly the moDC-activating capacity of WT and Δ Lc-p75 mutant *L. casei*. CD83 is a membrane-bound molecule whose expression is strongly correlated to the maturation status of moDCs. In our system, both *L. casei* strains induced the appearance of CD83 molecule on the surface of the moDCs regardless of the bacterial PGH mutation (**Figure 12A, 12B**).

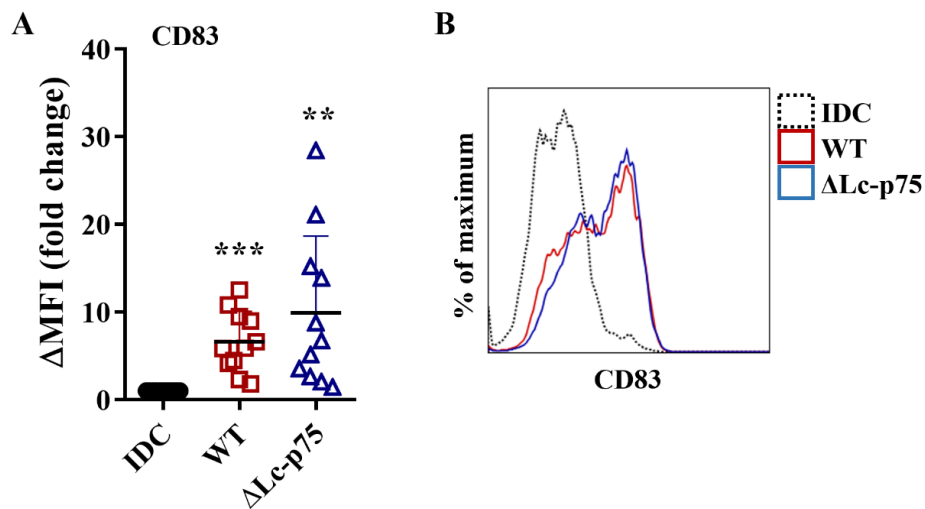


Figure 12. WT and Lc-p75 mutant *L. casei* BL23 increase the CD83 expression by bacteria-exposed moDCs regardless of the mutation. Five-day moDCs were activated with wild-type (WT) and mutant *L. casei* at a ratio of 1:4 for 24 h. Expression of CD83 was detected by flow cytometry. Fold change of median fluorescence intensity (MFI) compared to the unstimulated, control moDCs (IDC) was calculated from 11 independent donors indicated by black circles, red squares, and blue triangles \pm SD (A). Histograms show one representative experiment (B). Student's paired two-tailed *t*-test was used for statistical analysis with significance determined as * $p < 0.05$, ** $p < 0.01$, and *** $p < 0.001$ as compared to IDC.

Next, we tested the pro-inflammatory cytokine and chemokine secretion by bacteria-exposed moDCs. In contrast to the CD83 expression, we found significant differences between the WT and mutant *L. casei* strains in the induction of TNF- α , IL-1 β and IL-6 secretion by moDCs. Co-incubation with WT bacteria induced significantly higher inflammatory cytokine release from moDCs (Figure 13A). Interestingly, the production of the inflammatory chemokine, IL-8 did not show the same pattern as the cytokines; IL-8 secretion was triggered by both *L. casei* strains at the same efficiency (Figure 13B).

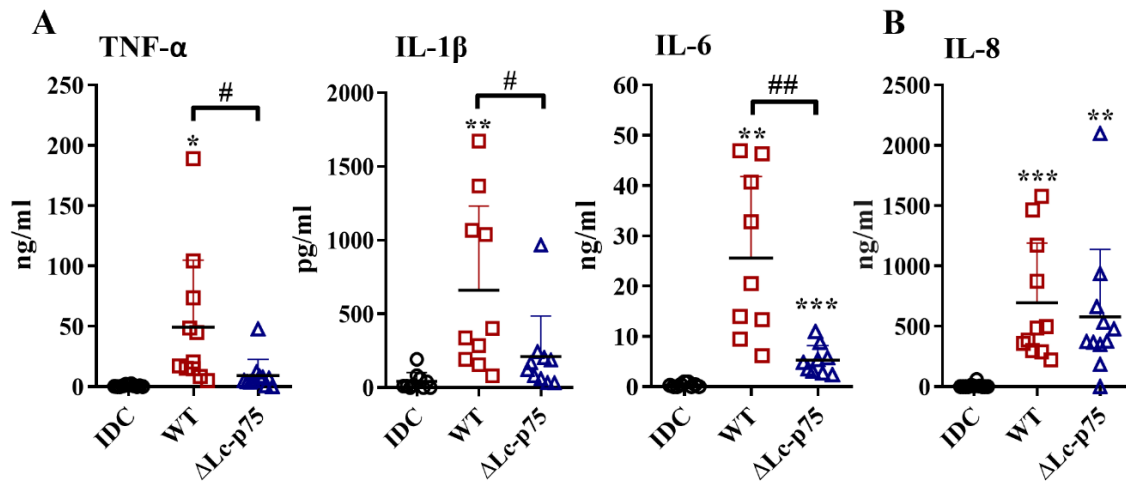


Figure 13. Deletion of Lc-p75 PGH influences the pro-inflammatory cytokine production but not IL-8 secretion by bacteria-exposed moDCs. Five-day moDCs were incubated with wild-type (WT) and Lc-p75 mutant *L. casei* for 24 h at a ratio of 1:4 and the concentration of TNF- α , IL-1 β , IL-6 (A) and IL-8 (B) was measured by ELISA from the collected supernatants of the moDC cultures. Figures show the individual donors (black circles, red squares, and blue triangles) and the mean of 9-11 independent experiments \pm SD. Statistical analysis was executed by paired, two-tailed Student's *t*-test with significance defined as * $p < 0.05$, ** $p < 0.01$ and *** $p < 0.001$ as compared to IDC. The difference between WT and Δ Lc-p75 was statistically significant determined as # $p < 0.05$ and ## $p < 0.01$.

To confirm, that the discrepancy between the WT and Δ Lc-p75 *L. casei* in moDC-activating capacity was not the consequence of the distinct levels of bacteria-induced cell death, we detected the frequency of dead moDCs using flow cytometry. Importantly, we could not distinguish significant changes in the dead cell frequency between the two bacteria-exposed moDC cultures and between the bacteria-exposed and unstimulated moDCs (Figure 14A, 14B).

These results suggest, that Lc-p75 deficient *L. casei* with abnormal cell wall structure and morphology induces a diminished inflammatory response by moDCs.

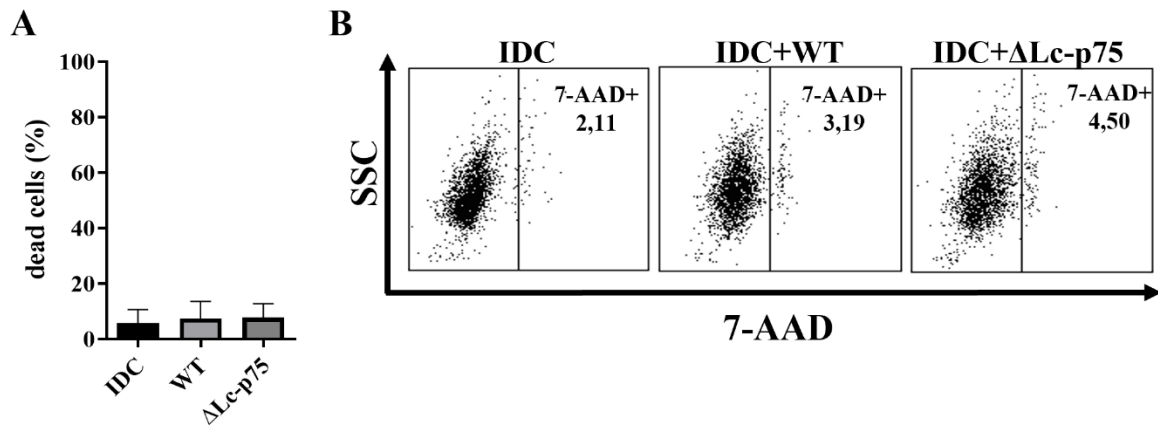


Figure 14. Exposure to WT and Lc-p75 mutant *L. casei* does not affect the viability of moDCs. After 5 days of in vitro moDC differentiation, the cells were exposed to wild-type (WT) *L. casei* and its Lc-p75 PGH mutant derivative for 24 h at a ratio of 1:4. Unstimulated moDCs (IDC) were used as a negative control. Frequency of dead cells was defined using 7-AAD fluorescent dye by flow cytometry (A). Dot plots show one representative experiment (B). Mean values were calculated from the results of 4-6 independent experiments \pm SD. Paired, two-tailed Student's *t*-test was used for the statistical analysis.

6.1.2. Absence of Lc-p75 in *L. casei* does not influence the antigen presentation and co-stimulation but promotes an attenuated T-cell response by bacteria-exposed moDCs

Immature, tissue-resident dendritic cells after pathogen recognition transform into powerful antigen-presenting, mature DCs which have the characteristics essential for the activation and polarization of Th cells in distinct directions. During the migration to the secondary lymphoid organs, DCs process the pathogens and increase the expression of MHCII and co-stimulatory molecules to activate naïve Th cells. Hence, the elevated level of HLA-DQ and CD80 and CD86 co-stimulatory molecules is considered a valuable marker of the stimulated, capable-of-T-cell-activation status of the DCs. In our experimental system, both *L. casei* strains induced increased expression of HLA-DQ, CD80, and CD86 molecules on the moDC surface independently of the bacterial PGH mutation (**Figure 15A, 15B**).

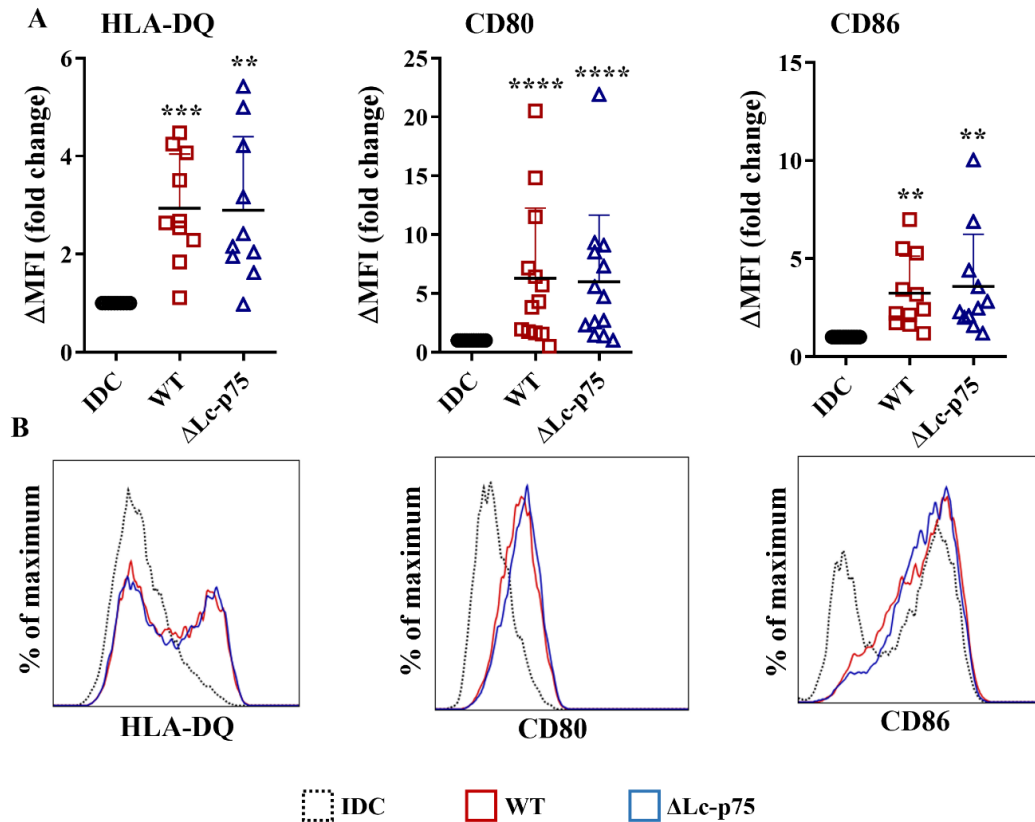


Figure 15. The absence of Lc-p75 PGH does not affect the antigen-presenting and co-stimulatory ability of bacteria-exposed moDCs. Five-day moDCs were exposed to wild-type (WT) and Lc-p75 mutant *L. casei* at a ratio of 1:4 for 24 h. The expression of HLA-DQ, CD80 and CD86 (A) was measured by flow cytometry. Fold change of MFI compared to the unstimulated, control moDCs was determined from 10-13 experiments \pm SD. Individual donors are represented with black circles, red squares, and blue triangles. Histogram overlays display one representative experiment (B). Student's paired two-tailed *t*-test was used in the statistical analysis with significance defined as * $p < 0.05$, ** $p < 0.01$ and *** $p < 0.001$ compared to IDC.

Besides the antigen presentation and co-stimulation, moDCs have to secrete soluble mediators to determine the direction of the naïve T-cell polarization. Similar to the inflammatory cytokines, WT bacteria caused elevated IL-10, IL-12 and IL-23 T-cell polarizing cytokine secretion by moDCs as compared to their mutant counterpart (Figure 16).

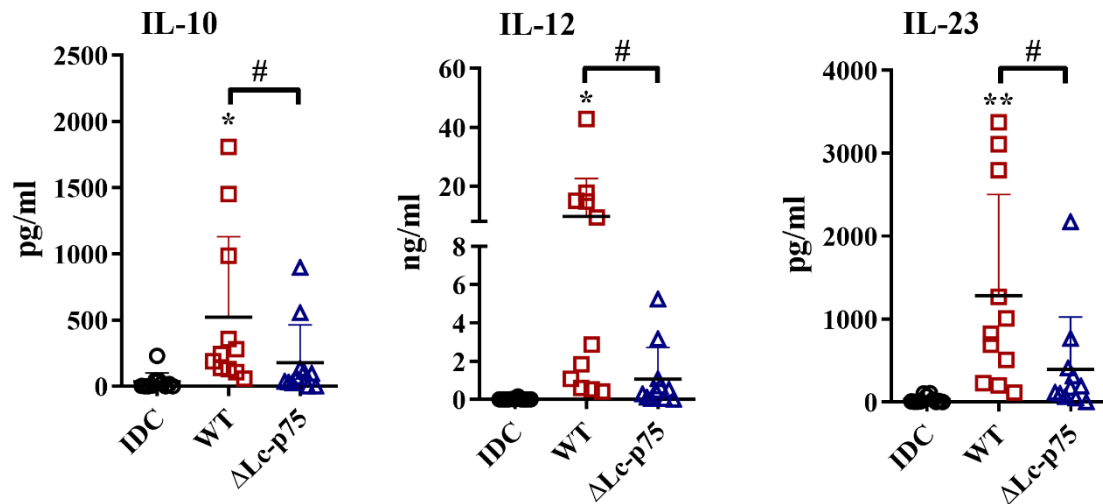


Figure 16. Lacking Lc-p75 PGH in *L. casei* diminishes the T-cell polarizing cytokine secretion by bacteria-exposed moDCs. Five-day moDCs were exposed to wild-type (WT) and Lc-p75 mutant *L. casei* at a ratio of 1:4 for 24 h. After collecting the cultures' supernatants, ELISA was used to measure the concentration of IL-10, IL-12 and IL-23 cytokines. Individual donors are represented by different types of glyphs (black circles, red squares, and blue triangles). Figures display the mean of 10-11 independent experiments \pm SD. Student's paired two-tailed t-test was used in the statistical analysis with significance illustrated as * $p < 0.05$ and ** $p < 0.01$ compared to IDC and # $p < 0.05$ between WT and Δ Lc-p75.

To get insight into how the discrepancy between the cell surface molecule expression and T-cell polarizing cytokine secretion is translated to the Th-cell responses, we cocultured bacteria-exposed moDCs with autologous PBLs. After 3 days T cells were subjected to IFN γ -, IL-17A-, and IL-4-specific ELISpot assays. We found that moDCs exposed to both *L. casei* strains increased the IFN γ - and IL-17A-producing T-cell numbers and the percentage of spot-covered well areas in comparison with unstimulated moDCs (**Figure 17A, 17B, 17C, 17D**). Prestimulation of moDCs with Lc-p75 mutant *L. casei* led to the reduction of IFN γ -secreting T-cell number and smaller area of spots compared to preactivation with WT *L. casei* (**Figure 17A, 17B**). Similarly, a significantly lower IL-17A-secreting T-cell number and less extensive spot-covered well area were promoted by moDCs pretreated with Lc-p75-defective bacteria in comparison with WT bacteria-exposed moDCs (**Figure 17C, 17D**). In contrast, a significant reduction in the IL-4-producing T-cell number and area coverage were induced by moDCs activated with *L. casei* strains compared to unstimulated moDCs regardless of the PGH mutation (**Figure 17E, 17F**). These results indicate that the Lc-p75 defective *L. casei* causes dampened Th1 and Th17 responses via the attenuated T-cell-polarizing cytokine secretion by the moDCs.

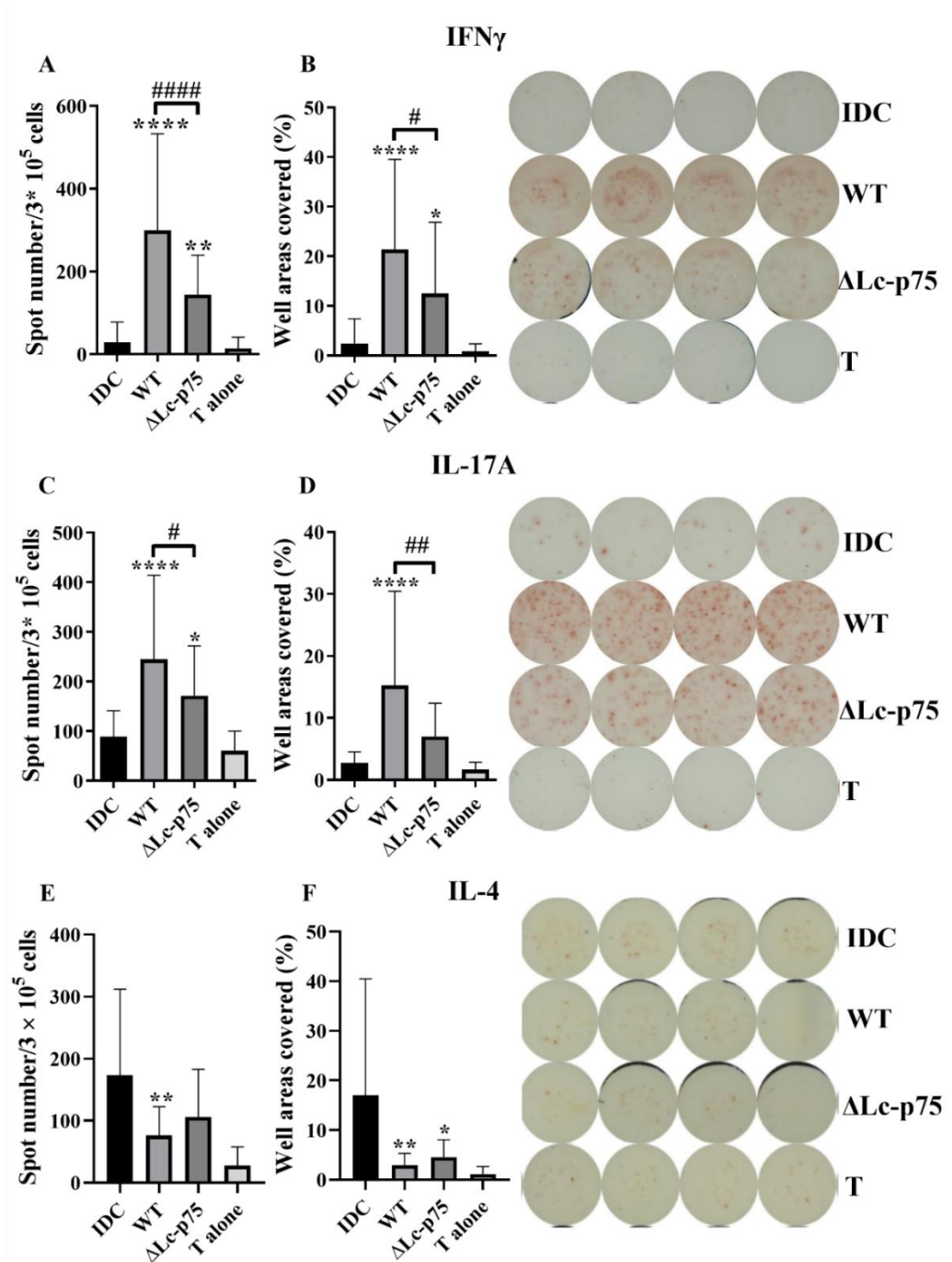


Figure 17. Removal of Lc-p75 PGH in *L. casei* BL23 affects the Th1- and Th17-polarizing capacity of bacteria-exposed moDCs but does not influence the Th2 activation by these cells. Wild-type (WT) and Lc-p75 mutant *L. casei*-exposed moDCs were washed, counted, and co-incubated with autologous T cells at a ratio of 1:20 for 3 days. The frequency of IFN γ - (A, B), IL-17A- (C, D), and IL-4-producing (E, F) T-lymphocytes was detected by ELISpot assays. The number of spots was counted, and the spot-covered area was calculated using a computer-assisted ELISpot image analyzer. The mean value of spot numbers (A, C, E) and well areas covered (B, D, F) were determined from 5 experiments with 4-6 parallel wells \pm SD. One-way ANOVA followed by Tukey's multiple comparison test was applied for statistical analysis. Significance is defined as * $p < 0.05$, ** $p < 0.01$, and **** $p < 0.0001$ compared to unstimulated, control samples (IDC). The differences between WT and Δ Lc-p75 were statistically significant described as # $p < 0.05$ and ## $p < 0.01$ and #### $p < 0.0001$.

6.1.3. Purified peptidoglycan extracted from WT or Lc-p75 mutant L. casei demonstrates similar moDC-activating potential

Lc-p75 deficiency causes modified composition and structure of the peptidoglycan, and aberrant bacterial morphology. Based on the above-detailed results, we raised the question whether the different moDC-activating potential of WT and Lc-p75 mutant strains is the straightforward consequence of the altered cell wall structure or indirectly connected to the transformed, long-chain forming morphology. Hence, we performed peptidoglycan purification derived from WT and Lc-p75 mutant *L. casei* strains and examined their moDC-activating capacity. Elevated pro-inflammatory TNF- α , IL-1 β and IL-6 production was observed by moDCs activated with PG preparations from both *L. casei* strains (**Figure 18A**). Similarly, PG from *L. casei* strains induced increased T-cell polarizing IL-10, IL-12, and IL-23 secretion by moDCs regardless of the PGH mutation (**Figure 18B**).

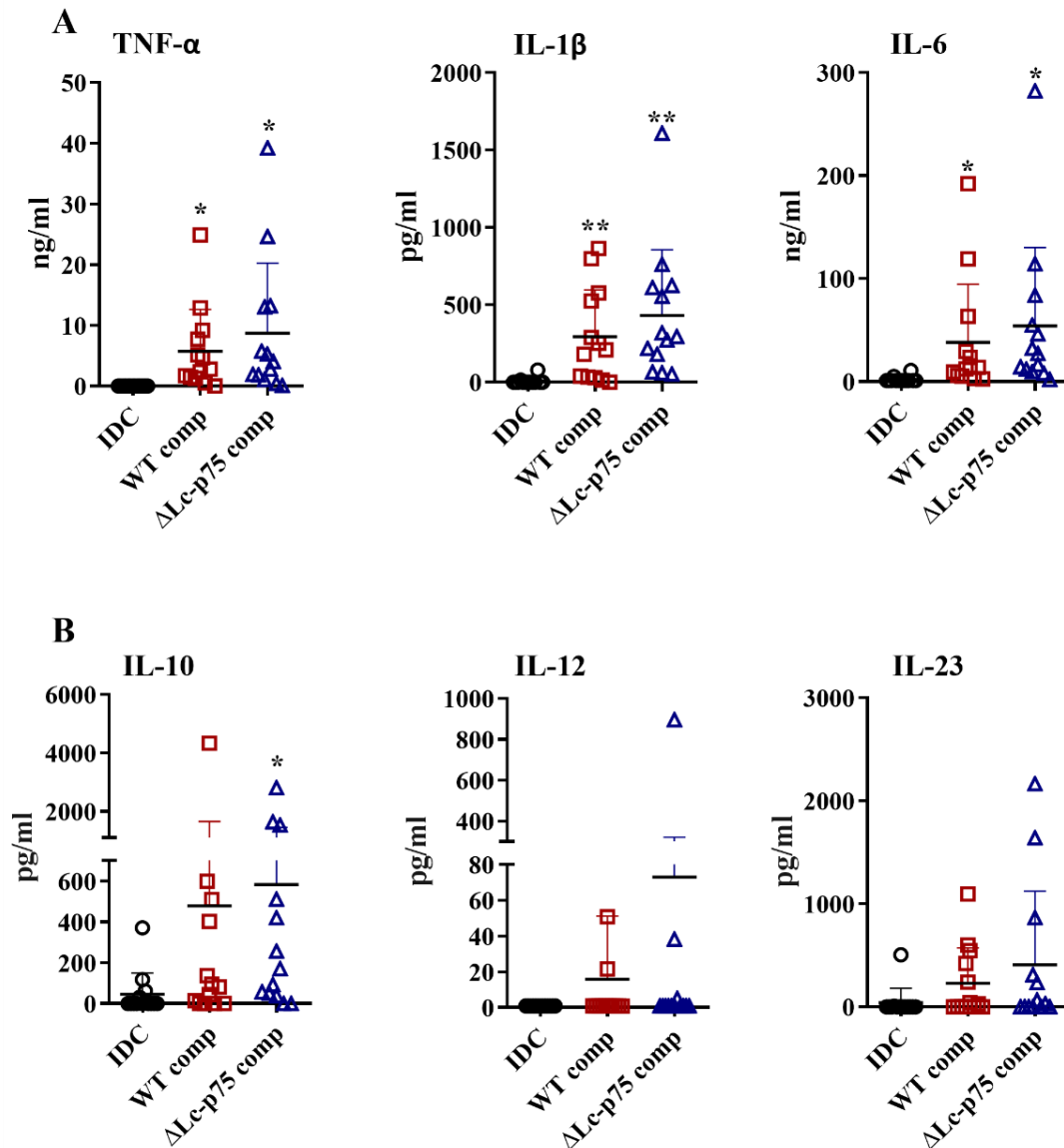


Figure 18. PG extracts derived from wild-type (WT) and Lc-p75 mutant *L. casei* strains promote elevated cytokine secretion by moDCs regardless of the PGH deletion. Five-day moDCs were activated with 10 μ g/ml purified PG components with both *L. casei* strains for 24 h. ELISA was used to determine the concentration of pro-inflammatory TNF- α , IL-1 β , and IL-6 cytokines (A) and of IL-10, IL-12, and IL-23 T-cell-polarizing cytokines (B) from the collected culture supernatants. Each glyph (black circles, red squares, and blue triangles) illustrates one individual donor. The mean of the concentration values was calculated from 11-13 experiments. Paired, two-tailed Student's *t*-test was applied in the statistical analysis with significance determined as * $p < 0.05$ and ** $p < 0.01$ compared to unstimulated control moDCs (IDC).

Moreover, moDCs activated with PG derived from WT and Lc-p75 mutant bacteria expressed a higher level of CD83 (Figure 19A, 19B), HLA-DQ (Figure 19C, 19D), CD80 (Figure 19E, 19F) and CD86 (Figure 19G, 19H) and produced more IL-8 (Figure 19I) than

the unstimulated moDCs independently of the targeted Lc-p75 mutation, similarly to the results obtained with live bacteria. Taken together, these results demonstrate that the alteration in PG structure due to the Lc-p75 mutation does not cause any differences in the purified PGs' moDC-activating capacity.

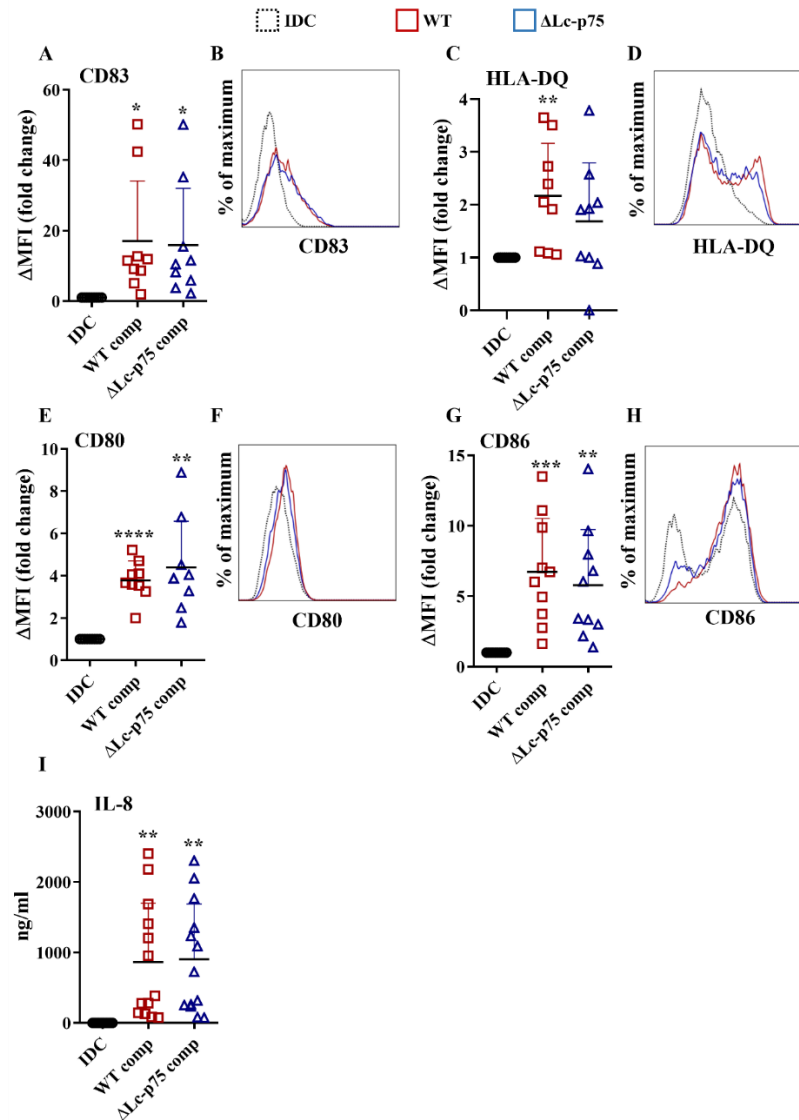


Figure 19. Exposure to purified PG components derived from wild-type (WT) and Lc-p75 mutant *L. casei* leads to elevated expression of CD83, HLA-DQ, CD80, and CD86 and enhanced IL-8 production by moDCs independently of bacterial PGH mutation. Five-day moDCs were stimulated with 10 $\mu\text{g/ml}$ PG extracts from WT and Lc-p75 mutant *L. casei*. Flow cytometry was used to detect the expression of CD83 (A, B), HLA-DQ (C, D), CD80 (E, F), and CD86 (G, H). Fold change of MFI to the control moDCs (IDC) was calculated from 7-9 independent experiments \pm SD (A, C, E, G). Histogram overlays show one representative experiment (B, D, F, H). IL-8 concentration was defined by ELISA from 12 independent donors and the mean values are shown \pm SD in the figures (I). Each glyph (black circle, red square, and blue triangle) represents one donor. Student's paired two-tailed *t*-test was applied for the statistical analysis. Significance is defined as * $p < 0.05$, ** $p < 0.01$, *** $p < 0.001$ and **** $p < 0.0001$ as compared to control samples (IDC).

6.1.4. Modified bacterial morphology leads to defective phagocytosis by moDCs

Since the PGs purified from the WT and Lc-p75 mutant *L. casei* showed similar moDC-activating capacity, we hypothesized that the diminished moDC activation triggered by the live Lc-p75 mutant bacteria is the aftermath of their impaired engulfment by moDCs. It has previously been shown that moDCs are able to internalize different *Lactobacillus* strains^{152–154}. In line with this, moDCs were able to phagocytose fluorescent mCherry-expressing WT (**Figure 20A**) and Lc-p75 mutant bacteria (**Figure 20B**) as shown by one Z-stack image of confocal microscopic picture.

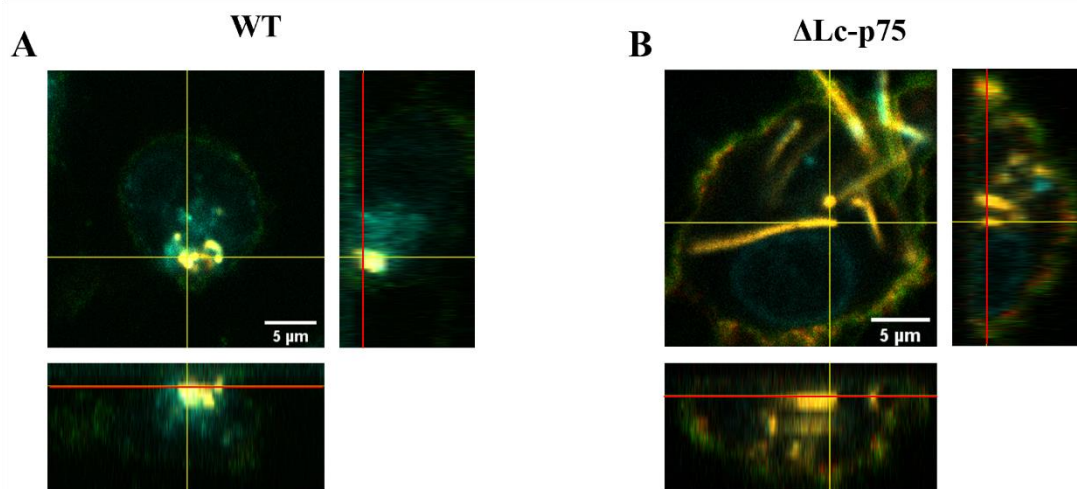


Figure 20. MoDCs internalize wild-type (WT) and Lc-p75 mutant bacteria. Five-day moDCs were co-incubated with mCherry-expressing WT and Lc-p75 *L. casei* at a ratio of 1:4 for 24 h. Uptake of WT (**A**) and Lc-p75 mutant (**B**) strains by moDCs was detected by confocal microscopy. MoDCs were stained with HLA-DQ (green), CD1a (red), and DAPI (cyan); mCherry was shown with yellow. Orthogonal views are shown in one Z-stack image. Z-projection in the X-Z direction is on the bottom, Z-projection in the Y-Z direction is on the right. The red lines illustrate the Z-depth of the optical slice and the orthogonal planes of the X-Z and Y-Z projections, respectively.

The fluorescent *L. casei* strains were used for the 3-h and 24-h phagocytosis assays, during which moDCs were co-incubated with WT and Lc-p75 mutant bacteria. After the incubation periods moDCs internalized both bacteria at 37°C, consequently becoming mCherry-positive; the frequency could be quantified by flow cytometry. We found remarkable differences in the moDCs' phagocytic capacity at 37°C and on ice, which represents active, temperature-dependent uptake of fluorescent bacteria after 3 (**Figure 21A, B**) and 24 h (**Figure 21C, D**). Importantly, a significant deviation was observed between WT and Lc-p75 mutant *L. casei*; WT bacteria were phagocytosed with higher intensity by moDCs than Lc-p75 defective bacteria after 3 h (**Figure 21A, B**) or 24 h (**Figure 21C, D**).

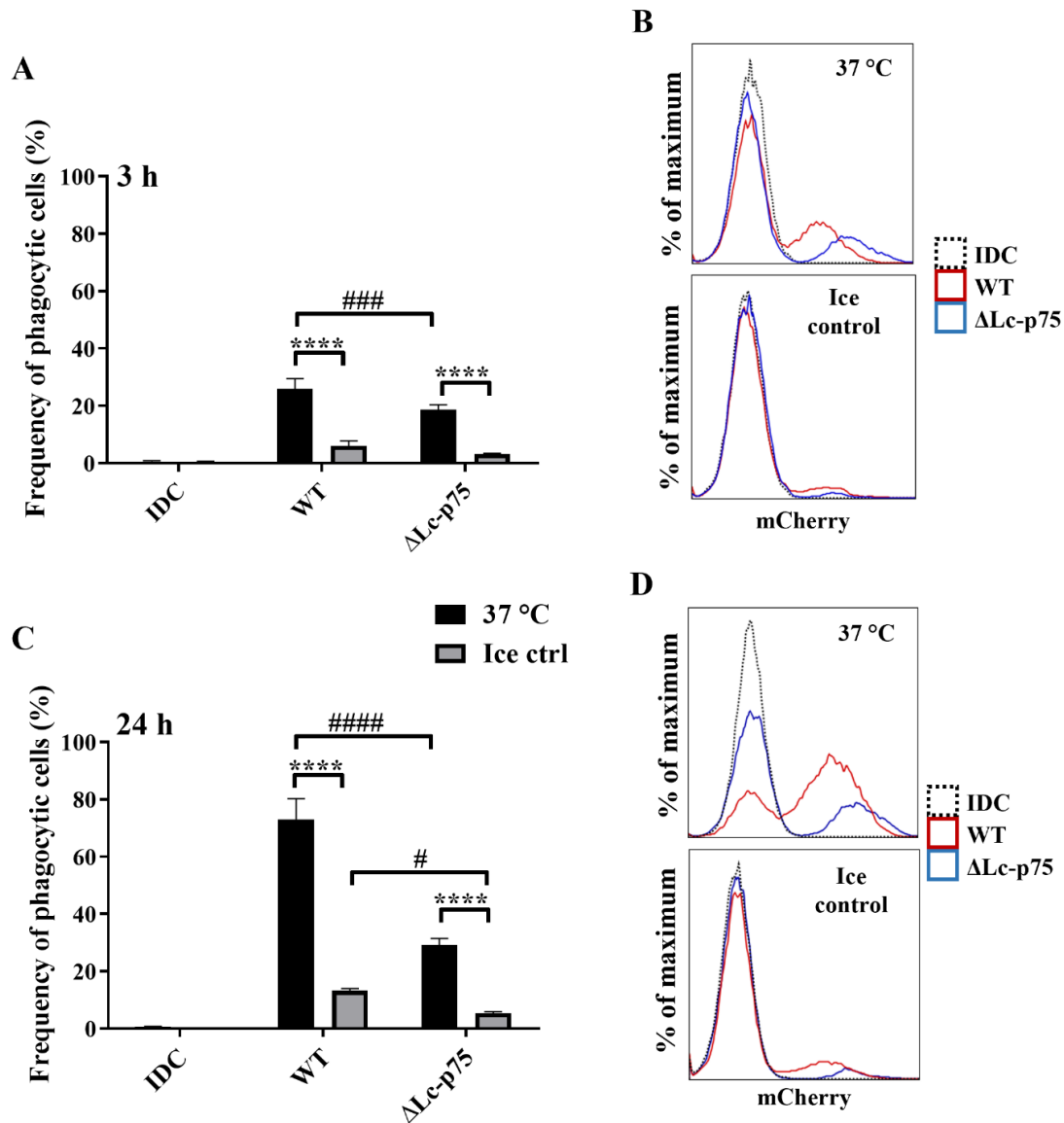


Figure 21. Deletion of Lc-p75 PGH in *L. casei* BL23 modifies the efficiency of phagocytosis by moDCs. Five-day moDCs were exposed to mCherry-expressing wild-type (WT) and Lc-p75 deficient *L. casei* strains for 3 and 24 h at a ratio of 1:4 at 37°C and on ice as a control. The internalizing capacity of moDCs was determined by detecting the frequency of mCherry-expressing moDCs after 3 h (A) and after 24 h (C) by flow cytometry. Histograms show one representative experiment about the uptake of WT (B) and Lc-p75 (D) mutant *L. casei* by moDCs. Mean values of the frequency of phagocytic cells from 3 independent experiments are shown \pm SD. Two-way ANOVA followed by Tukey's post hoc test was used in the statistical analysis. Significance defined as **** $p < 0.0001$ showing the differences between the samples incubated at 37°C and on ice. The differences between WT and Δ Lc-p75 were statistically significant determined as # $p < 0.05$, ### $p < 0.001$ and ##### $p < 0.0001$.

In 2007, Gogolak et al reported, that the CD1a⁺ and CD1a⁻ subpopulations of *in vitro* generated moDCs differ in their *E. coli*-internalizing ability¹⁵⁵. However, in our experimental system, lacking CD1a molecule on the surface of moDCs did not cause insufficient uptake of *L. casei* bacteria; CD1a⁺ and CD1a⁻ cells internalized WT and Lc-p75 mutant *L. casei* bacteria

to a similar extent (**Figure 22A, 22B**). This is in good agreement with the study by Seshadri et al, in which they observed no differences between CD1a⁺ and CD1a⁻ cells' *E. coli*-phagocytosing capacity¹⁵⁶. These results suggest that the targeted mutation of *L. casei* Lc-p75 alters the mutant bacteria's fate due to their blocked phagocytosis by moDCs regardless of the cell surface expression of the CD1a molecule. This observation can be linked to the long-chain morphology of the mutant *L. casei* strain.

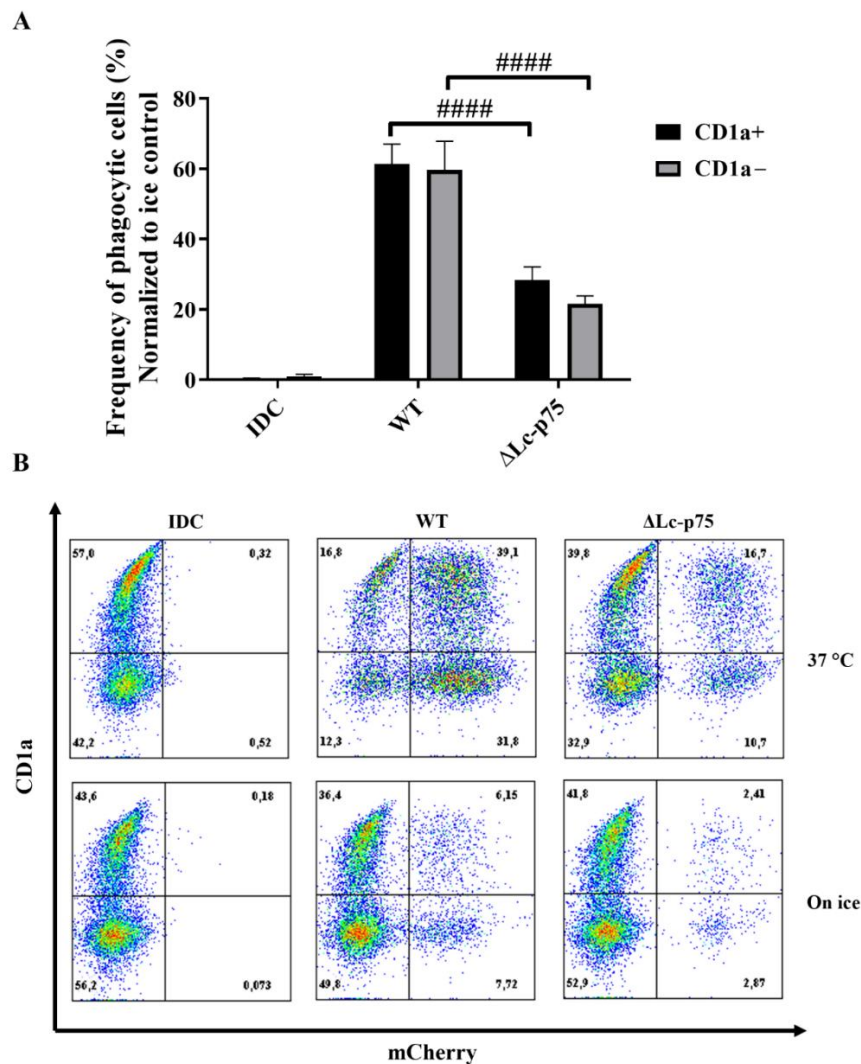


Figure 22. Expression of CD1a does not influence the phagocytic effectiveness of *L. casei*-activated moDCs. Five-day moDCs were treated with mCherry-labeled wild-type (WT) and Lc-p75 deficient *L. casei* BL23 for 24 h at 37°C and on ice. The frequency of phagocytic CD1a⁺ and CD1a⁻ moDC subsets was defined by detecting mCherry-expressing moDCs with flow cytometry (A). The frequency of internalizing cells was normalized to ice control. The mean values of 3 independent experiments are shown ± SD. Panel B illustrates dot plots from one experiment representing the CD1a and mCherry expression of moDCs. Two-way ANOVA followed by Tukey's multiple comparison tests was applied for the statistical analysis. Differences between WT and ΔLc-p75 were statistically significant, determined as ##### $p < 0.0001$.

6.1.5. Blocked uptake of WT *L. casei* induces diminished inflammatory and T-cell polarizing moDC responses

To further examine that the internalization of WT bacteria is an essential element in moDC activation, actin polymerization, which is the initial step of phagocytosis was inhibited by cytochalasin D (CyD). Firstly, we detected the engulfment of mCherry-expressing WT *L. casei* by CyD-treated and non-treated moDCs using flow cytometry and confocal microscopy. Our results showed an extreme drop in the frequency of mCherry-positive, CyD-treated moDCs (**Figure 23A, 23B**). The montage and the orthogonal views of one Z-stack image of the confocal microscopic pictures revealed that moDCs without any CyD treatment could uptake WT bacteria (**Figure 23C, 23D**). In contrast, CyD-pretreated moDCs could not engulf WT bacteria (**Figure 23E, 23F**). Moreover, CyD treatment caused remarkable morphological changes in moDCs, in agreement with a previous study, in which CyD treatment generated tubular protrusions and invaginations in neutrophil granulocytes¹⁵⁷.

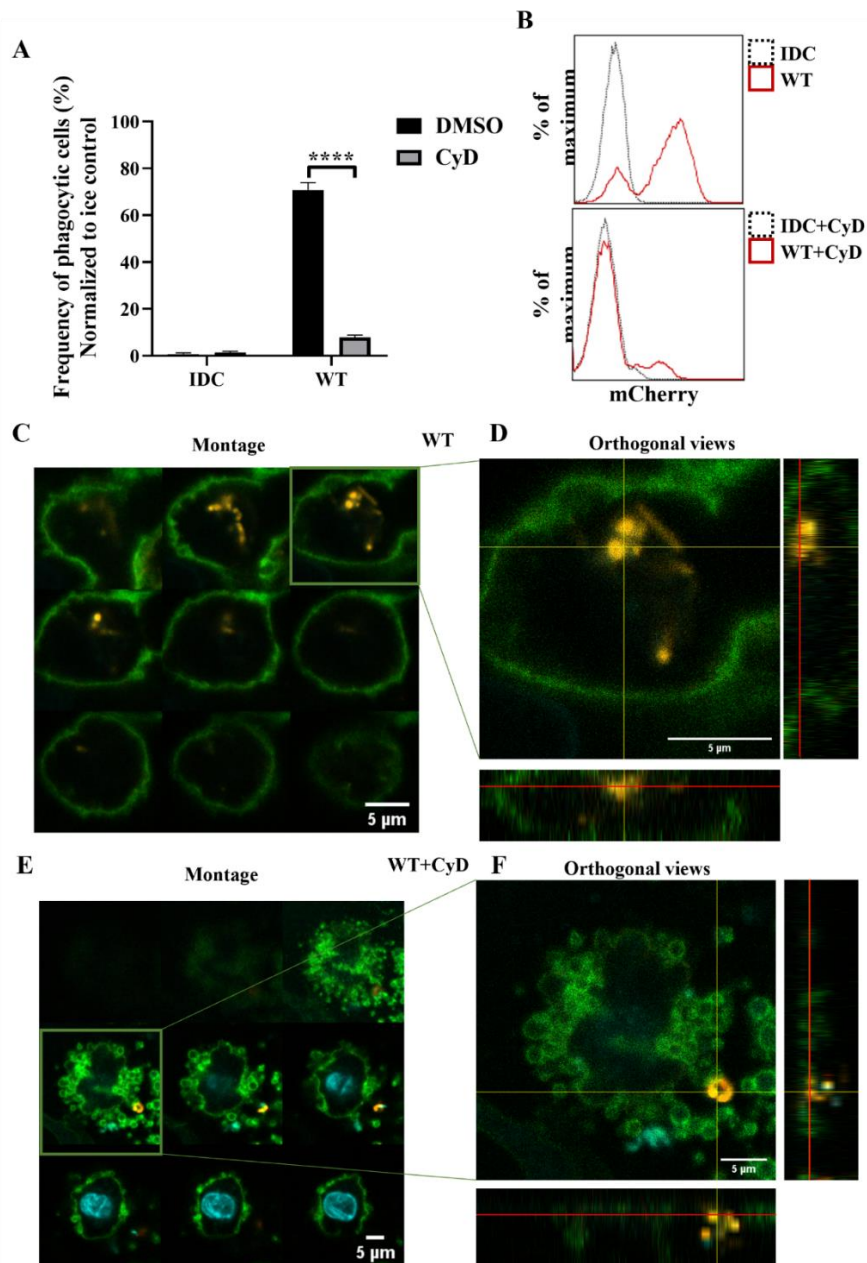


Figure 23. Cytochalasin D treatment leads to defective phagocytic efficiency by moDCs. On day 5 of moDC differentiation, the immature DCs were pre-treated with 15 μ M cytochalasin D (CyD) or its vehicle control DMSO for 30 min. After that, IDCs were incubated with mCherry-expressing wild-type (WT) *L. casei* BL23 at a ratio of 1:4 for 24 h. Control cells (IDC) received only DMSO or CytD treatment, not bacteria. The frequency of the phagocytic moDCs was determined by detecting the mCherry-expressing moDCs by flow cytometry. The frequency of phagocytic cells was normalized to ice control and was calculated from 3 independent experiments \pm SD (A). Histograms show one representative experiment (B). For the confocal microscopic pictures, moDCs were stained with HLA-DQ (green) and DAPI (cyan); mCherry was illustrated with yellow. In figure left, montage pictures (C, E) represent the Z-stack images per 1 μ m from the bottom to the top of the cell. In figure right the orthogonal views (D, F) are shown in one Z-stack image. Z-projection in the X-Z direction is on the bottom, and the Z-projection in the Y-Z direction is on the right. The red lines show the Z-depth of the optical slice and the orthogonal planes of the X-Z and Y-Z projections, respectively. Two-way ANOVA

followed by Tukey's post hoc test was applied for the statistical analysis. The difference between the non-treated and CyD-treated moDCs was statistically significant, determined as **** $p < 0.0001$.

To confirm, that the differences in the WT bacteria uptake between CyD-treated and non-treated moDCs were not triggered by the CyD-induced increased cell death, the frequency of dead cells was evaluated by flow cytometry. Importantly, we did not detect any differences in the cell death frequencies between CyD-treated and non-treated moDCs after co-incubation with WT bacteria (**Figure 24A, 24B**). It should be noted that CyD pretreatment induced a significant increase in the frequency of unstimulated dead moDC, however, it did not reach 10 % in the moDC cultures.

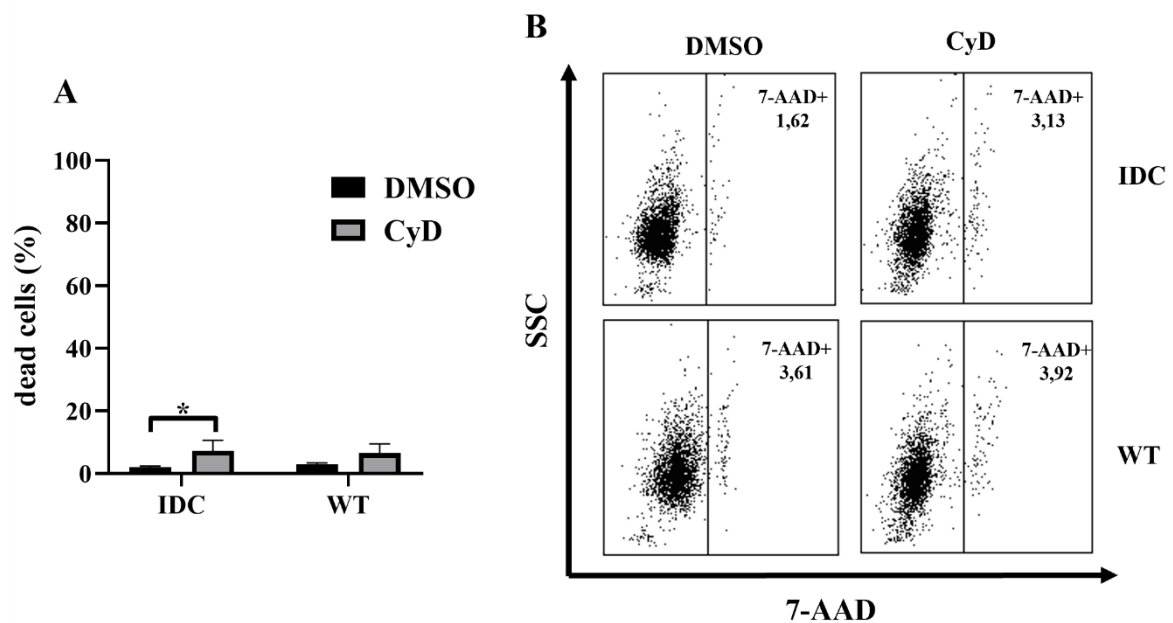


Figure 24. CyD treatment does not influence the viability of *L. casei*-activated moDCs. On day 5 of moDC differentiation, the immature DCs were pre-treated with 15 μ M cytochalasin D (CyD) or DMSO for 30 min. After that, moDCs were incubated with wild-type (WT) *L. casei* BL23 at a ratio of 1:4 for 24 h. Control IDCs were not activated with WT bacteria. The percentage of dead moDCs was detected using 7-AAD fluorescent dye by flow cytometry. Mean values of the dead cell percentage were determined from 3 independent experiments \pm SD (**A**). Dot plots illustrate one representative experiment (**B**). Two-way ANOVA followed by Tukey's post hoc test was applied for statistical analysis. Significance is defined as * $p < 0.05$ compared to DMSO-treated moDCs.

Next, we analyzed whether the inhibition of the WT bacteria uptake had a blocking effect on moDCs' functional responses. Firstly, we tested the pro-inflammatory TNF- α , IL-1 β and IL-6 (**Figure 25A**) secretion by moDCs. We found that CyD-pretreatment caused a highly significant decline in the pro-inflammatory cytokine secretion by moDCs. Similarly, CyD-treated moDCs produced significantly less T-cell-polarizing IL-10, IL-12, and IL-23 cytokines

by moDCs (**Figure 25B**), and consequently diminished IFN γ - and IL-17A-producing T-cell numbers in the moDC-T-cell cocultures (**Figure 25C, 25D**).

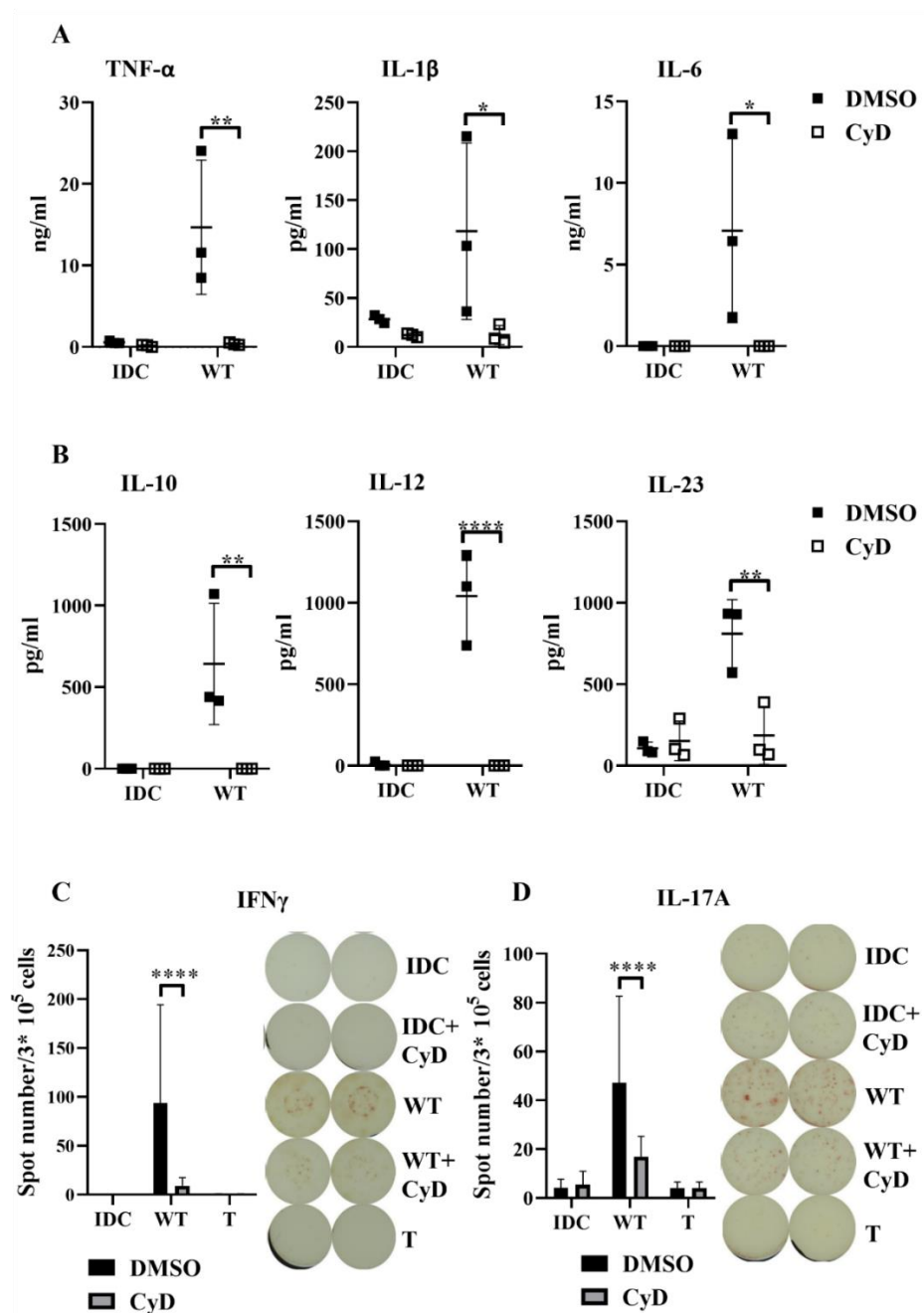


Figure 25. CyD treatment attenuates the cytokine secretion and T-cell polarizing ability of *L. casei*-exposed moDCs. Five-day moDCs were preincubated with 15 μ M CyD or its vehicle control DMSO for 30 min. After that, immature DCs were treated with wild-type (WT) *L. casei* BL23 at a ratio of 1:4 for 24 h. Control cells were not activated with bacteria and remained immature (IDC). The concentration of pro-inflammatory TNF- α , IL-1 β , IL-6 (**A**) cytokines, and the T-cell-polarizing IL-10, IL-12, and IL-23 (**B**) was measured from the collected supernatants of moDCs cultures using ELISA. Figures show the mean of 3 independent experiments \pm SD. Each square represents one donor. CyD- or DMSO-treated and *L. casei*-activated moDCs were washed, counted, and co-incubated with autologous T cells at a ratio of 1:20 for 3 days. Then, the cultured cells were subjected to ELISpot assays. The number of IFN γ - (**C**) and IL-17A-secreting (**D**) T cells was calculated from 3 experiments with 4 parallel wells.

*Figures represent the mean values of the spot numbers \pm SD. Paired, two-tailed Student's *t*-test was used for the statistical analysis (A-F). Two-way ANOVA followed by Tukey's multiple comparison test was applied for statistical analysis. Significance between DMSO- and CyD-treated moDCs was defined as * $p < 0.05$, ** $p < 0.01$, and **** $p < 0.0001$.*

In addition to this, we tested the effect of CyD pretreatment on cell surface marker expression and IL-8 chemokine secretion by moDCs. Previously we could not find differences in these functions between WT and Lc-p75 mutant bacteria-activated moDCs. Similarly, CyD-treated and WT bacteria-stimulated moDCs expressed CD83 (**Figure 26A, 26B**), HLA-DQ (**Figure 26C, 26D**) and co-stimulatory CD80 (**Figure 26E, 26F**) and CD86 (**Figure 26G, 26H**) molecules at a similar level as DMSO- and WT bacteria-treated moDCs.

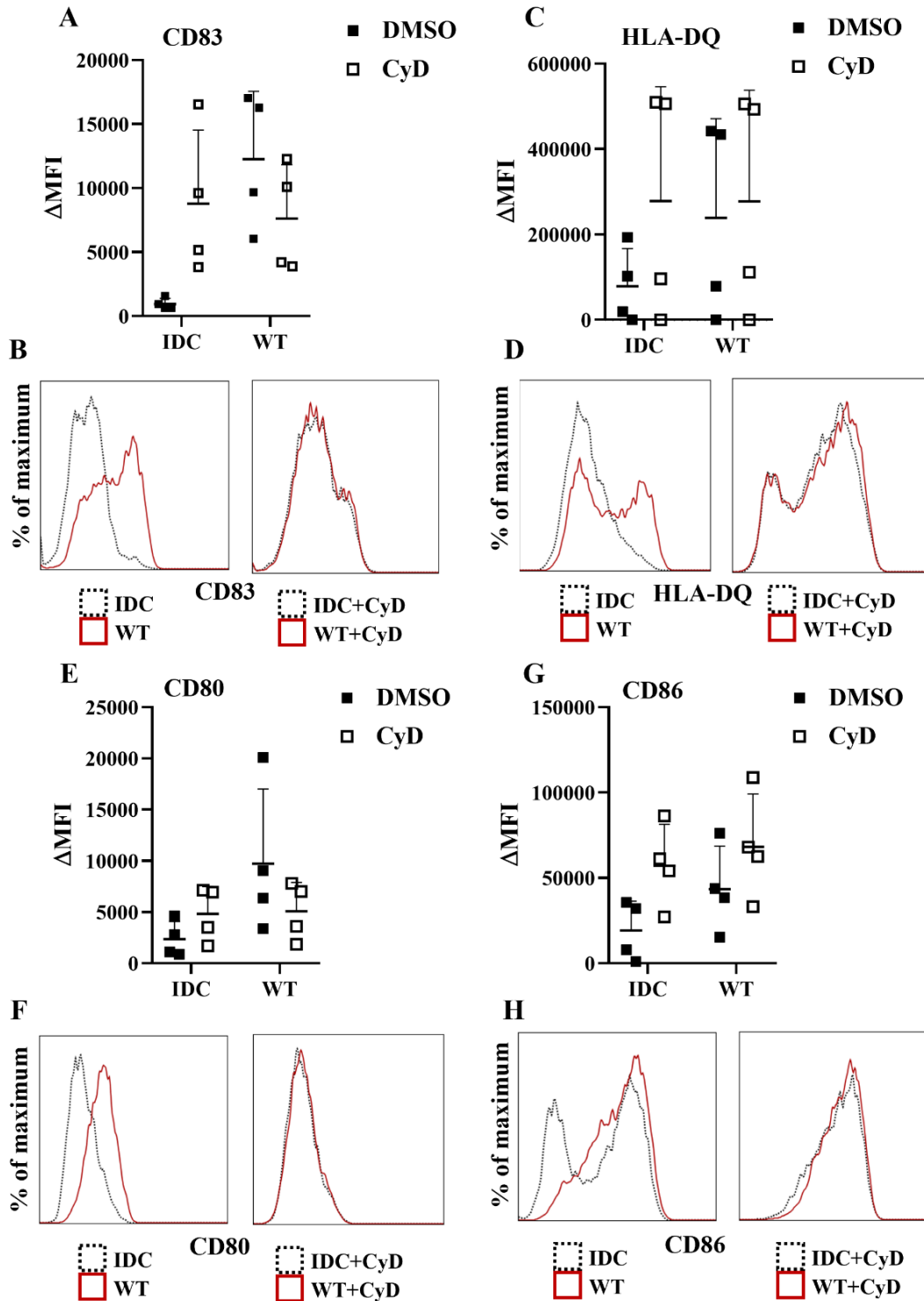


Figure 26. Cytochalasin D treatment does not modify the expression of activation and co-stimulatory cell surface markers of moDCs independently of the bacterial presence. 5-day moDCs were preincubated with 15 μ M CyD or its vehicle control DMSO for 30 min. After that, moDCs were treated with WT *L. casei* BL23 at a ratio of 1:4 for 24 h. Expression of CD83 (A), HLA-DQ (C), CD80 (E) and CD86 (G) was detected by flow cytometry. MFI was calculated from 4 experiments \pm SD. Histograms (B, D, F, H) illustrate one representative experiment. Each squares represent one donor. Two-way ANOVA followed by Tukey's post hoc test was applied for statistical analysis.

The same was true for the IL-8 production by CyD-treated and non-treated, WT *L. casei*-exposed moDCs (**Figure 27**). However, it is worth noting that CyD treatment alone also triggered significantly elevated IL-8 secretion, related to previous results obtained with human retinal pigment epithelial cells¹⁵⁸.

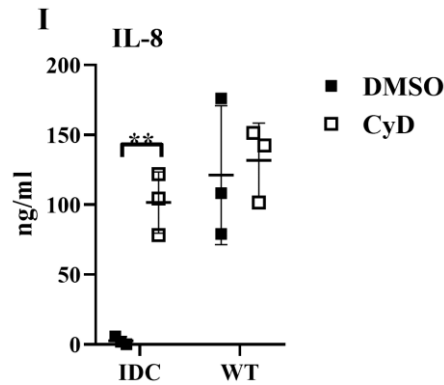


Figure 27. Cytochalasin D treatment enhances the IL-8 secretion by moDCs regardless of the bacterial presence. 5-day moDCs were preincubated with 15 μ M CyD or its vehicle control DMSO for 30 min. After that, moDCs were treated with WT *L. casei* BL23 at a ratio of 1:4 for 24 h. The concentration of IL-8 chemokine was defined from the collected supernatants of the moDC cultures. Mean values were determined from 3 independent experiments \pm SD (**I**). Each square represents one donor. Two-way ANOVA followed by Tukey's post hoc test was applied for statistical analysis. Significance between DMSO- and CyD-treated moDCs was defined as ** $p < 0.01$.

Overall, these results indicate that bacteria engulfment is a crucial step in WT *L. casei*-triggered moDC activation, representing that the attenuated phagocytic uptake of Lc-p75 mutant *L. casei* may lead to diminished moDC-activating capacity and consequently reduced Th1 and Th17 cell responses.

6.2. Part II. Studying the effects of different tumor cell line-derived soluble factors on the differentiation program and phagocytic potential of moDCs

6.2.1. TU-CMs alter the phenotypic properties of moDCs

It is well known that different tumor types can alter the differentiation program and T-cell-polarizing activities of myeloid cells such as DCs. Therefore, we analyzed the typical differentiation markers including CD14, CD209, CD1a, and CD1d, as well as the molecules that participated in T-cell activation (HLA-ABC, HLA-DR, CD86 and PD-L1) of TU-CM-educated moDCs.

CD14 expression is continuously decreasing during the moDC differentiation process, while CD209/DC-SIGN is increasing¹⁵⁹. We found that control moDCs showed reduced CD14 and elevated CD209 expression (**Figure 28A, 28B, 28C, 28D**). However, dexDCs maintained the CD14 expression on their surface, while expressed CD209 (**Figure 28A, 28B, 28C, 28D**). TU-CM tendentially upregulated the expression of CD14; significant differences were observed between HT29-CM- and WM278-CM-conditioned moDCs and the control moDCs (**Figure 28A, 28B**). Interestingly, WM983A primary melanoma cell line supernatant significantly decreased the CD14 expression by moDCs as compared to dexDCs and the other primary melanoma cell line, WM278-conditioned moDCs. Besides, CD209 expression was generally reduced by TU-CM on the moDC surface in a non-significant manner (**Figure 28C, 28D**). Two exceptions were found: WM983A-CM and its metastatic counterpart, WM983B-CM significantly down-regulated the expression of CD209 by moDCs.

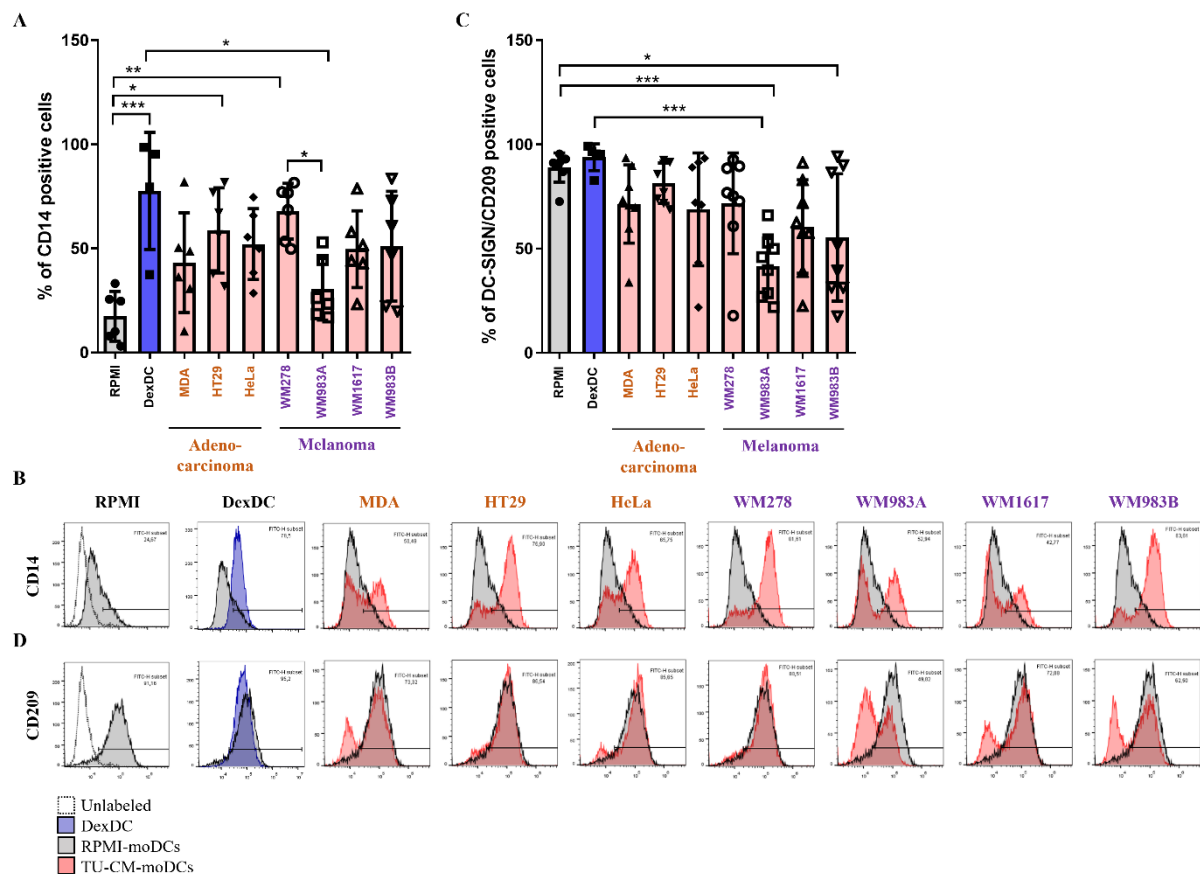


Figure 28. TU-CM modify the CD14 and CD209 expression by moDCs. Monocytes were differentiated in the presence of MDA-MB231-, HeLa-, HT29-, WM278-, WM1617-, WM983A- and WM983B-CM or 0.25 μ M dexamethasone for 4 days. Frequency of CD14- (A, B) and CD209- (C, D) expressing cells was detected by flow cytometry. Mean values of the positive cell percentage were calculated from 4 independent experiments \pm SD. Histograms (B, D) represent one representative experiment. One-way ANOVA followed by Tukey's post hoc test was used for the statistical analysis. Significance is defined as * $p < 0.05$, ** $p < 0.01$, *** $p < 0.001$.

Next, we aimed to test how the TU-CM influence the CD1a and CD1d expression of moDCs. Members of the CD1 family are readily expressed by the moDCs¹⁶⁰. In our system, TU-CM along with the dexamethasone significantly decreased the CD1a expression by moDCs; however, MDA-CM could only non-significantly attenuate the moDCs' CD1a expression (**Figure 29A, 29B**). In contrast, CD1d expression was not altered by any TU-CM-exposed moDCs as compared to RPMI-moDCs (**Figure 29C, 29D**). We found only one significant difference between dexDC and WM278-CM-exposed moDCs in the CD1d expression.

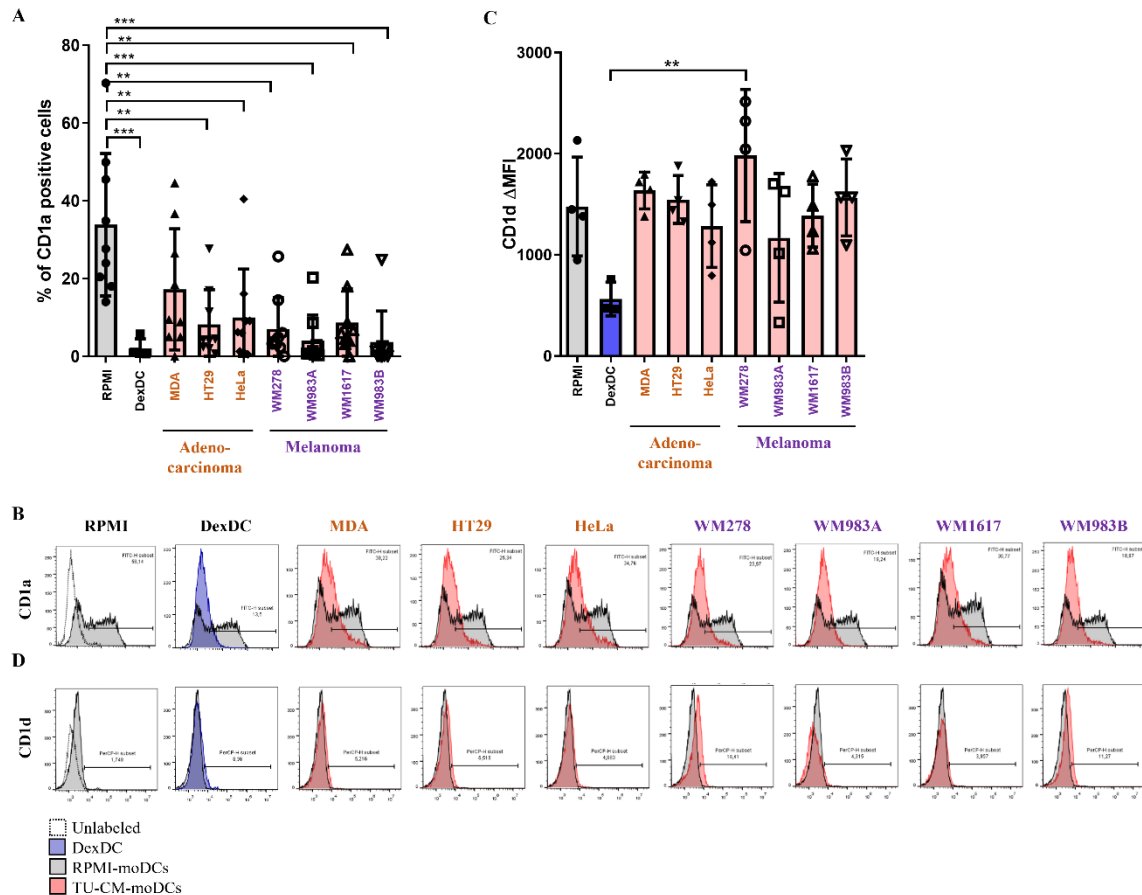


Figure 29. TU-CM modify the CD1a and CD1d expression by moDCs. Monocytes were differentiated in the presence of MDA-MB231-, HeLa-, HT29-, WM278-, WM1617-, WM983A- and WM983B-CM or 0.25 μ M dexamethasone for 4 days. Expression of CD1a and CD1d was detected by flow cytometry. Mean values of the percentage of CD1a-positive cells (**A**) and of the MFI of CD1d expression (**C**) were calculated from 4 independent experiments \pm SD. Histograms (**B**, **D**) represent one representative experiment. One-way ANOVA followed by Tukey's post hoc test was used for the statistical analysis. Significance is defined as ** $p < 0.01$, *** $p < 0.001$.

For presenting the antigens to the T cells, moDCs increase the expression of MHC I and MHC II molecules. Therefore, in the next step we analyzed the expression of HLA-ABC and HLA-DR molecules by TU-CM-educated moDCs. We found, that neither HLA-ABC, nor HLA-DR expression was changed to any TU-CM exposure on the surface of moDCs as

compared to RPMI-moDCs (**Figure 30A, 30B, 30C, 30D**). In contrast, significant differences were observed between dexDCs and WM983A-CM and its metastatic counterpart WM983B-CM-conditioned moDCs in HLA-ABC expression (**Figure 30A, 30B**). In addition, dexamethasone treatment induced significantly increased HLA-DR expression by moDCs compared to RPMI-moDCs and all the tumor cell line-educated moDCs except HT29 (**Figure 30C, 30D**).

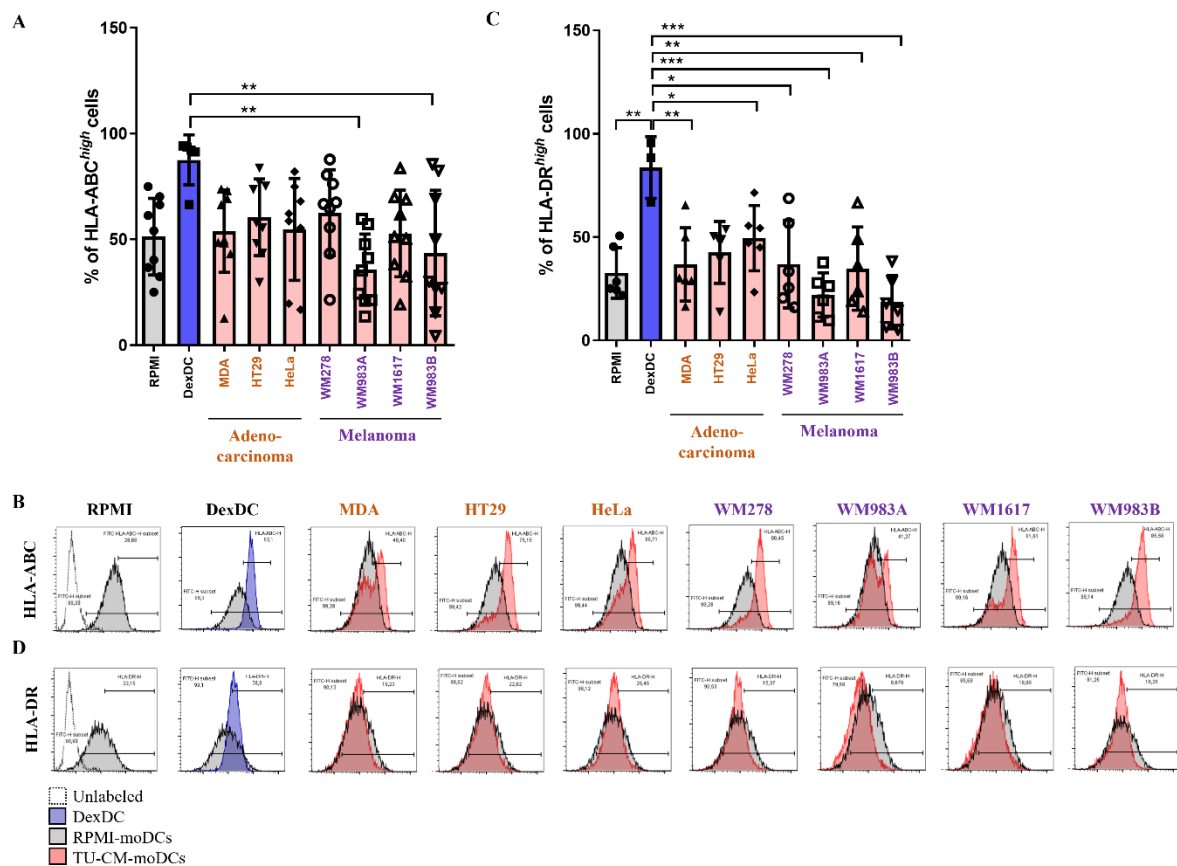


Figure 30. TU-CM modify the antigen-presenting capacity of moDCs. Monocytes were differentiated in the presence of MDA-MB231-, HeLa-, HT29-, WM278-, WM1617-, WM983A- and WM983B-CM or 0.25 μM dexamethasone for 4 days. Expression of HLA-ABC and HLA-DR was detected by flow cytometry. Mean values of the percentage of HLA-ABC^{high} (A) and HLA-DR^{high} (C) cells were calculated from 4 independent experiments \pm SD. Histograms (B, D) represent one representative experiment. One-way ANOVA followed by Tukey's post hoc test was used for the statistical analysis. Significance is defined as * $p < 0.05$, ** $p < 0.01$, *** $p < 0.001$.

Besides the antigen-presenting molecules, DCs increase the expression of co-stimulatory and co-inhibitory molecules upon T-cell activation. Hence, in the next step we studied the expression of co-stimulatory CD86 and co-inhibitory PD-L1 expression by TU-CM-exposed moDCs. CD86 expression was decreased due to dexamethasone treatment of moDCs (**Figure 31A, 31B**). In HT29 and HeLa adenocarcinoma cell lines and WM278 and WM983A

primary melanoma cell CM-treated moDCs, we observed a significantly higher CD86 expression than in dexDCs (**Figure 31A, 31B**).

PD-L1 expression was completely diminished by dexamethasone-exposed moDCs (**Figure 31C, 31D**). Adenocarcinoma cell line-CM caused significantly elevated PD-L1 expression by moDCs as compared to dexDCs. Interestingly, the two primary melanoma cell lines behaved differently; WM278 induced significantly increased PD-L1 expression as compared to WM983A-derived CM by moDCs. Similarly, their metastatic counterparts showed similar effects on the PD-L1 expression to the primary melanomas (**Figure 31C, 31D**).

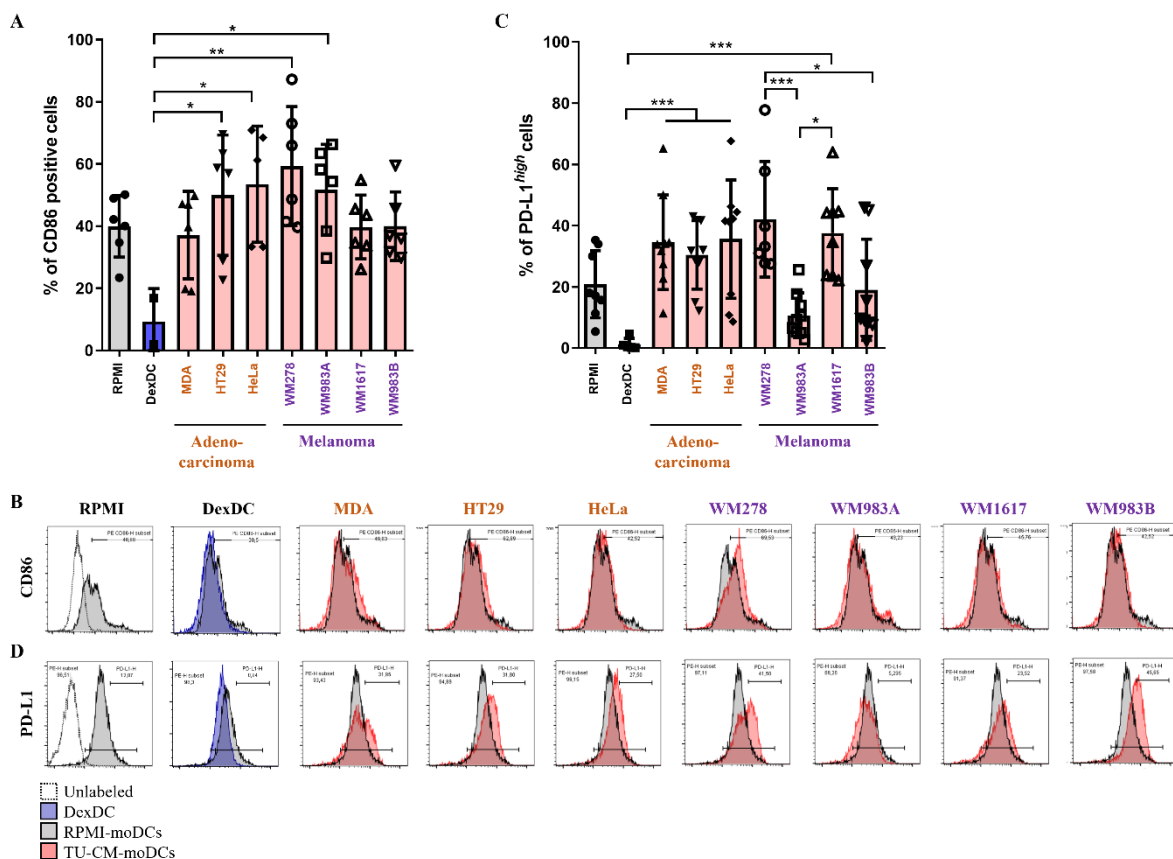


Figure 31. TU-CM modify the co-stimulatory and co-inhibitory ability of moDCs. Monocytes were differentiated in the presence of MDA-MB231-, HeLa-, HT29-, WM278-, WM1617-, WM983A- and WM983B-CM or 0.25 μ M dexamethasone for 4 days. Expression of CD86 and PD-L1 was detected by flow cytometry. Mean values of the percentage of CD86-positive (A) and PD-L1^{high} (C) cells were calculated from 4 independent experiments \pm SD. Histograms (B, D) represent one representative experiment. One-way ANOVA followed by Tukey's post hoc test was used for the statistical analysis. Significance is defined as * $p < 0.05$, ** $p < 0.01$, *** $p < 0.001$.

6.2.2. Mediators derived from different tumor cell lines modify the phagocytic capacity of moDCs

Several studies demonstrate that probiotic bacteria, including different *Lactobacillus* species can have beneficial effects on different tumors such as human papillomavirus-induced cervical cancer, melanoma, or gastrointestinal cancers^{161–163}. However, little is known about how the different tumor-derived soluble mediators can influence the phagocytic activity of professional phagocytes like DCs. It was revealed in the flow cytometric measurements that moDCs internalized wild-type *L. casei* at 37°C but the phagocytosis was inhibited at 4°C (**Figure 32**). *L. casei* uptake with the highest frequency was observed by dexDCs; further significant differences were detected between the control moDCs and two melanoma cell lines, WM278- and its metastatic counterpart WM1617-educated moDCs. In contrast, any adenocarcinoma cell line did not change the *L. casei* uptake by moDCs (**Figure 32**). These results show that certain melanoma cell lines indirectly modify the *L. casei*-internalizing capacity of moDCs.

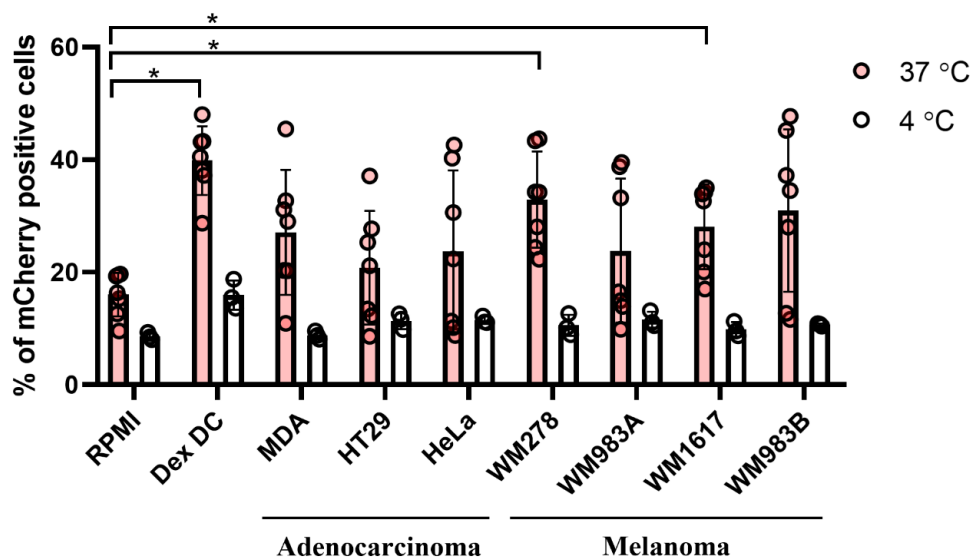


Figure 32. TU-CM modify the internalizing capacity of moDCs. Monocytes were differentiated in the presence of MDA-MB231-, HeLa-, HT29-, WM278-, WM1617-, WM983A- and WM983B-CM or 0.25 μ M dexamethasone for 4 days. On day 4, cells were co-cultured with mCherry-expressing *L. casei* BL23 at a ratio of 1:4 for 4 h at 37°C and 4°C as a control. The phagocytic efficiency of moDCs was defined by detecting the mCherry-positive moDCs with flow cytometry. Dot plots show the gating strategy using the data of MDA-CM-exposed moDCs (A). Figure shows the mean of the frequency of mCherry-positive cells from 7 (37°C) and 3 (4°C) independent experiments \pm SD. Each dot represents one donor. One-way ANOVA followed by Tukey's post hoc test was used for the statistical analysis. Significance is defined as * $p < 0.05$.

With the application of heatmaps we could make more specific statements regarding the relationships between markers/phagocytosis and the different TU-CM-educated moDCs dividing into two groups: adenocarcinoma and melanoma.

In the adenocarcinoma group, the relationship between the markers/phagocytosis and the different cell line-educated moDCs showed a diverse pattern, each cell line had its unique profile. MDA-CM moDCs had a positive link with CD1a expression and phagocytosis, while had a strong negative relationship with CD14, HLA-DR and CD86 expression. HT29-CM-conditioned moDCs displayed high HLA-ABC, CD14 and CD209 expression but were strongly negatively connected to PD-L1 and phagocytosis. HeLa-CM-educated moDCs had an intense positive relationship with HLA-DR expression and a strongly negative one with CD1d expression (*Figure 33A*).

Among melanoma cell lines, WM278-CM-moDCs had a positive relationship with every marker and the phagocytosis at various extents, while the other primary melanoma cell line, the WM983A-CM-educated moDCs had a negative link to all markers and phagocytosis, except a slight positive relation to CD86. Interestingly, WM278-CM- and its metastatic counterpart WM1617-CM-educated moDCs behaved completely differently regarding almost every marker and phagocytosis with the most prominent difference in the CD1a and CD86 expression. In contrast, the other melanoma pair, WM983A- and WM983B-CM acted similarly on the marker expression and phagocytosis by moDCs (*Figure 33B*).

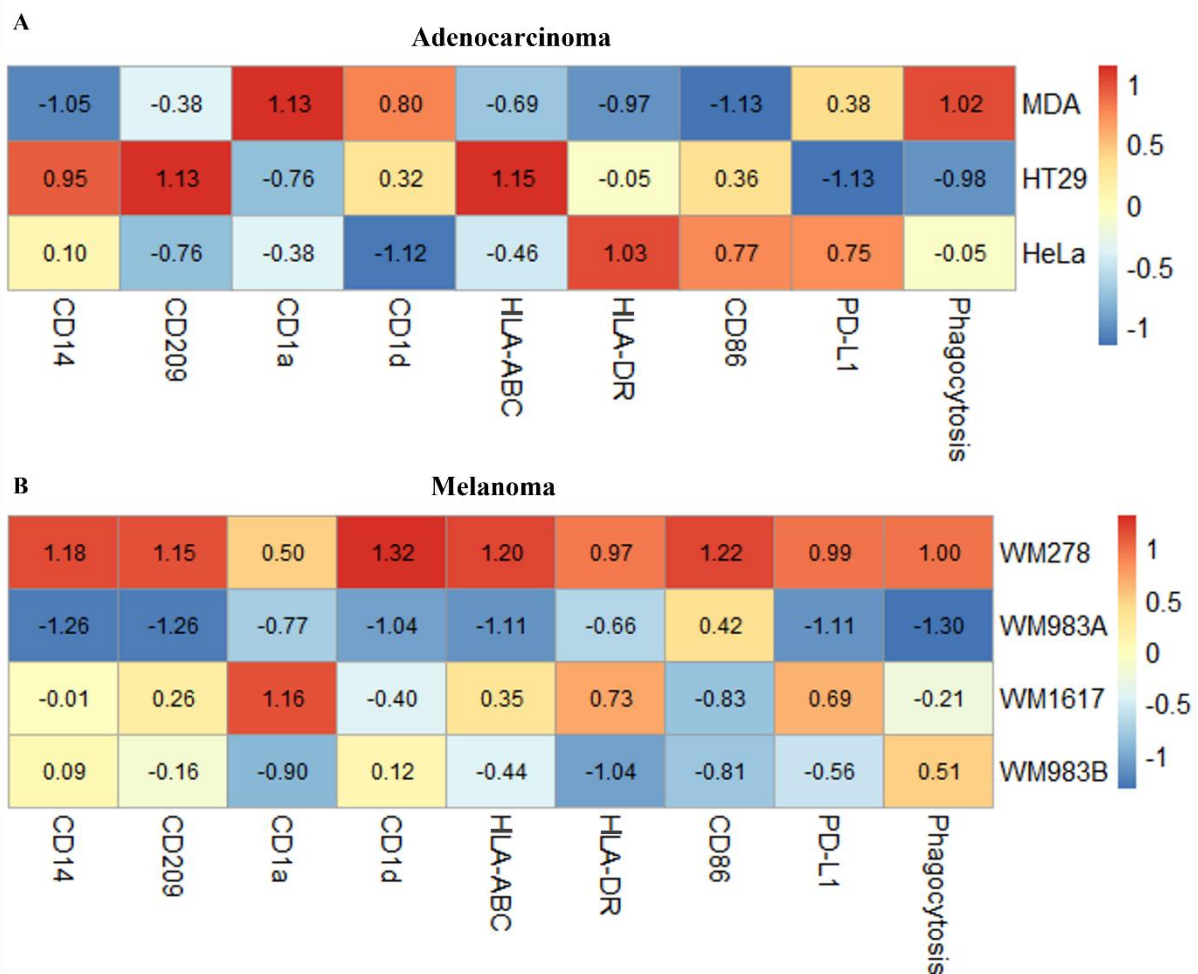


Figure 33. Heatmaps show positive and negative relationships between cell surface marker expression, phagocytic ability and the different TU-CM-educated moDCs. Raw data of cell surface marker expression and phagocytosis without RPMI and dexDC data were used for plotting heatmaps with pheatmap package in RStudio. The dataset was divided into two groups: adenocarcinoma (A) and melanoma (B). Raw data were normalized with z-score and scaled by column. Markers/phagocytosis are displayed on the bottom, while the different tumors are shown on the right. Red indicates positive relationship; negative link is displayed in blue. Normalized values are shown in the boxes.

6.2.3. Correlation analyses reveal associations between the expression of different cell surface markers and phagocytosis by adenocarcinoma- or melanoma-derived CM-educated moDCs

To analyze the degree of the correlations between the markers and phagocytic activity, we performed correlation analyses of the two groups in R Studio. The results were displayed with correlograms.

In the group of adenocarcinoma-CM-conditioned moDCs strong positive correlations were found between the phagocytic activity and CD1a and PD-L1 expression. Interestingly, phagocytosis was negatively correlated with CD14, CD209, HLA-ABC and CD86. In addition,

we found strong positive correlations between CD86 and CD14, CD86 and HLA-DR, HLA-ABC and CD14, HLA-ABC and CD209 and finally, CD14 and CD209. On the contrary, PD-L1 negatively correlated with CD1a, CD209 and HLA-ABC; CD86 and HLA-DR had a strong negative correlation with CD1a and CD1d. Moreover, HLA-ABC is anticorrelated with CD1a and CD1a with CD14 (*Figure 34*).

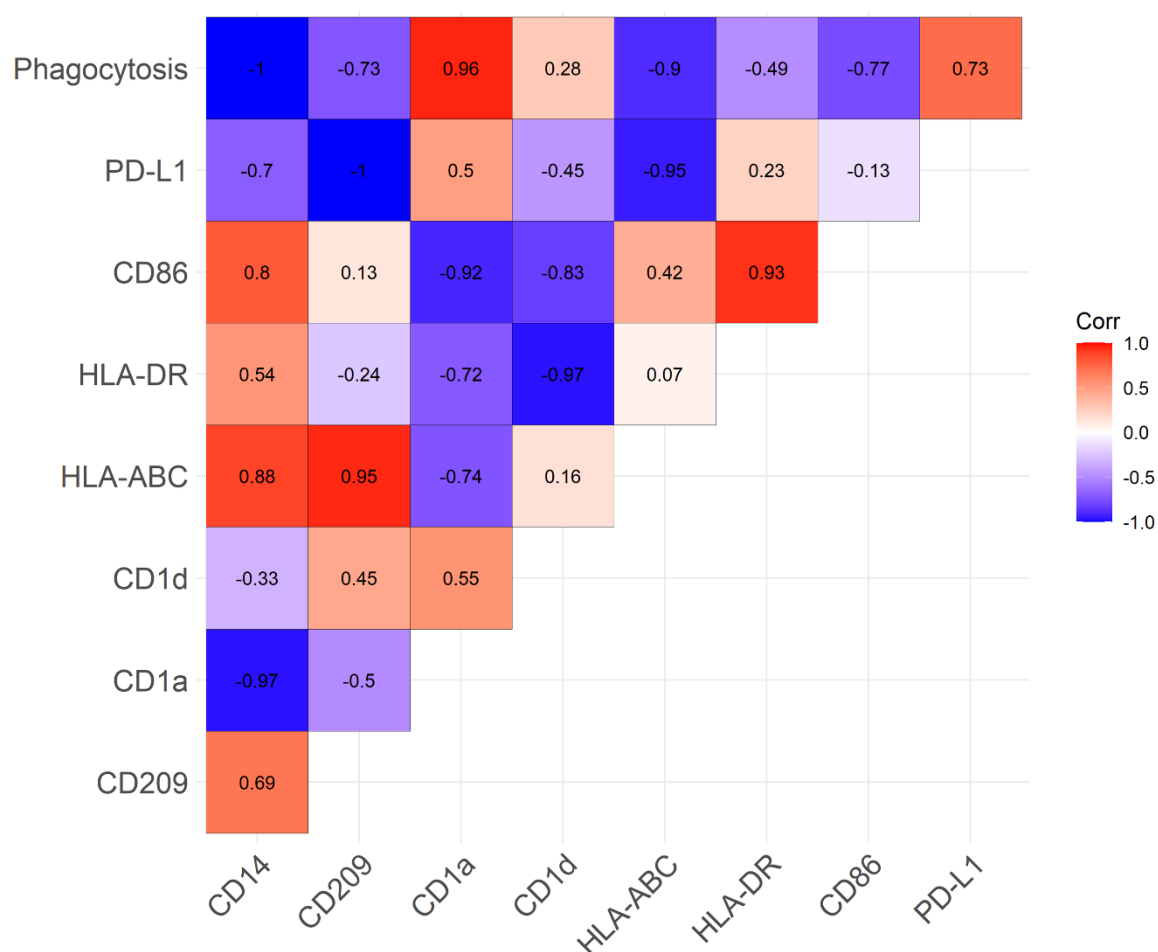


Figure 34. Correlation analyses revealed differences between the cell surface marker expression and internalizing capacity of adenocarcinoma-CM-educated moDCs. Correlation matrices were generated from the raw data of adenocarcinoma-CM-conditioned moDCs; RPMI and dexDCs were excluded from the analyses. Correlograms were visualized using ggcorrplot package in RStudio. Positive correlations are shown in red, while negative correlations are displayed in blue. Correlation coefficients are demonstrated in the boxes.

Surprisingly, in the group of melanoma-CM-educated moDCs only positive correlations were found between the phagocytosis and cell surface marker expressions at various degrees; between CD86 and CD1a no correlation was observed (*Figure 35*).

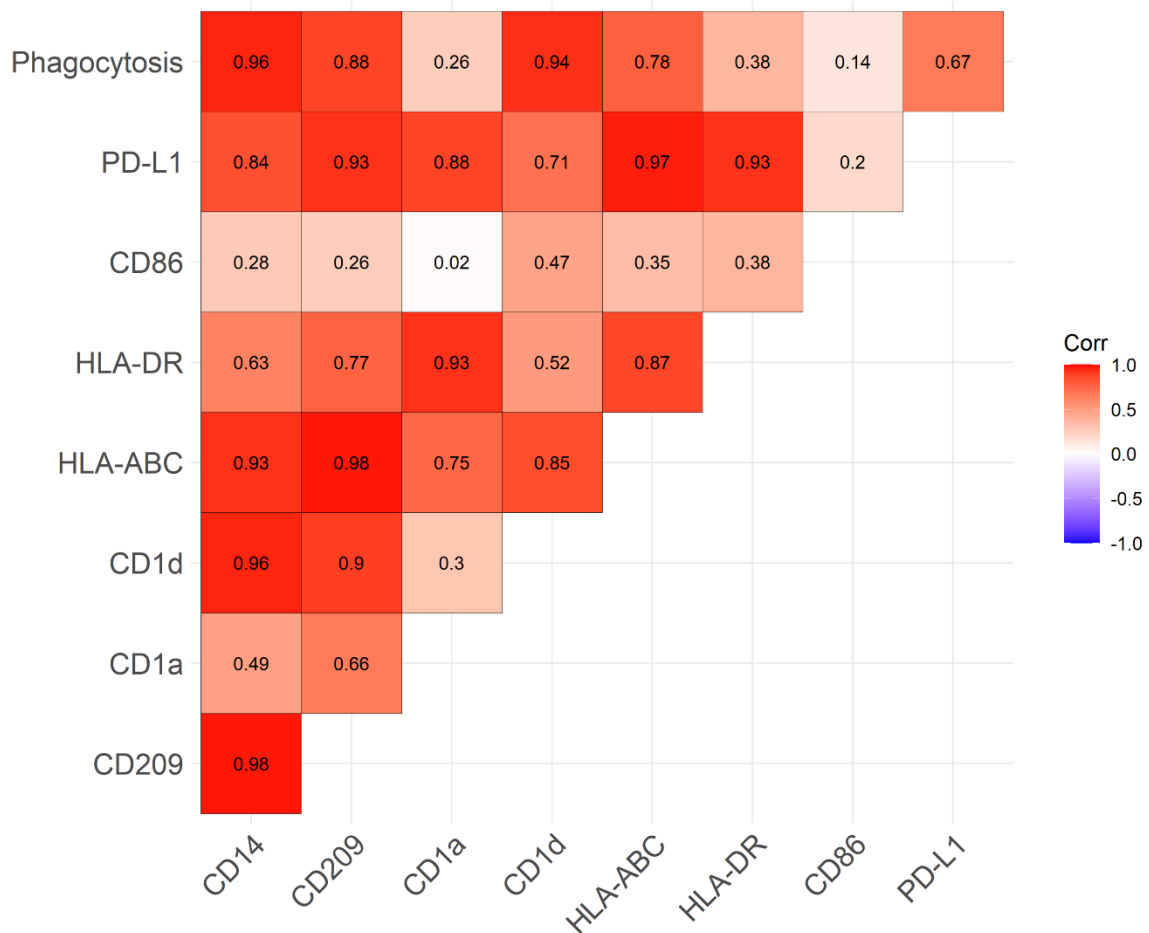


Figure 35. Correlation analyses show differences between the cell surface marker expression and phagocytic capacity of melanoma-CM-educated moDCs. Correlation matrices were generated from the raw data of melanoma-CM-conditioned moDCs; RPMI and dexDCs were excluded from the analyses. Correlograms were visualized using ggcorrplot package in RStudio. Positive correlations are shown in red, while negative correlations are displayed in blue. Correlation coefficients are demonstrated in the boxes.

Taken together, our results indicate that diverse tumor types are able to indirectly manipulate the phenotype and phagocytic activity of moDCs in different ways. Our results also emphasize that primary and metastatic melanoma cells act differently on the differentiation, phenotype, and phagocytic activity of moDCs.

7. DISCUSSION

The human body is continuously exposed to various external and internal stimuli, which can threaten the integrity of homeostasis. Mucosal surfaces and the skin are a frequent entry for potentially dangerous molecules or microorganisms; however, on the other hand these surfaces are covered by beneficial mutualistic and commensal microbiota including LAB in the gastrointestinal system. Various favorable effects are attributed to LAB members; hence the main function of the mucosal immune system is to distinguish between dangerous and non-dangerous materials and induce immunogenic or tolerogenic immune responses suitable for the features of the antigens. Dendritic cells organize immune responses by bridging innate and adaptive immunity¹⁶⁴. DCs continuously sample the microenvironment by micropinocytosis, receptor-mediated endocytosis and phagocytosis⁹⁸ and are able to mediate inflammatory or tolerogenic responses. Furthermore, their unique, naïve T-cell-activating capacity makes them the primary promoters of tolerance against the microbiota.

Disruption of the delicate immunological balance between host cells and microbiota may lead to serious consequences, for example inflammatory disorders like Crohn's disease (CD), chronic obstructive pulmonary disease, atopic dermatitis, or autoimmune disorders such as multiple sclerosis or even cancer. Therefore, the interactions between mutualistic microorganisms including LAB members like lactobacilli and immune cells are under intensive investigation. Despite the heterogeneous results due to the extreme strain-specificity, we must attempt to harvest and describe the immunomodulatory actions of each microbiota member as precisely as possible.

In contrast to microbiota, tolerance induced by the dendritic cell subsets in the tumor microenvironment is linked with poor prognosis in patients. Widening the knowledge about the regulation of dendritic cell differentiation and functions by different tumor types is important in the development of future therapies against cancers.

7.1. Peptidoglycan modifications of *L. casei* BL23 influence the inflammation-inducing capacity of monocyte-derived dendritic cells

PG as an essential component of the bacterium plays a remarkable role in host-microbe interactions. Host cells can interact with PG or its fragments in different ways and respond to them. PG fragments can be generated by the actions of PGHs which cleave the PG macromolecule at explicit sites. Alterations in PG structure due to the absence of different PGHs can influence the host's response to the PG. In our work, we managed to generate an *L. casei* BL23 strain deficient in Lc-p75 PGH which is a γ -D-glutamyl-L-lysyl endopeptidase, a

major PGH in *L. casei* BL23 and study its moDC- and consequently the T-cell-activating potential.

Besides their prominent probiotic effects, LAB strains such as lactobacilli and their metabolites/components are able to activate dendritic cells, however, the outcomes are varied between studies. A study from Foligne et al demonstrated that *L. salivarius*, *L. rhamnosus* and *L. acidophilus* differentially activated bone marrow derived DCs (BMDCs)¹⁶⁵. BMDCs produced various levels of pro-inflammatory cytokines and chemokines and IL-10. Moreover, bacteria induced elevated expression of MHCII, CD86, and CD40 but the expressional level varied between each lactobacillus-activated BMDCs¹⁶⁵. In another study, the effects of VSL#3 a probiotic cocktail containing *B. longum*, *B. infantis*, *B. breve*, *L. acidophilus*, *L. casei*, *L. delbrueckii* subsp. *bulgaricus*, *L. plantarum* and *Streptococcus salivarius* subsp. *thermophilus* on BMDCs were investigated at different bacterial cell numbers¹⁶⁶. It was revealed, that increasing VSL#3 bacterial load induced more mature BMDC indicated by elevated MHCII and co-stimulatory CD80, CD86, and CD40 expression. When *L. casei* was selected to compare the BMDC-activating potential to a nonpathogenic *E. coli* ATCC 25922 strain, the authors found, that *L. casei* could not cause IL-10 and IL-12 secretion by BMDCs and IFN γ production by T cells¹⁶⁶. Christensen et al also demonstrated that *L. casei* subsp *alactus*-activated BMDCs did not produce IL-10, but secreted IL-12, IL-6, and TNF- α and expressed MHCII and CD86¹⁶⁷. In another interesting study, the *in vitro* and *in vivo* immunomodulatory capacity of different LAB strains was compared¹⁶⁸. The strains induced various concentrations of IL-10 and IL-12; *L. casei* BL23 caused moderate IL-10 production by human PBMC and less IL-12 but could significantly improve the symptoms of TNBS-induced colitis in BALB/c mice. In line with these data, our results showed that wild-type *L. casei* BL23 induced the maturation of moDCs indicated by the elevated expression of CD83, MHCII, and co-stimulatory molecules. Additionally, WT *L. casei*-activated moDCs secreted pro-inflammatory cytokines and chemokines, and T-cell polarizing cytokines as well. Moreover, WT *L. casei*-exposed moDCs induced the activation of IFN γ and IL-17A-producing T cells. These observations emphasize the strain- and condition-dependent immunomodulatory actions of different LAB strains and prove the difficulties of microbiota research.

One of many beneficial effects attributed to LAB is inhibiting the adherence, colonization, and biofilm formation of pathogens and pathobionts. The colonization resistance may be executed in many ways, including competition for nutrients and energy sources, by soluble factors like bile acids or antimicrobial peptides and proteins¹⁶⁹. In addition to this, it has previously been explored that some Lactobacillus strains have high adhesion and aggregation

potential which may be efficient against pathogenic biofilm formation and mediate modulatory mechanisms to the host cells^{170,171}. Inactivation of Lc-p75 in *L. casei* BL23 led to the formation of long-chain, aggregated phenotype which induced significantly less inflammatory and T-cell-polarizing cytokine secretion by moDCs as compared to wild-type bacteria in our experimental system. Moreover, Lc-p75 defective *L. casei* caused reduced Th1 and Th17 responses via the attenuated T-cell-polarizing cytokine secretion by moDCs. Intriguingly, the expression of CD83, HLA-DQ, CD80, and CD86 molecules on the moDCs was not affected by the Lc-p75 mutation in *L. casei* BL23. It has been published that DCs from Crohn's disease patients bearing a Nod2fs mutation had a normal maturation indicated by the elevated level of CD80 and CD86 molecules after TLR stimulation¹⁷². Besides, IL-12p70, TNF- α , and IL-10 production remained also unaffected by the DCs derived from CD patients upon TLR activation. However, NOD2 ligand MDP-exposed DCs patients failed to induce the expression of co-stimulatory molecules and the cytokine secretion was completely abrogated by the DCs. In contrast to this, in a paper in which the moDC-modulatory capacity of *L. reuteri* ATCC PTA 6475 and its CmbA, a mucus-binding protein inactivated counterpart was studied, it was found that wild-type and CmbA-mutant *L. reuteri* ATCC PTA 6475 induced the expression of CD83, CD80, CD86, and HLA-DR at a similar level, while WT *L. reuteri* promoted more TNF- α , IL-12 and IL-1 β secretion by moDCs than its mutant counterpart¹⁵⁴. Similar to the cell surface markers, Lc-p75 mutation in *L. casei* BL23 did not influence the IL-8 production by moDCs in our experiments. In good agreement with this, in a study executed with human macrophages it was found that nuclear I κ B α inhibited the release of TNF α , IL-1 β , and IL-6 upon LPS stimulation, however, IL-8 production remained unaffected¹⁷³. Another study demonstrated that the inactivation of Regulator of G-protein Signaling 16 (RGS16) in THP-1 cell line induced elevated TNF α , IL-1 β and IL-6 production but not IL-8¹⁷⁴. These results suggest that the regulation of the IL-8 gene expression differs from the inflammatory cytokines. Indeed, it has recently been published that ERK3 controls the IL-8 production by gut epithelial cells, but there is no available information about its contribution to the regulation of cytokine production¹⁷⁵.

To further analyze, that the observed discrepancy between live WT and Δ Lc-p75 mutant *L. casei* in inflammatory-inducing capacity by moDCs is the direct outcome of the altered bacterial PG components, we investigated the moDC-activating ability of purified PG from the WT and Lc-p75 mutant strains. Inactivation of Lc-p75 in *L. casei* results in a decreased amount of disaccharide-dipeptide fragments¹³¹. Based on our results, we concluded that the modified PG in Δ Lc-p75 mutant could activate its receptor on moDCs with similar efficiency as the fragments derived from WT bacteria. Indeed, analyses of PG components of pathogenic

bacteria¹⁷⁶ and *L. acidophilus*¹²⁰ uncovered that disaccharide units regardless of the number of peptide residues can trigger innate immune responses. In contrast to this, previously, Grangette et al. showed that *L. plantarum* with modified teichoic acid (TA) could diminish the inflammatory cytokine secretion by human PBMC *in vitro* and reduce inflammation in colitis model *in vivo*¹¹¹. However, they found that the purified TA behaved similarly to the whole bacteria, so the structural modification of the TA determined the inflammatory-provoking potential of *L. plantarum*.

Besides the altered composition of PG, the Lc-p75 defective *L. casei* BL23 strain has significant morphological alterations consisting of the formation of long cell chains, we concluded that its low/moderate DC-activating capacity may be the consequence of its impaired phagocytic uptake.

7.2. Phagocytosis of *L. casei* BL23 is an elemental step in the induction of moDC activation

Dendritic cells can continuously monitor the extracellular space around them and ingest various substances by different endocytic processes, such as pinocytosis, receptor-mediated endocytosis, and phagocytosis⁹⁸. Many studies have shown that DCs can engulf various Lactobacillus strains. In a study with porcine APCs, *L. jensenii* TL2937 was efficiently phagocytosed and increased the production of IL-1 β , IL-12p70, and IL-10 by moDCs¹⁵². In another study, *L. rhamnosus* JB-1 bacteria were actively internalized by human moDCs causing weak co-stimulatory molecule expression and cytokine secretion¹⁵³. In accordance with these data, moDCs were able to efficiently phagocytose *L. casei* BL23; however, Lc-p75 mutant strain with long-chain forming morphology was weakly engulfed by moDCs. Similarly, it has been shown that wild-type *L. reuteri* ATCC 6475 and ATCC 53608 strains were actively phagocytosed, but their CmbA and mucus-binding proteins deficient counterparts were less engulfed by moDCs¹⁵⁴.

The phagocytic process depends on various factors, including the participating receptors, duration and affinity of the binding and the physical features of the target like the size and shape^{97,177}. It has previously been demonstrated that the size of the bacterial aggregates determines the efficiency of the phagocytosis by polymorphonuclear leukocytes (PMNs) affecting the killing capacity of the PMNs¹⁷⁸. Hence, the properties of the internalization process may guide the nature of the emerging immune responses. When heat-killed *S. aureus* was added to mouse macrophages, the phagocytosis and intracellular Nod proteins also contributed to the cytokine production¹⁷⁹. In our experimental system, the long-chain-forming mutant counterpart of *L. casei* BL23 induced only a limited inflammatory and T-cell-polarizing

cytokine production by moDCs as compared to WT *L. casei*. The relevance of phagocytosis was also corroborated by its blockade with cytochalasin D, which caused a robust reduction in the pro-inflammatory and T-cell-polarizing cytokine secretion by moDCs, similarly to the Lc-p75 mutant bacteria-activated moDCs. This observation is in good agreement with a study obtained with human monocytes activated by *Candida albicans* and *Saccharomyces cerevisiae*¹⁸⁰. Cytochalasin D strongly decreased the pro-inflammatory and IL-10 secretion by monocytes.

Morphological plasticity like forming long chains by inhibiting cell septation is a survival strategy for pathogens¹⁸¹, such as uropathogenic *E. coli* to avoid phagocytosis by the immune cells or increase antibiotic resistance⁶⁵. Moreover, the filamentous form of *Haemophilus influenzae* can participate in biofilm formation and can cause otitis media in the chinchilla's inner ear¹⁸². On the contrary, long cell chains of *Enterococcus faecalis* mutants were reported to be more susceptible to phagocytosis and thus less virulent¹⁸³.

Based on our findings and the literature, we can interpret our results relevant to *in vivo* situations in the following ways: 1) Direct interaction of the moDCs with *L. casei* BL23 induces an inflammatory response, which is sufficient to promote adaptive, memory Th1 and Th17 responses and at the same time drives IL-10 secretion which is crucial for the maintenance of tolerance against mutualistic microbes in the gut. 2) Aggregated, filamentous *L. casei* BL23 due to the successful evasion of its phagocytosis by moDCs induces reduced inflammation and adaptive immune responses to avoid excessive activation of the immune cells and thus harmful reactions to the healthy tissues.

Overall, these results demonstrated that the immunomodulatory mechanisms exerted by *L. casei* BL23 are strikingly dependent on their internalization by moDCs. The uptake defines the cytokine production by moDCs, which can be translated to the inflammatory response and to stimulatory Th1/Th17-driven adaptive immune responses. The long-chain-forming Lc-p75 mutant *L. casei* bacteria, which are less efficiently phagocytosed, cause moderate moDC and T cell responses, similar to the moDCs unable to phagocytose wild-type *L. casei* due to the action of cytochalasin D (**Figure 36**).

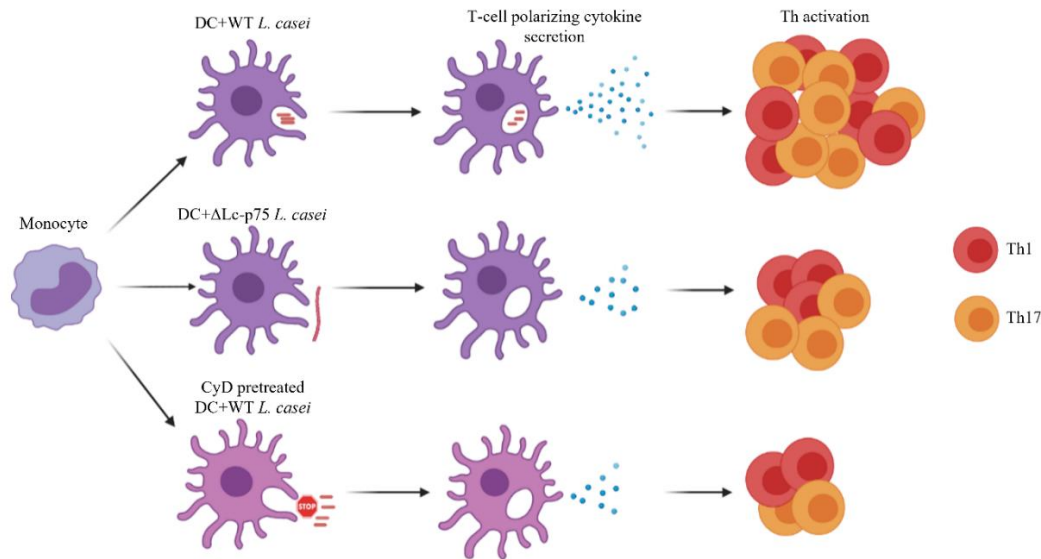


Figure 36. Schematic representation of the immunomodulatory role of wild-type (WT) and Lc-p75 mutant *L. casei* BL23. Monocytes were differentiated to DCs and were exposed to WT, Lc-p75 mutant *L. casei* and CyD inhibiting the actin polymerization. WT bacteria were phagocytosed by moDCs thus, enhanced the Th1- and Th17-stimulating capacity of these cells and consequently the number of Th1 and Th17 cells. In contrast to this, *L. casei* BL23 inactivated in Lc-p75 were internalized with less efficiency by moDCs which led to reduced T-cell activation by these cells and hence fewer T-cell numbers similar to the CyD-treated moDCs exposed to WT bacteria. Created in BioRender.

7.3. Soluble mediators derived from melanoma and adenocarcinoma cell lines differentially affect the differentiation and phagocytic activity of moDCs

DC subsets form an important part of the tumor microenvironment due to their action as APCs and contribute significantly to the antitumor or tumor-promoting responses via orchestrating the T-cell activities¹⁸⁴. Regulatory DCs can be generated from monocytes but the divergencies in cancer types, tissue of origin, the stage of tumor progression, and the slight differences in the tumor microenvironment can lead to a variety of phenotypical and functional properties¹⁸⁵.

Tumors secrete soluble mediators/factors which manipulate the differentiation and functions of the DC subtypes. During the differentiation from CD14⁺ monocytes, DCs begin to express CD209/DC-SIGN and parallelly they lose the CD14 from their surface via epigenetic changes¹⁵⁹. However, CD14⁺ DCs can be found normally in the dermis¹⁸⁶, either induced by stromal cell-derived factors¹⁸⁷ or at increased frequency in many diseases including rheumatoid and psoriatic arthritis¹⁸⁸ and in various types of cancers^{146,189}. In line with these data, melanoma, and adenocarcinoma-derived soluble factors could induce the expression of CD14 to varying degrees, while CD209 expression remained unaffected except WM983A, primary melanoma cells and their metastatic counterpart WM983B cells.

Besides CD209, CD1a, a group 1 CD1 molecule is increasingly expressed on the surface of moDCs upon differentiation¹⁵⁵. Since CD1a presents lipid or glycolipid antigens to T cells, tumor cells readily reduce its expression by the DCs thereby evading the tumor antigen presentation¹⁶⁰. All the examined tumor CM in our experiments downregulated the expression of CD1a by the DCs. Furthermore, it has been demonstrated that tumors and tumor-derived molecules decrease the capacity of peptide antigen presentation and co-stimulation by the DCs¹⁹⁰. In our experiments neither HLA-ABC, HLA-DR nor CD86 expression was altered significantly by the tumor-derived factors in comparison with non-treated control cells indicating that these moDCs retained their ability to activate T cells.

Antigen processing by APCs requires the uptake of the antigens by any endocytic pathway. Owing to the largely expressed “don’t eat me” signals by the tumor cells, they successfully evade the phagocytosis and the subsequent tumor antigen presentation by the APCs. In a clinical approach these phagocytosis inhibitory signals such as CD47-SIRP α and PD-1-PD-L1 serve as phagocytosis checkpoint therapies against different tumor types including solid tumors and lymphomas as well¹⁹¹. In our experimental setting, phagocytosis of the *L. casei* BL23 was not blocked by the TU-CM, and parallel they tended to elevate the frequency of PD-L1^{high} moDCs except WM983A. Despite PD-L1 negatively affects phagocytosis we found a positive correlation between phagocytosis and PD-L1 expression by both adenocarcinoma- and melanoma-CM-exposed moDCs.

It has been illustrated by multiple studies that certain bacterial strains from the microbiota including *Bifidobacterium longum* (*B. longum*), *Enterococcus faecium*, Faecalibacterium species and *A. muciniphila* were linked to the increased efficiency of anti-PD-1-PD-L1 therapy in melanoma patients and in mouse experiments^{192,193}. Moreover, it has recently been reported that four Bifidobacterium species, *B. bifidum*, *B. longum*, *B. lactis* and *B. breve* could be detected in the colonic tumor tissues and enhanced the efficacy of the anti-CD47 immunotherapy¹⁹⁴. In both cases, DCs were the targeted cells by the microbiota members, however the precise interactions between the bacteria, tumor cells and DCs remained unclear.

Taken together, we provided a comprehensive analysis of the differentiation and functions of several tumor-derived soluble factor-exposed moDCs facilitating the *in vitro* differentiation of tumor-conditioned moDCs. Correlation analyses showed tumor type-specific actions on the differentiation and phagocytic potential of moDCs. The exerted immunomodulatory actions did not depend on the tissue origin or the stage of tumor growth.

8. SUMMARY

“All disease begins in the gut” said Hippocrates more than 2000 years ago and it is now becoming increasingly clear that he was right, owing to the numerous studies attempted to investigate the relationship between microbiota and the human host. Many beneficial and modulatory actions are attributed to the mutualistic bacteria in our gastrointestinal tract. Disruption of their delicate balance can lead to serious diseases, including inflammatory disorders, autoimmunity and even cancer.

Considering the complex organizing functions of the different DC subsets, it is evident that these cell types are excellent targets for studying the symbiotic bacteria-exerted immunomodulatory effects, which are commonly context- and strain-dependent. In our work, we aimed to set up an *in vitro* experimental system in which the moDC-modulatory properties of *L. casei* and its altered PG can be analyzed. We found that the presence of WT *L. casei* induced more prominent inflammatory and Th1 and Th17 responses by moDCs than the mutant *L. casei*-induced ones. The morphological differences between the wild-type and mutant bacterial strains were behind these observations. Phagocytic efficiency of moDCs was impaired in the presence of the long-chain forming mutant bacteria like in the actin-polymerization-inhibited WT *L. casei*-exposed moDCs.

Phagocytosis is an essential element in the interaction between transformed cells and immune cells. Cancer cells efficiently evade the recognition and uptake by the immune cells due to their strong direct and indirect immunomodulatory actions, in which DCs are also excellent targets. Cancer cells are able to manipulate the differentiation and functions of all DC subtypes favoring the generation and maintenance of a suppressive microenvironment. However, the exerted immunomodulatory activities by the cancers are context and tumor-type specific. In our work, we attempted to compare the regulatory actions of different adenocarcinoma- and melanoma cell line derived soluble factors on the differentiation and functions of moDCs. Our results stress the differences in the impacts of distinct tumor cell-lines in the regulation of moDC differentiation and phagocytic activity regardless of origin and primary or metastatic activity.

Collectively, by targeting the moDCs by external factors such as altered microbiota members or different cancer cell-derived factors, the moDC-mediated immune responses can be fundamentally changed. These collected observations may help in the deeper understanding of the complex interactions between the innocent microbiota members and DCs, as well as the dangerous cancer cells and the DCs.

9. ÖSSZEFOGLALÁS

“Minden betegség a belekben kezdődik” mondta több mint 2000 évvel ezelőtt Hippokratész. A kijelentés igaza mostanában kezd tisztázódni köszönhetően annak a rengeteg tanulmánynak, amelyek a számos előnyös tulajdonsággal rendelkező mikrobióta és a gazdaszervezet kölcsönhatásaival foglalkoznak. A mikrobióta és a gazdaszervezet kényes egyensúlyának felbomlása súlyos állapotok kialakulásának kedvez úgy, mint gyulladásoz megbetegedések, autoimmun betegségek és tumoros állapotok.

Tekintve a különféle dendritikus sejt (DS) alpopulációk komplex szabályozó szerepét, ezek a sejtek kitűnő jelöltek arra, hogy nyomon kövessük a különféle mikrobióta tagok által kiváltott immunmoduláló hatásokat, amelyek nem egyszer környezet- és fajspecifikusak. Munkánk során célul tűztük ki, hogy beállítsunk egy olyan *in vitro* rendszert, amelyben a vad típusú és PG-módosított *L. casei* BL23 baktériumnak a monocita-eredetű DS-eket (moDS) szabályozó hatásait tudjuk vizsgálni. Eredményeink azt mutatták, hogy a vad típusú *L. casei*-vel kezelt moDS-ek gyulladásoz, valamint Th1 és Th17 polarizáló válaszai sokkal kifejezettebbek voltak, mint a mutáns baktériumoknak kitett moDS-eké. Ennek hátterében a baktériumok közötti morfológiai különbségek állnak. A hosszú láncokat alkotó mutáns baktériumokat a moDS-ek nem képesek hatékonyan felvenni, hasonlóan ahhoz, ahogy az aktin polimerizációban gátolt moDS-ek sem tudják hatékonyan bekebelezni a vad típusú *L. casei* sejteket.

A fagocitózis folyamata nélkülözhetetlen szerepet játszik a megváltozott tumoros sejtek és immunsejtek közötti kölcsönhatásban is. A tumoros sejtek sikeresen képesek kivédeni az immunsejtek általi felismerést és felvételt, amelyet közvetlen és közvetett immunmodulációval érnek el tumor- és környezetspecifikus módon. A megváltozott sejtek képesek befolyásolni a DS-ek differenciációját és funkcióit, azért, hogy olyan sejtípust hozzanak létre, amely támogatja a szuppresszív mikrokörnyezet kialakulását és fenntartását. Munkánk során összehasonlítottunk azokat a szabályozó folyamatokat, amelyeket adenokarcinóma és melanoma sejtvonalakból származó faktorok okoztak az moDS-ek differenciációjában és fagocitózis képességében. Eredményeink szerint, a tumorok közvetett hatásai nagyon heterogének, függetlenek a szöveti eredettől és a metasztatikus állapottól.

Összefoglalva elmondható, hogy az olyan külső faktorok, mint megváltozott mikrobióta tagok, illetve különböző tumor típusokból származó faktorok alapjaiban véve változtatják meg az moDS-ek által kiváltott immunválaszokat. Remélhetőleg a megfigyeléseink hozzájárulnak azon komplex kölcsönhatások jobb megismeréséhez, amelyek az ártalmatlan mikrobióta tagok és a DS-ek, valamint a veszélyes transzformálódott sejtek és a DS-ek között zajlanak.

10. REFERENCES

1. Proctor, L. What's next for the human microbiome? *Nature* **569**, 623 (2017).
2. Marchesi, J. R. & Ravel, J. The vocabulary of microbiome research: a proposal. *Microbiome* **3**, 1–3 (2015).
3. Berg, G. *et al.* Microbiome definition re-visited: old concepts and new challenges. *Microbiome* **8**, 1–22 (2020).
4. Martino, C. *et al.* Microbiota succession throughout life from the cradle to the grave. *Nat. Rev. Microbiol.* **0123456789**, (2022).
5. Hou, K. *et al.* Microbiota in health and diseases. *Signal Transduct. Target. Ther.* **7**, 135 (2022).
6. Donaldson, G. P., Lee, S. M. & Mazmanian, S. K. Gut biogeography of the bacterial microbiota. *Nat. Rev. Microbiol.* **14**, 20–32 (2015).
7. Thursby, E. & Juge, N. Introduction to the human gut microbiota. *Biochem. J.* **474**, 1823–1836 (2017).
8. Hornef, M. Pathogens, commensal symbionts, and pathobionts: Discovery and functional effects on the host. *ILAR J.* **56**, 159–162 (2015).
9. Ren, C. *et al.* Protective effects of lactic acid bacteria on gut epithelial barrier dysfunction are Toll like receptor 2 and protein kinase C dependent. *Food Funct.* **11**, 1230–1234 (2020).
10. Natividad, J. M. M. & Verdu, E. F. Modulation of intestinal barrier by intestinal microbiota: Pathological and therapeutic implications. *Pharmacol. Res.* **69**, 42–51 (2013).
11. Bäumlner, A. J. & Sperandio, V. Interactions between the microbiota and pathogenic bacteria in the gut. *Nature* **535**, 85–93 (2016).
12. Campana, R., Van Hemert, S. & Baffone, W. Strain-specific probiotic properties of lactic acid bacteria and their interference with human intestinal pathogens invasion. *Gut Pathog.* **9**, 1–12 (2017).
13. LeBlanc, J. G., Levit, R., Savoy de Giori, G. & de Moreno de LeBlanc, A. Application of vitamin-producing lactic acid bacteria to treat intestinal inflammatory diseases. *Appl. Microbiol. Biotechnol.* **104**, 3331–3337 (2020).
14. Den Besten, G. *et al.* The role of short-chain fatty acids in the interplay between diet, gut microbiota, and host energy metabolism. *J. Lipid Res.* **54**, 2325–2340 (2013).
15. Resta, S. C. Effects of probiotics and commensals on intestinal epithelial physiology: Implications for nutrient handling. *J. Physiol.* **587**, 4169–4174 (2009).
16. Vieira, A. T., Teixeira, M. M. & Martins, F. S. The role of probiotics and prebiotics in inducing gut immunity. *Front. Immunol.* **4**, 1–12 (2013).
17. Yan, F. & Polk, D. B. Probiotics and immune health. *Curr. Opin. Gastroenterol.* **27**, 496–501 (2011).
18. Gensollen, T., Iyer, S. S., Kasper, D. L. & Blumberg, R. S. How colonization by microbiota in early life shapes the immune system. *Science (80-.)*. **352**, 539–544 (2016).
19. Risnes, K. R., Belanger, K., Murk, W. & Bracken, M. B. Antibiotic exposure by 6 months and asthma and allergy at 6 years: Findings in a cohort of 1,401 US children. *Am. J. Epidemiol.* **173**, 310–318 (2011).
20. Kronman, M. P., Zaoutis, T. E., Haynes, K., Feng, R. & Coffin, S. E. Antibiotic exposure and IBD development among children: A population-based cohort study. *Pediatrics* **130**, (2012).
21. Azad, M. B., Bridgman, S. L., Becker, A. B. & Kozyrskyj, A. L. Pediatric original article infant antibiotic exposure and the development of childhood overweight and central adiposity. *Int. J. Obes.* **38**, 1290–1298 (2014).
22. Boursi, B., Mamtani, R., Haynes, K. & Yang, Y. X. The effect of past antibiotic exposure on diabetes risk. *Eur. J. Endocrinol.* **172**, 639–648 (2015).
23. Randall, T. D. & Mebius, R. E. The development and function of mucosal lymphoid tissues: A balancing act with micro-organisms. *Mucosal Immunol.* **7**, 455–466 (2014).
24. Elmore, S. A. Enhanced Histopathology of Mucosa-Associated Lymphoid Tissue. *Toxicol. Pathol.* **34**, 687–696 (2006).
25. Herath, M., Hosie, S., Bornstein, J. C., Franks, A. E. & Hill-Yardin, E. L. The Role of the Gastrointestinal Mucus System in Intestinal Homeostasis: Implications for Neurological Disorders. *Front. Cell. Infect. Microbiol.* **10**, (2020).

26. Johansson, M. E. V., Sjövall, H. & Hansson, G. C. The gastrointestinal mucus system in health and disease. *Nat. Rev. Gastroenterol. Hepatol.* **10**, 352–361 (2013).
27. Rogier, E. W., Frantz, A. L., Bruno, M. E. C. & Kaetzel, C. S. Secretory IgA is concentrated in the outer layer of colonic mucus along with gut bacteria. *Pathogens* **3**, 390–403 (2014).
28. Sicard, J. F., Bihan, G. Le, Vogeleer, P., Jacques, M. & Harel, J. Interactions of intestinal bacteria with components of the intestinal mucus. *Front. Cell. Infect. Microbiol.* **7**, (2017).
29. Berry, D. *et al.* Host-compound foraging by intestinal microbiota revealed by single-cell stable isotope probing. *Proc. Natl. Acad. Sci. U. S. A.* **110**, 4720–4725 (2013).
30. Nava, G. M., Friedrichsen, H. J. & Stappenbeck, T. S. Spatial organization of intestinal microbiota in the mouse ascending colon. *ISME J.* **5**, 627–638 (2011).
31. KORELITZ, B. I. & JANOWITZ, H. D. The physiology of intestinal absorption. *J. Mt. Sinai Hosp. N. Y.* **24**, 181–205 (1957).
32. Lee, S. H. Intestinal Permeability Regulation by Tight Junction: Implication on Inflammatory Bowel Diseases. *Intest. Res.* **13**, 11 (2015).
33. Fukata, M. & Arditì, M. The role of pattern recognition receptors in intestinal inflammation. *Mucosal Immunol.* **6**, 451–463 (2013).
34. Kagnoff, M. F. The intestinal epithelium is an integral component of a communications network. *J. Clin. Invest.* **124**, 2841–2843 (2014).
35. Bevins, C. L. & Salzman, N. H. Paneth cells, antimicrobial peptides and maintenance of intestinal homeostasis. *Nat. Rev. Microbiol.* **9**, 356–368 (2011).
36. Kobayashi, K. S. *et al.* Nod2-dependent regulation of innate and adaptive immunity in the intestinal tract. *Science (80-.)*. **307**, 731–734 (2005).
37. Petnicki-Ocwieja, T. *et al.* Nod2 is required for the regulation of commensal microbiota in the intestine. *Proc. Natl. Acad. Sci. U. S. A.* **106**, 15813–15818 (2009).
38. Mei, X., Gu, M. & Li, M. Plasticity of Paneth cells and their ability to regulate intestinal stem cells. *Stem Cell Res. Ther.* **11**, 1–13 (2020).
39. Gribble, F. M. & Reimann, F. Function and mechanisms of enteroendocrine cells and gut hormones in metabolism. *Nat. Rev. Endocrinol.* **15**, 226–237 (2019).
40. Hendel, S. K. *et al.* Tuft Cells and Their Role in Intestinal Diseases. *Front. Immunol.* **13**, 1–13 (2022).
41. Mörbe, U. M. *et al.* Human gut-associated lymphoid tissues (GALT); diversity, structure, and function. *Mucosal Immunol.* **14**, 793–802 (2021).
42. Mowat, A. M. & Agace, W. W. Regional specialization within the intestinal immune system. *Nat. Rev. Immunol.* **14**, 667–685 (2014).
43. Mabbott, N. A., Donaldson, D. S., Ohno, H., Williams, I. R. & Mahajan, A. Microfold (M) cells: Important immunosurveillance posts in the intestinal epithelium. *Mucosal Immunol.* **6**, 666–677 (2013).
44. Schulz, O. & Pabst, O. Antigen sampling in the small intestine. *Trends Immunol.* **34**, 155–161 (2013).
45. Barone, F., Patel, P., Sanderson, J. D. & Spencer, J. Gut-associated lymphoid tissue contains the molecular machinery to support T-cell-dependent and T-cell-independent class switch recombination. *Mucosal Immunol.* **2**, 495–503 (2009).
46. Reboldi, A. *et al.* Mucosal immunology: IgA production requires B cell interaction with subepithelial dendritic cells in Peyer’s patches. *Science (80-.)*. **352**, (2016).
47. Stagg, A. J. Intestinal Dendritic Cells in Health and Gut Inflammation. **9**, 1–10 (2018).
48. Junker, Y. *et al.* Comparative analysis of mononuclear cells isolated from mucosal lymphoid follicles of the human ileum and colon. *Clin. Exp. Immunol.* **156**, 232–237 (2009).
49. Verbrugge, P., Kujala, P., Waelput, W., Peters, P. J. & Cuvelier, C. A. Clusterin in human gut-associated lymphoid tissue, tonsils, and adenoids: Localization to M cells and follicular dendritic cells. *Histochem. Cell Biol.* **129**, 311–320 (2008).
50. Granot, T. *et al.* Dendritic Cells Display Subset and Tissue-Specific Maturation Dynamics over Human Life. *Immunity* **46**, 504–515 (2017).
51. Senda, T. *et al.* Microanatomical dissection of human intestinal T-cell immunity reveals site-specific changes in gut-associated lymphoid tissues over life. *Mucosal Immunol.* **12**, 378–389 (2019).

52. Zhao, Y. *et al.* Spatiotemporal segregation of human marginal zone and memory B cell populations in lymphoid tissue. *Nat. Commun.* **9**, (2018).
53. Langman, J. M. & Rowland, R. The number and distribution of lymphoid follicles in the human large intestine. *J. Anat.* **149**, 189–94 (1986).
54. Fenton, T. M. *et al.* Immune Profiling of Human Gut-Associated Lymphoid Tissue Identifies a Role for Isolated Lymphoid Follicles in Priming of Region-Specific Immunity. *Immunity* **52**, 557-570.e6 (2020).
55. Spencer, J. & Sollid, L. M. The human intestinal B-cell response. *Mucosal Immunol.* **9**, 1113–1124 (2016).
56. Macpherson, A. J. & Smith, K. Mesenteric lymph nodes at the center of immune anatomy. *J. Exp. Med.* **203**, 497–500 (2006).
57. Huang, F. P. *et al.* A discrete subpopulation of dendritic cells transports apoptotic intestinal epithelial cells to T cell areas of mesenteric lymph nodes. *J. Exp. Med.* **191**, 435–443 (2000).
58. Sun, M., He, C., Cong, Y. & Liu, Z. Regulatory immune cells in regulation of intestinal inflammatory response to microbiota. *Mucosal Immunol.* **8**, 969–978 (2015).
59. Okumura, R. & Takeda, K. Maintenance of gut homeostasis by the mucosal immune system. *Proc. Japan Acad. Ser. B Phys. Biol. Sci.* **92**, 423–435 (2016).
60. Ma, H., Qiu, Y. & Yang, H. Intestinal intraepithelial lymphocytes: Maintainers of intestinal immune tolerance and regulators of intestinal immunity. *J. Leukoc. Biol.* **109**, 339–347 (2021).
61. Thorburn, A. N. *et al.* Evidence that asthma is a developmental origin disease influenced by maternal diet and bacterial metabolites. *Nat. Commun.* **6**, (2015).
62. Sequeira, R. P., McDonald, J. A. K., Marchesi, J. R. & Clarke, T. B. Commensal Bacteroidetes protect against *Klebsiella pneumoniae* colonization and transmission through IL-36 signalling. *Nat. Microbiol.* **5**, 304–313 (2020).
63. Panwar, R. B., Sequeira, R. P. & Clarke, T. B. Microbiota-mediated protection against antibiotic-resistant pathogens. *Genes Immun.* **22**, 255–267 (2021).
64. Kim, S. G. *et al.* Microbiota-derived lantibiotic restores resistance against vancomycin-resistant *Enterococcus*. *Nature* **572**, 665–669 (2019).
65. Justice, S. S., Hunstad, D. A., Seed, P. C. & Hultgren, S. J. Filamentation by *Escherichia coli* subverts innate defenses during urinary tract infection. *Proc. Natl. Acad. Sci. U. S. A.* **103**, 19884–19889 (2006).
66. Qian, Z. *et al.* Probiotic *Lactobacillus* Sp. Strains inhibit growth, adhesion, biofilm formation, and gene expression of bacterial vaginosis-inducing *Gardnerella vaginalis*. *Microorganisms* **9**, (2021).
67. Madsen, K. L. Enhancement of epithelial barrier function by probiotics. *J. Epithel. Biol. Pharmacol.* **5**, 55–59 (2012).
68. Erturk-Hasdemir, D. *et al.* Symbionts exploit complex signaling to educate the immune system. *Proc. Natl. Acad. Sci. U. S. A.* **116**, 26157–26166 (2019).
69. Ivanov, I. I. *et al.* Induction of Intestinal Th17 Cells by Segmented Filamentous Bacteria. *Cell* **139**, 485–498 (2009).
70. Amlan, B., Petnicki-Ocwieja, T. & Kobayashi, K. S. Nod2: a key regulator linking microbiota to intestinal mucosal immunity. *J. Mol. Med.* **90**, 15–24 (2012).
71. Fox, B. E., Vilander, A., Abdo, Z. & Dean, G. A. NOD2 signaling in CD11c + cells is critical for humoral immune responses during oral vaccination and maintaining the gut microbiome. *Sci. Rep.* **12**, 1–14 (2022).
72. Clark, M. A., Hirst, B. H. & Jepson, M. A. M-cell surface β 1 integrin expression and invasion-mediated targeting of *Yersinia pseudotuberculosis* to mouse Peyer’s patch M cells. *Infect. Immun.* **66**, 1237–1243 (1998).
73. Chiba, S. *et al.* Listerial invasion protein internalin B promotes entry into ileal Peyer’s patches in vivo. *Microbiol. Immunol.* **55**, 123–129 (2011).
74. Mantis, N. J. *et al.* Selective Adherence of IgA to Murine Peyer’s Patch M Cells: Evidence for a Novel IgA Receptor. *J. Immunol.* **169**, 1844–1851 (2002).
75. Rochereau, N. *et al.* Dectin-1 Is Essential for Reverse Transcytosis of Glycosylated SIgA-Antigen Complexes by Intestinal M Cells. *PLoS Biol.* **11**, (2013).
76. Lelouard, H., Fallet, M., De Bovis, B., Méresse, S. & Gorvel, J. Peyer’s patch dendritic cells

- sample antigens by extending dendrites through M cell-specific transcellular pores. *Gastroenterology* **142**, 592-601.e3 (2012).
77. Lelouard, H. *et al.* Pathogenic Bacteria and Dead Cells Are Internalized by a Unique Subset of Peyer's Patch Dendritic Cells That Express Lysozyme. *Gastroenterology* **138**, 173-184.e3 (2010).
 78. Sakhony, O. S. *et al.* M cell-derived vesicles suggest a unique pathway for trans-epithelial antigen delivery. *Tissue Barriers* **3**, 37-41 (2015).
 79. Komban, R. J. *et al.* Activated Peyer's patch B cells sample antigen directly from M cells in the subepithelial dome. *Nat. Commun.* **10**, 1-15 (2019).
 80. Bonnardel, J. *et al.* Innate and Adaptive Immune Functions of Peyer's Patch Monocyte-Derived Cells. *Cell Rep.* **11**, 770-784 (2015).
 81. Wagner, C. *et al.* Differentiation Paths of Peyer's Patch LysoDCs Are Linked to Sampling Site Positioning, Migration, and T Cell Priming. *Cell Rep.* **31**, (2020).
 82. Da Silva, C., Wagner, C., Bonnardel, J., Gorvel, J. P. & Lelouard, H. The Peyer's patch mononuclear phagocyte system at steady state and during infection. *Front. Immunol.* **8**, (2017).
 83. Iwasaki, A. & Kelsall, B. L. Unique Functions of CD11b + , CD8 α + , and Double-Negative Peyer's Patch Dendritic Cells . *J. Immunol.* **166**, 4884-4890 (2001).
 84. Fleeton, M. N. *et al.* Peyer ' s Patch Dendritic Cells Process Viral Antigen from Apoptotic Epithelial Cells in the Intestine of Reovirus-infected Mice The Journal of Experimental Medicine. *J. Exp. Med.* **200**, (2004).
 85. Jaensson, E. *et al.* Small intestinal CD103+ dendritic cells display unique functional properties that are conserved between mice and humans. *J. Exp. Med.* **205**, 2139-2149 (2008).
 86. Watchmaker, P. B. *et al.* Comparative transcriptional and functional profiling defines conserved programs of intestinal DC differentiation in humans and mice. *Nat. Immunol.* **15**, 98-108 (2014).
 87. Sun, T., Nguyen, A. & Gommerman, J. L. Dendritic Cell Subsets in Intestinal Immunity and Inflammation. *J. Immunol.* **204**, 1075-1083 (2020).
 88. Niess, J. H. *et al.* CX3CR1-mediated dendritic cell access to the intestinal lumen and bacterial clearance. *Science (80-.)*. **307**, 254-258 (2005).
 89. Rescigno, M. *et al.* Dendritic cells express tight junction proteins and penetrate gut epithelial monolayers to sample bacteria. *Nat. Immunol.* **2**, 361-367 (2001).
 90. Farache, J. *et al.* Luminal Bacteria Recruit CD103+ Dendritic Cells into the Intestinal Epithelium to Sample Bacterial Antigens for Presentation. *Immunity* **38**, 581-595 (2013).
 91. McDole, J. R. *et al.* Goblet cells deliver luminal antigen to CD103 + dendritic cells in the small intestine. *Nature* **483**, 345-349 (2012).
 92. Yoshida, M. *et al.* Human neonatal Fc receptor mediates transport of IgG into luminal secretions for delivery of antigens to mucosal dendritic cells. *Immunity* **20**, 769-783 (2004).
 93. Mazzini, E., Massimiliano, L., Penna, G. & Rescigno, M. Oral Tolerance Can Be Established via Gap Junction Transfer of Fed Antigens from CX3CR1+ Macrophages to CD103+ Dendritic Cells. *Immunity* **40**, 248-261 (2014).
 94. Brode, S. & MacAry, P. A. Cross-presentation: Dendritic cells and macrophages bite off more than they can chew! *Immunology* **112**, 345-351 (2004).
 95. Kumari, S., Mg, S. & Mayor, S. Endocytosis unplugged: Multiple ways to enter the cell. *Cell Res.* **20**, 256-275 (2010).
 96. Garrett, W. S. *et al.* Developmental control of endocytosis in dendritic cells by Cdc42. *Cell* **102**, 325-334 (2000).
 97. Underhill, D. M. & Goodridge, H. S. Information processing during phagocytosis. *Nat. Rev. Immunol.* **12**, 492-502 (2017).
 98. Liu, Z. & Roche, P. A. Macropinocytosis in phagocytes: Regulation of MHC class-II-restricted antigen presentation in dendritic cells. *Front. Physiol.* **6**, 1-6 (2015).
 99. Mercanti, V. *et al.* Selective membrane exclusion in phagocytic and macropinocytic cups. *J. Cell Sci.* **119**, 4079-4087 (2006).
 100. von Delwig, A. *et al.* Inhibition of macropinocytosis blocks antigen presentation of type II collagen in vitro and in vivo in HLA-DR1 transgenic mice. *Arthritis Res. Ther.* **8**, 1-11 (2006).
 101. Marina-García, N. *et al.* Clathrin- and Dynamin-Dependent Endocytic Pathway Regulates Muramyl Dipeptide Internalization and NOD2 Activation. *J. Immunol.* **182**, 4321-4327 (2009).

102. Popescu, N. I. *et al.* Internalization of Polymeric Bacterial Peptidoglycan Occurs through Either Actin or Dynamin Dependent Pathways. *Microorganisms* **10**, (2022).
103. Loh, L. N., Gao, G. & Tuomanen, E. I. Dissecting bacterial cell wall entry and signaling in eukaryotic cells: An actin-dependent pathway parallels platelet-activating factor receptor-mediated endocytosis. *MBio* **8**, (2017).
104. Bastos, P. A. D., Wheeler, R. & Boneca, I. G. Uptake, recognition and responses to peptidoglycan in the mammalian host. *FEMS Microbiol. Rev.* **45**, 1–25 (2021).
105. Chapot-Chartier, M. P. & Kulakauskas, S. Cell wall structure and function in lactic acid bacteria. *Microb. Cell Fact.* **13**, 1–23 (2014).
106. Sukhithasri, V., Nisha, N., Biswas, L., Anil Kumar, V. & Biswas, R. Innate immune recognition of microbial cell wall components and microbial strategies to evade such recognitions. *Microbiol. Res.* **168**, 396–406 (2013).
107. Bastos, P. A. D., Wheeler, R. & Boneca, I. G. Uptake, recognition and responses to peptidoglycan in the mammalian host. *FEMS Microbiol. Rev.* **45**, 1–25 (2021).
108. Crump, G. M., Mashayekh, S., Zhou, J. & Grimes, C. L. Revisiting peptidoglycan sensing: interactions with host immunity and beyond. *Chem. Commun.* (2020) doi:10.1039/x0xx00000x.
109. Hansen, J. M. *et al.* N-glycolylated peptidoglycan contributes to the immunogenicity but not pathogenicity of mycobacterium tuberculosis. *J. Infect. Dis.* **209**, 1045–1054 (2014).
110. Shida, K., Kiyoshima-Shibata, J., Nagaoka, M., Watanabe, K. & Nanno, M. Induction of interleukin-12 by Lactobacillus strains having a rigid cell wall resistant to intracellular digestion. *J. Dairy Sci.* **89**, 3306–3317 (2006).
111. Grangette, C. *et al.* Enhanced antiinflammatory capacity of a Lactobacillus plantarum mutant synthesizing modified teichoic acids. *Proc. Natl. Acad. Sci. U. S. A.* **102**, 10321–10326 (2005).
112. Abdalla, A. K. *et al.* Exopolysaccharides as Antimicrobial Agents: Mechanism and Spectrum of Activity. *Front. Microbiol.* **12**, (2021).
113. Clarke, T. B. *et al.* Recognition of peptidoglycan from the microbiota by Nod1 enhances systemic innate immunity. *Nat. Med.* **16**, 228–231 (2010).
114. Tosoni, G., Conti, M. & Diaz Heijtz, R. Bacterial peptidoglycans as novel signaling molecules from microbiota to brain. *Curr. Opin. Pharmacol.* **48**, 107–113 (2019).
115. Arentsen, T. *et al.* The bacterial peptidoglycan-sensing molecule Pglyrp2 modulates brain development and behavior. *Mol. Psychiatry* **22**, 257–266 (2017).
116. Liu, Y., Defourny, K. A. Y., Smid, E. J. & Abee, T. Gram-positive bacterial extracellular vesicles and their impact on health and disease. *Front. Microbiol.* **9**, 1–8 (2018).
117. Nagakubo, T., Tahara, Y. O., Miyata, M., Nomura, N. & Toyofuku, M. Mycolic acid-containing bacteria trigger distinct types of membrane vesicles through different routes. *iScience* **24**, 102015 (2021).
118. Viala, J. *et al.* Nod1 responds to peptidoglycan delivered by the Helicobacter pylori cag pathogenicity island. *Nat. Immunol.* **5**, 1166–1174 (2004).
119. Nakamura, N. *et al.* Endosomes are specialized platforms for bacterial sensing and NOD2 signalling. *Nature* **509**, 240–244 (2014).
120. Bersch, K. L. *et al.* Bacterial Peptidoglycan Fragments Differentially Regulate Innate Immune Signaling. *ACS Cent. Sci.* **7**, 688–696 (2021).
121. Do, T., Page, J. E. & Walker, S. Uncovering the activities, biological roles, and regulation of bacterial cell wall hydrolases and tailoring enzymes. *J. Biol. Chem.* **295**, 3347–3361 (2020).
122. Heidrich, C. *et al.* Involvement of N-acetylmuramyl-L-alanine amidases in cell separation and antibiotic-induced autolysis of Escherichia coli. *Mol. Microbiol.* **41**, 167–178 (2001).
123. Vollmer, W. Bacterial growth does require peptidoglycan hydrolases. *Mol. Microbiol.* **86**, 1031–1035 (2012).
124. Hashimoto, M., Ooiwa, S. & Sekiguchi, J. Synthetic lethality of the lytE cw10 genotype in Bacillus subtilis is caused by lack of D, L-endopeptidase activity at the lateral cell wall. *J. Bacteriol.* **194**, 796–803 (2012).
125. Russell, A. B. *et al.* Type VI secretion delivers bacteriolytic effectors to target cells. *Nature* **475**, 343–349 (2011).
126. Yan, F. *et al.* Soluble Proteins Produced by Probiotic Bacteria Regulate Intestinal Epithelial Cell Survival and Growth. *Gastroenterology* **132**, 562–575 (2007).

127. Yan, F. *et al.* Colon-specific delivery of a probiotic-derived soluble protein ameliorates intestinal inflammation in mice through an EGFR-dependent mechanism. *J. Clin. Invest.* **121**, 2242–2253 (2011).
128. Wang, Y. *et al.* An LGG-derived protein promotes IgA production through upregulation of APRIL expression in intestinal epithelial cells. *Mucosal Immunol.* **10**, 373–384 (2017).
129. Bäuerl, C., Pérez-Martínez, G., Yan, F., Polk, D. B. & Monedero, V. Functional analysis of the p40 and p75 proteins from lactobacillus casei BL23. *J. Mol. Microbiol. Biotechnol.* **19**, 231–241 (2011).
130. Bäuerl, C. *et al.* P40 and P75 are singular functional muramidases present in the lactobacillus casei/paracasei/rhamnosus Taxon. *Front. Microbiol.* **10**, 1–17 (2019).
131. Regulski, K. *et al.* Analysis of the peptidoglycan hydrolase complement of lactobacillus casei and characterization of the major γ -D-Glutamyl-L-Lysyl-endopeptidase. *PLoS One* **7**, (2012).
132. Bancalari, E., Castellone, V., Bottari, B. & Gatti, M. Wild Lactobacillus casei Group Strains: Potentiality to ferment plant derived juices. *Foods* **9**, (2020).
133. Johansson, M. A., Sjögren, Y. M., Persson, J. O., Nilsson, C. & Sverremark-Ekström, E. Early colonization with a group of Lactobacilli decreases the risk for allergy at five years of age despite allergic heredity. *PLoS One* **6**, 1–8 (2011).
134. Hill, D. *et al.* The Lactobacillus casei group: History and health related applications. *Front. Microbiol.* **9**, 1–12 (2018).
135. Bravo, J. A. *et al.* Ingestion of Lactobacillus strain regulates emotional behavior and central GABA receptor expression in a mouse via the vagus nerve. *Proc. Natl. Acad. Sci. U. S. A.* **108**, 16050–16055 (2011).
136. Tiptiri-Kourpeti, A. *et al.* Lactobacillus casei exerts anti-proliferative effects accompanied by apoptotic cell death and up-regulation of TRAIL in colon carcinoma cells. *PLoS One* **11**, 1–20 (2016).
137. He, J. F., Jin, D. X., Luo, X. G. & Zhang, T. C. LHH1, a novel antimicrobial peptide with anti-cancer cell activity identified from Lactobacillus casei HZ1. *AMB Express* **10**, (2020).
138. Lenoir, M. *et al.* Lactobacillus casei BL23 regulates Treg and Th17 T-cell populations and reduces DMH-associated colorectal cancer. *J. Gastroenterol.* **51**, 862–873 (2016).
139. Takagi, A. *et al.* Enhancement of natural killer cytotoxicity delayed murine carcinogenesis by a probiotic microorganism. *Carcinogenesis* **22**, 599–605 (2001).
140. Takagi, A. *et al.* Relationship between the in vitro response of dendritic cells to Lactobacillus and prevention of tumorigenesis in the mouse. *J. Gastroenterol.* **43**, 661–669 (2008).
141. Iwanowycz, S. *et al.* Type 2 dendritic cells mediate control of cytotoxic t cell resistant tumors. *JCI Insight* **6**, (2021).
142. Chao, M. P., Weissman, I. L. & Majeti, R. The CD47-SIRP α pathway in cancer immune evasion and potential therapeutic implications. *Curr. Opin. Immunol.* **24**, 225–232 (2012).
143. Barkal, A. A. *et al.* CD24 signalling through macrophage Siglec-10 is a target for cancer immunotherapy. *Nature* **572**, 392–396 (2019).
144. Chao, M. P., Majeti, R. & Weissman, I. L. Programmed cell removal: A new obstacle in the road to developing cancer. *Nat. Rev. Cancer* **12**, 58–67 (2012).
145. Clappaert, E. J., Murgaski, A., Damme, H. Van, Kiss, M. & Laoui, D. Diamonds in the rough: Harnessing tumor-Associated myeloid cells for cancer therapy. *Front. Immunol.* **9**, 1–20 (2018).
146. Spary, L. K. *et al.* Tumor stroma-derived factors skew monocyte to dendritic cell differentiation toward a suppressive CD14 + PD-L1 + phenotype in prostate cancer . *Oncoimmunology* **3**, e955331 (2014).
147. Pillai, K., Pourgholami, M. H., Chua, T. C. & Morris, D. L. MUC1 as a potential target in anticancer therapies. *Am. J. Clin. Oncol. Cancer Clin. Trials* **38**, 108–118 (2015).
148. Scanlon, C. S. *et al.* Galanin modulates the neural niche to favour perineural invasion in head and neck cancer. *Nat. Commun.* **6**, (2015).
149. Zong, J., Keskinov, A. A., Shurin, G. V. & Shurin, M. R. Tumor-derived factors modulating dendritic cell function. *Cancer Immunol. Immunother.* **65**, 821–833 (2016).
150. Xia, C. Q., Peng, R., Beato, F. & Clare-Salzler, M. J. Dexamethasone induces IL-10-producing monocyte-derived dendritic cells with durable immaturity. *Scand. J. Immunol.* **62**, 45–54 (2005).
151. Wang, G. *et al.* Stimulation of tolerogenic dendritic cells using dexamethasone and 1,25-

- dihydroxyvitamin D3 represses autologous T cell activation and chondrocyte inflammation. *Exp. Ther. Med.* **17**, 679–688 (2019).
152. Tsukida, K. *et al.* Immunoregulatory effects triggered by immunobiotic *Lactobacillus jensenii* TL2937 strain involve efficient phagocytosis in porcine antigen presenting cells. *BMC Immunol.* **17**, 1–12 (2016).
 153. Konieczna, P. *et al.* Human dendritic cell DC-SIGN and TLR-2 mediate complementary immune regulatory activities in response to *Lactobacillus rhamnosus* JB-1. *PLoS One* **10**, 1–14 (2015).
 154. Bene, K. P. *et al.* *Lactobacillus reuteri* surface mucus adhesins upregulate inflammatory responses through interactions with innate C-Type lectin receptors. *Front. Microbiol.* **8**, 1–16 (2017).
 155. Gogolak, P. *et al.* Differentiation of CD1a⁻ and CD1a⁺ monocyte-derived dendritic cells is biased by lipid environment and PPAR γ . *Blood* **109**, 643–652 (2007).
 156. Seshadri, C. *et al.* Human CD1a Deficiency Is Common and Genetically Regulated. *J. Immunol.* **191**, 1586–1593 (2013).
 157. Galkina, S. I. *et al.* Erratum to “mold alkaloid cytochalasin d modifies the morphology and secretion of FMLP-, LPS-, or PMA-stimulated neutrophils upon adhesion to fibronectin” (Mediators of Inflammation (2017) 2017 (4308684) DOI: 10.1155/2017/4308684). *Mediators Inflamm.* **2018**, (2018).
 158. Gao, M. *et al.* The influence of actin depolymerization induced by Cytochalasin D and mechanical stretch on interleukin-8 expression and JNK phosphorylation levels in human retinal pigment epithelial cells. *BMC Ophthalmol.* **17**, 4–9 (2017).
 159. Bullwinkel, J., Lüdemann, A., Debarry, J. & Singh, P. B. Epigenotype switching at the CD14 and CD209 genes during differentiation of human monocytes to dendritic cells. *Epigenetics* **6**, 45–51 (2011).
 160. Coventry, B. & Heinzl, S. CD1a in human cancers: A new role for an old molecule. *Trends Immunol.* **25**, 242–248 (2004).
 161. Luo, M. *et al.* Preventive effect of *Lactobacillus reuteri* on melanoma. *Biomed. Pharmacother.* **126**, (2020).
 162. Yang, X. *et al.* Role of *Lactobacillus* in cervical cancer. *Cancer Manag. Res.* **10**, 1219–1229 (2018).
 163. Javanmard, A. *et al.* Gastroenterology and Hepatology From Bed to Bench. Probiotics and their role in gastrointestinal cancers prevention and treatment; an overview. (2018).
 164. Twetman, L., Larsen, U., Fiehn, N. E., Steckésn-Blicks, C. & Twetman, S. Coaggregation between probiotic bacteria and caries-associated strains: An in vitro study. *Acta Odontol. Scand.* **67**, 284–288 (2009).
 165. Foligne, B. *et al.* A key role of dendritic cells in probiotic functionality. *PLoS One* **2**, (2007).
 166. Drakes, M., Blanchard, T. & Czinn, S. Bacterial probiotic modulation of dendritic cells. *Infect. Immun.* **72**, 3299–3309 (2004).
 167. Christensen, H. R., Frøkiær, H. & Pestka, J. J. *Lactobacilli* Differentially Modulate Expression of Cytokines and Maturation Surface Markers in Murine Dendritic Cells. *J. Immunol.* **168**, 171–178 (2002).
 168. Foligne, B. *et al.* Correlation between in vitro and in vivo immunomodulatory properties of lactic acid bacteria. *World J. Gastroenterol.* **13**, 236–243 (2007).
 169. Sorbara, M. T. & Pamer, E. G. Interbacterial mechanisms of colonization resistance and the strategies pathogens use to overcome them. *Mucosal Immunol.* **12**, (2019).
 170. de Souza, B. M. S., Borgonovi, T. F., Casarotti, S. N., Todorov, S. D. & Penna, A. L. B. *Lactobacillus casei* and *Lactobacillus fermentum* Strains Isolated from Mozzarella Cheese: Probiotic Potential, Safety, Acidifying Kinetic Parameters and Viability under Gastrointestinal Tract Conditions. *Probiotics Antimicrob. Proteins* **11**, 382–396 (2019).
 171. Tuo, Y. *et al.* Aggregation and adhesion properties of 22 *Lactobacillus* strains. *J. Dairy Sci.* **96**, 4252–4257 (2013).
 172. Kramer, M. Impaired dendritic cell function in Crohn’s disease patients with NOD2 3020insC mutation. *J. Leukoc. Biol.* **79**, 860–866 (2006).
 173. Ghosh, C. C. *et al.* Gene-Specific Repression of Proinflammatory Cytokines in Stimulated Human Macrophages by Nuclear I κ B α . *J. Immunol.* **185**, 3685–3693 (2010).

174. Suurväli, J. *et al.* RGS16 restricts the pro-inflammatory response of monocytes. *Scand. J. Immunol.* **81**, 23–30 (2015).
175. Bogucka, K. *et al.* ERK3/MAPK6 controls IL-8 production and chemotaxis. *Elife* **9**, 1–40 (2020).
176. Kusumoto, S., Fukase, K. & Shiba, T. Key structures of bacterial peptidoglycan and lipopolysaccharide triggering the innate immune system of higher animals: Chemical synthesis and functional studies. *Proc. Japan Acad. Ser. B Phys. Biol. Sci.* **86**, 322–337 (2010).
177. Doshi, N. & Mitrugotri, S. Macrophages recognize size and shape of their targets. *PLoS One* **5**, 1–6 (2010).
178. Alhede, M. *et al.* Bacterial aggregate size determines phagocytosis efficiency of polymorphonuclear leukocytes. *Med. Microbiol. Immunol.* **209**, 669–680 (2020).
179. Kapetanovic, R. *et al.* Contribution of phagocytosis and intracellular sensing for cytokine production by Staphylococcus aureus-activated macrophages. *Infect. Immun.* **75**, 830–837 (2007).
180. Camilli, G. *et al.* Impaired phagocytosis directs human monocyte activation in response to fungal derived β -glucan particles. *Eur. J. Immunol.* **48**, 757–770 (2018).
181. Justice, S. S., Hunstad, D. A., Lynette, C. & Hultgren, S. J. Morphological plasticity as a bacterial survival strategy. *Nat. Rev. Microbiol.* **6**, 162–168 (2008).
182. Leroy, M. *et al.* Multiple consecutive lavage samplings reveal greater burden of disease and provide direct access to the nontypeable Haemophilus influenzae biofilm in experimental otitis media. *Infect. Immun.* **75**, 4158–4172 (2007).
183. Salamaga, B. *et al.* Bacterial size matters: Multiple mechanisms controlling septum cleavage and diplococcus formation are critical for the virulence of the opportunistic pathogen Enterococcus faecalis. *PLoS Pathog.* **13**, 1–26 (2017).
184. Gerhard, G. M., Bill, R., Messemaker, M., Klein, A. M. & Pittet, M. J. Tumor-infiltrating dendritic cell states are conserved across solid human cancers. *J. Exp. Med.* **218**, (2021).
185. Olingy, C. E., Dinh, H. Q. & Hedrick, C. C. Monocyte heterogeneity and functions in cancer. *J. Leukoc. Biol.* **106**, 309–322 (2019).
186. van de Ven, R., Lindenberg, J. J., Oosterhoff, D. & de Gruijl, T. D. Dendritic cell plasticity in tumor-conditioned skin: CD14+ cells at the cross-roads of immune activation and suppression. *Front. Immunol.* **4**, 1–7 (2013).
187. Mázló, A. *et al.* MSC-like cells increase ability of monocyte-derived dendritic cells to polarize IL-17-/IL-10-producing T cells via CTLA-4. *iScience* **24**, (2021).
188. Marzaioli, V. *et al.* CD209/CD14+ Dendritic Cells Characterization in Rheumatoid and Psoriatic Arthritis Patients: Activation, Synovial Infiltration, and Therapeutic Targeting. *Front. Immunol.* **12**, 1–16 (2022).
189. Han, Y., Chen, Z., Yang, Y., Jiang, Z. & Cao, X. Human CD14+CTLA-4+ Regulatory Dendritic Cells Suppress T-Cell Response by Cytotoxic T-Lymphocyte Antigen-4-Dependent IL-10 and Indoleamine- 2,3-Dioxygenase Production in Hepatocellular Carcinoma. *Hepatology* **59**, 567–579 (2014).
190. Bandola-Simon, J. & Roche, P. A. Dysfunction of Antigen Processing and Presentation by Dendritic Cells in Cancer. *Mol. Immunol.* **113**, 31–37 (2019).
191. Feng, M. *et al.* Phagocytosis checkpoints as new targets for cancer immunotherapy. *Nat. Rev. Cancer* **19**, 568–586 (2019).
192. Matson, V. *et al.* The commensal microbiome is associated with anti-PD-1 efficacy in metastatic melanoma patients. *Science (80-.)*. **359**, 104–108 (2018).
193. Gopalakrishnan, V., Spencer, C. N., Nezi, L. & Wargo, J. A. Gut microbiome modulates response to anti-PD-1 immunotherapy in melanoma patients. *Science (80-.)*. **13**, 1–16 (2017).
194. Shi, Y. *et al.* Intratumoral accumulation of gut microbiota facilitates CD47-based immunotherapy via STING signaling. *J. Exp. Med.* **217**, (2020).

11. PUBLICATION LIST PREPARED BY THE KENÉZY LIFE SCIENCES LIBRARY



UNIVERSITY of
DEBRECEN

UNIVERSITY AND NATIONAL LIBRARY
UNIVERSITY OF DEBRECEN

H-4002 Egyetem tér 1, Debrecen

Phone: +3652/410-443, email: publikaciok@lib.unideb.hu

Registry number: DEENK/2/2023.PL
Subject: PhD Publication List

Candidate: Márta Tóth
Doctoral School: Doctoral School of Molecular Cellular and Immune Biology
MTMT ID: 10059109

List of publications related to the dissertation

1. Burai, S., Kovács, R., Molnár, T., **Tóth, M.**, Szendi-Szatmári, T., Jenei, V., Bíró-Debreceni, Z., Brisco, S., Balázs, M., Bácsi, A., Koncz, G., Türk-Mázló, A.: Comprehensive analysis of different tumor cell-line produced soluble mediators on the differentiation and functional properties of monocyte-derived dendritic cells.
PLoS One. 17 (10), 1-23, 2022.
DOI: <http://dx.doi.org/10.1371/journal.pone.0274056>
IF: 3.752 (2021)
2. **Tóth, M.**, Muzsai, S., Regulski, K., Szendi-Szatmári, T., Czimmerer, Z., Rajnavölgyi, É., Chapot-Chartier, M. P., Bácsi, A.: The phagocytosis of *Lactocaseibacillus casei* and its immunomodulatory properties on human monocyte-derived dendritic cells depend on the expression of Lc-p75, a bacterial peptidoglycan-hydrolase.
Int. J. Mol. Sci. 23 (14), 1-19, 2022.
DOI: <http://dx.doi.org/10.3390/ijms23147620>
IF: 6.208 (2021)

List of other publications

3. Jenei, V., Burai, S., Molnár, T., Kardos, B., Mácsik, R., **Tóth, M.**, Debreceni, Z., Bácsi, A., Türk-Mázló, A., Koncz, G.: Comparison of the immunomodulatory potential of platinum-based anti-cancer drugs and anthracyclins on human monocyte-derived cells.
Cancer Chemother. Pharmacol. 91 (1), 53-66, 2023.
DOI: <http://dx.doi.org/10.1007/s00280-022-04497-1>
IF: 3.288 (2021)
4. Szénási, T., Varga, A., Hajas, G., **Tóth, M.**, Czimmerer, Z., Bácsi, A.: "Trained" immunitás memória kialakulása a veleszületett immunválaszok során.
Immunol. Szle. 14 (1), 15-21, 2022.





5. Szénási, T., Varga, A., **Tóth, M.**, Hajas, G., Muzsai, S., Czimmerer, Z., Bácsi, A.: A BCG-oltás és a koronavírus-fertőzés immunológiai kapcsolata.
Immunol. Szle. 14 (1), 23-29, 2022.
6. **Tóth, M.**, Bácsi, A.: A súlyos eozinofil asztma biológiai terápiás lehetőségei és az eozinofil sejtek fiziológiás szerepe.
Orvostovábbk. szle. 29 (3), 47-52, 2022.
7. **Tóth, M.**, Dajnoki, Z., Szegedi, A., Bácsi, A.: "Harmadik típusú találkozás" a 2-es típusú gyulladással.
Immunol. Szle. 13 (4), 41-49, 2021.
8. Ivanovics, B., Gazsi, G., Reining, M., Berta, I., Póliska, S., **Tóth, M.**, Domokos, A., Nagy, B. J., Staszny, Á., Cserhádi, M., Csősz, É., Bácsi, A., Csenki-Bakos, Z., Ács, A., Urbányi, B., Czimmerer, Z.: Embryonic exposure to low concentrations of aflatoxin B1 triggers global transcriptomic changes, defective yolk lipid mobilization, abnormal gastrointestinal tract development and inflammation in zebrafish.
J. Hazard. Mater. 416, 1-15, 2021.
DOI: <http://dx.doi.org/10.1016/j.jhazmat.2021.125788>
IF: 14.224
9. Türk-Mázló, A., Kovács, R., Miltner, N., **Tóth, M.**, Veréb, Z., Szabó, K., Bacskai, I., Pázmándi, K. L., Apáti, Á., Bíró, T., Bene, K., Rajnavölgyi, É., Bácsi, A.: MSC-like cells increase ability of monocyte-derived dendritic cells to polarize IL-17-/IL-10-producing T cells via CTLA-4.
iScience. 24 (4), 1-25, 2021.
DOI: <http://dx.doi.org/10.1016/j.isci.2021.102312>
IF: 6.107
10. Majai, G., Gogolák, P., **Tóth, M.**, Hodrea, J., Horváth, D., Fésüs, L., Rajnavölgyi, É., Bácsi, A.: Autologous apoptotic neutrophils inhibit inflammatory cytokine secretion by human dendritic cells, but enhance Th1 responses.
FEBS Open Bio. 10 (8), 1492-1502, 2020.
DOI: <http://dx.doi.org/10.1002/2211-5463.12904>
IF: 2.693
11. Dogra, P., Rancan, C., Ma, W., **Tóth, M.**, Senda, T., Carpenter, D. J., Kubota, M., Matsumoto, R., Thapa, P., Szabó, P. A., Li Poon, M. M., Li, J., Arakawa-Hoyt, J., Shen, Y., Fong, L., Lanier, L. L., Farber, D. L.: Tissue Determinants of Human NK Cell Development, Function, and Residence.
Cell. 180 (4), 749-763, 2020.
DOI: <http://dx.doi.org/10.1016/j.cell.2020.01.022>
IF: 41.582
12. Bene, K., **Tóth, M.**, Al-Taani, S., Tóth, L., Türk-Mázló, A., Rajnavölgyi, É., Bácsi, A.: A humán bélmikrobiom szerepe fiziológiás és patológias immunológiai folyamatokban.
Immunol. Szle. 11 (2), 14-24, 2019.





13. Kalló, G., Chatterjee, A., **Tóth, M.**, Rajnavölgyi, É., Csutak, A., Tózsér, J., Csósz, É.: Relative quantification of human [béta]-defensins by a proteomics approach based on selected reaction monitoring.
Rapid Commun. Mass Spectrom. 29 (18), 1623-1631, 2015.
IF: 2.226

Total IF of journals (all publications): 80,08

Total IF of journals (publications related to the dissertation): 9,96

The Candidate's publication data submitted to the iDEa Tudóstér have been validated by DEENK on the basis of the Journal Citation Report (Impact Factor) database.

09 January, 2023



12. KEYWORDS

12.1 Keywords

Microbiota, Lactobacillus, peptidoglycan, peptidoglycan-hydrolase, monocyte-derived dendritic cell, inflammation, phagocytosis, T cell, adenocarcinoma, melanoma, tumor cell line-derived soluble factors, differentiation

12.2 Kulcsszavak

Mikrobióta, Lactobacillus, peptidoglikán, peptidoglikán-hidroláz, monocita-eredetű dendritikus sejt, gyulladás, fagocitózis, T-sejt, adenokarcinóma, melanóma, tumor sejtvonal-eredetű oldott faktorok, differenciáció

13. ACKNOWLEDGEMENTS

One page is not enough to express my deep thanks to those, who helped me during this period of my life.

Firstly, I would like to thank my supervisor, *Prof. Dr. Attila Bácsi* for his continuous and essential support finalizing my PhD years. He always helped me with his outstanding professional knowledge and brilliant insights through the emerging troubles. His door was always open for the scientific and personal problems even the smallest ones. He taught me new point of views communicating our results more scientifically and clearly.

I am also very grateful to my former supervisor, *Prof. Dr. Éva Rajnavölgyi*, who allowed my MSc studies and fostered my PhD and pre-doctoral studies. She introduced me to the scientific world and taught how to present our results in a precise way.

I also say thanks to the previous Head of the Department, *Prof. Dr. Tamás Bíró* for the encouragement going to the US for a short-study program.

I am very thankful to *Dr. Donna L. Farber* for allowing me to work in her laboratory in the Columbia University and *Dr. Pranay Dogra* for teaching me that the errors in the RStudio do not necessarily mean bad.

I would like to express my special thanks to my present (and forever) roommate and friend *Dr. Anett Türk-Mázló* that she was attaching me like her MSC1 cells attach to the flask in every Microsoft error and making the workdays feel like home. I also would like to thank *Dr. Krisztián Bene*, my friend and former roommate for the laughing, and experiences we shared together with Anett.

I am also very grateful to the past member of the Bácsi's lab, *Dr. Brahma V. Kumar*, my friend and "American connection". Additionally, I am also thankful for the present members of the lab *Dr. Aliz Varga*, *Dr. György Hajas* and *Szabolcs Muzsai* and the honorary member of the lab, *Dr. Adrienn Gyöngyösi* for the talks about scientific and real-life problems.

I would like to thank all my colleagues, my students, and collaborators especially *Dr. Marie-Pierre Chapot-Chartier* and *Dr. Krzysztof Regulski* for fixing every problem I ever had, the support and advice. I would like to say special thanks to *Katalin Orosz-Tóth* for teaching me the precise lab work, her continuous support and encouragement starting the PhD. I am also very grateful to *Erzsike Nagyné Kovács*, *Zsuzsanna Bíró-Debreceni* and *Andrea Justyákné Tóth* for their excellent assistance and advice in the lab work.

The acknowledgement would not be complete without expressing my deep thanks to my partner, *Dr. Zsolt Czimmerer*, who taught me that everything starts with the genes. He inspires

me every day and with his completely different scientific vision, he always encourages me to improve myself.

Finally, I would like to deeply thank to my “non-work” friends, my supporting family, my mother *Márta*, my father *István*, my brother *István Jr.*, my aunt *Kati* for their patience and love and our dog, *Netti*, who helped me reduce (and sometimes intensify) the stress.

The work was supported by TAMOP-4.2.2.A-11/1/KONV-2012 0023 project implemented through the New Hungary Development Plan, and the National Research, Development and Innovation Office (NKFIH PD132570, NK 101538, NN 114423, K 125337, K 125224 and K 142930) and by TKP2021-EGA-19 project implemented with the support provided from the National Research, Development, and Innovation Fund of Hungary, financed under the TKP2021-EGA funding scheme. The work was also supported by GINOP-2.3.2-15-2016-00050 project. The project is co-financed by the European Union and the European Regional Development Fund.

14. APPENDIX

Sára Burai, Ramóna Kovács, Tamás Molnár, **Márta Tóth**, Tímea Szendi-Szatmári, Viktória Jenei, Zsuzsanna Bíró-Debreceni, Shlomie Brisco, Margit Balázs, Attila Bácsi, Gábor Koncz, Anett Mázló: *Comprehensive analysis of different tumor cell-line produced soluble mediators on the differentiation and functional properties of monocyte-derived dendritic cells*, Plos One, 2022, DOI: 10.1371/journal.pone.0274056.

Márta Tóth, Szabolcs Muzsai, Krzysztof Regulski, Tímea Szendi-Szatmári, Zsolt Czimmerer, Éva Rajnavölgyi, Marie-Pierre Chapot-Chartier, Attila Bácsi: *The Phagocytosis of Lactocaseibacillus casei and Its Immunomodulatory Properties on Human Monocyte-Derived Dendritic Cells Depend on the Expression of Lc-p75, a Bacterial Peptidoglycan Hydrolase*, Int. J. Mol. Sci., 2022, DOI: 10.3390/ijms23147620.